UNIVERSITY OF CALIFORNIA SAN DIEGO

Investigations into the Electronic Nature of Naphthalene in Push-Pull dyes

A Thesis submitted in partial satisfaction of the
requirements for the degree
Master of Science

in

Chemistry

by

Kevin I. Nguyen

Committee in charge:

Professor Emmanuel Theodorakis, Chair
Professor Francesco Paesani
Professor Jerry Yang

2019

The Thesis of Kevin I. Nguyen is approved, and is acceptable in quality and form for publication on microfilm and electronically:

_____

_____

_____

Chair

University of California San Diego

2019

Table of Contents

List of Figures

List of Schemes

List of Tables

ACKNOWLEGEMENTS

I would like to thank Professor Emmanuel Theodorakis for his support and guidance. I have not encountered many people who have supernatural patience to deal with my idiosyncrasies. I am not a conventional person, and I don't fit in conventional molds. This is more often considered a negative trait than a positive one, and I'm thankful that Emmanuel could see the good from it. When I first joined his lab, he told me that he only had room for scientists that could think independently. Although I think he sometimes laments telling me that, because I took it to the extreme, deep down he probably still encourages it.

I would also like to think Professors Francesco Paesani and Jerry Yang for their advice and feedback. Often times it takes outside perspective for me to realize that there are aspects I need to improve, such as being more conscientious and refined.

Thank you Mo and Jordi for working with me on my project and providing the electrochemical and computational data.

Thank you to Jeff Rances, who went out of his way to help me through the thesis process. I have a problem with adhering to deadlines, and this experience has been eye-opening.

Thank you to Alex, Josh, and Jamie, who were instrumental in helping to rebuild the lab.

Thank you Jessica Brown for being so helpful.

I would like to thank Nam Do for everything she has done for me.

The Thesis is currently being prepared for submission for publication of the material. Nguyen, Kevin; Melaimi, Mohand; Cirera, Jordi. The Thesis author was the primary investigator and author of this material.

ABSTRACT OF THE THESIS

Investigations into the Electronic Nature of Naphthalene in Push-Pull dyes

by

Kevin I. Nguyen

Master of Science in Chemistry

University of California San Diego, 2019

Professor Emmanuel A. Theodorakis, Chair

The understanding of a dye's electronic nature is fundamentally important as well as vital to the rational design of subsequent dyes. The elucidation of the conjugation

path in a naphthalene dye, substituted by a donor and acceptor on the long axis, is reported. This was accomplished *via* a combination of theoretical and empirical methods aimed at measuring the results of perturbing the electronic pi-structure. The replacement of methine units in naphthalene with nitrogen through the synthesis of analogues resulted in characteristic changes to the optical and electrochemical properties. These observations are consistent with the donor and acceptor being conjugated to specific positions in naphthalene. The results add to fundamental knowledge about the electronic nature of push-pull naphthalene, while directly providing a map of sites on naphthalene that may be synthetically targeted and altered to obtain bespoke dyes with desired photophysical or electrochemical properties.

Introduction

The development of organic dyes for pigments, biological probes, or other applications has consistently contended with the question of how structure influences property[1-3]. Over the years, this problem has been addressed both theoretically and empirically to provide several models and trends[4-7]. Among the oldest and most pervasive relationships involves pi-conjugation and energy, i.e., systems with longer conjugation generally absorb light of longer wavelengths[1]. Early theoretical models, such as the free-electron model, have explained this relationship in simple systems and predicted successfully the properties of several structures[6]. However, in pi-structures of greater length or complexity, these models fail to replicate experimental findings. As more advanced computational models emerged, the simple definition of conjugation evolved[8]. This is most evidently observed by the replacement of valence bond (VB) theory with molecular orbital (MO) theory in modern studies of conjugation. Within the context of leading MO theory treatments, such as density-functional theory (DFT), an active area of research is focused on developing more accurate models to describe aspects of pi-conjugation. This in essence suggests that the rational design of organic dyes for modern applications is a multivariate problem contingent on grasping a dynamic definition of conjugation, one that relies on the symbiosis of new empirical evidence and its theoretical explanation.

Dyes with donors (D) conjugated to acceptors (A) through a pi-unit, known as “push-pull” dyes[9], present an additional challenge to the understanding of conjugation. These dyes have gained popularity due to ease of synthesis and tunability through modular variation of the subunits[10-11]. The potential charge-transfer (CT) character in the

ground- or excited-states is desirable for applications such as dye-sensitized solar cells, molecular electronics, and fluorescent probes[9-10, 12]. However, the characterization of conjugation in push-pull dyes remains elusive. Strong donor-acceptor interaction that gives rise to the CT character significantly perturbs the electronic structure of the original pi-unit, such that the extent of electron delocalization is often ambiguous[8]. In the case of a push-pull dye (Figure 1) with D and A substituted on the long-axis of naphthalene[13-14], the true structure is depicted as an aromatic-quinoid resonance pair (Figure 2a), where the weight of each resonance structure depends on the nature of D and A. The problem is further complicated by multiple resonance structures of the aromatic form (Figure 2b), resulting in multiple possible conjugation paths (Figure 2c) to the quinoid form. It is clear that this valance-bond analysis, and the depiction of conjugation as single- and double-bond alternation in the Lewis structures, fails to convey adequate fundamental information about the dye that would allow for rational design.

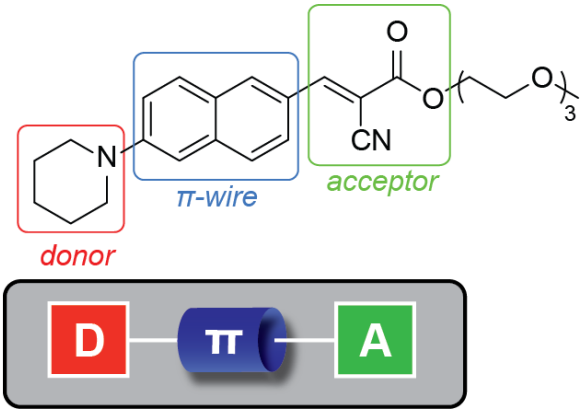

Figure 1: Example of a push-pull naphthalene dye. D and A denotes donor and acceptor, respectively.

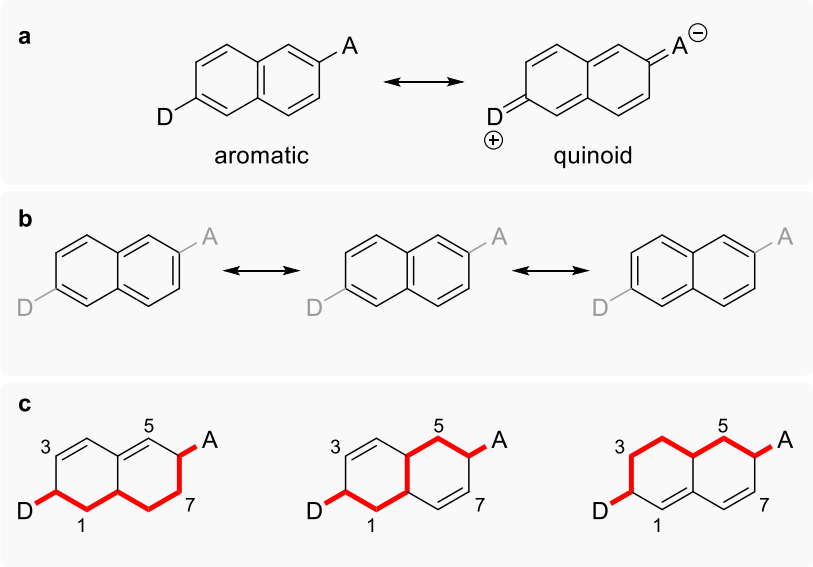

Figure 2: a) Aromatic and quinoid mesomeric structures of the naphthalene push-pull dye. b) resonance structures of aromatic naphthalene push-pull dye. c) possible conjugation pathways given the aromatic resonance structures

Fortunately, MO theory offers a more palpable description of conjugation in push-pull systems. Because molecular orbitals arise from a linear combination of atomic orbitals (LCAO), the size of the coefficients represents the weight of contribution of the atomic orbital to the overall MO[15]. Thus, the conjugation path can be seen as occurring along the connected atoms with the most significant coefficients (or, more precisely, the square of the coefficients) in the highest-occupied molecular orbital (HOMO) and the lowest-unoccupied molecular orbital (LUMO). In other words, conjugation is governed by the topologies of the frontier molecular orbitals[8]. Experimental studies of polymethine[2], a simple linear-conjugated hydrocarbon chain, have shown that perturbation by heteroatom substitution at C-H (methine units) with the largest squared-coefficients give rise to considerable spectral shifts (Figure 3). Specifically, electronegative heteroatoms such as nitrogen red-shifts the absorption when substitution occurs at odd-numbered methines,

which are positions in the LUMO with greatest squared-coefficients[2]. Conversely, the replacement of even-numbered methines (i.e. HOMO sites with the largest squared-coefficients) results in a blue shift.

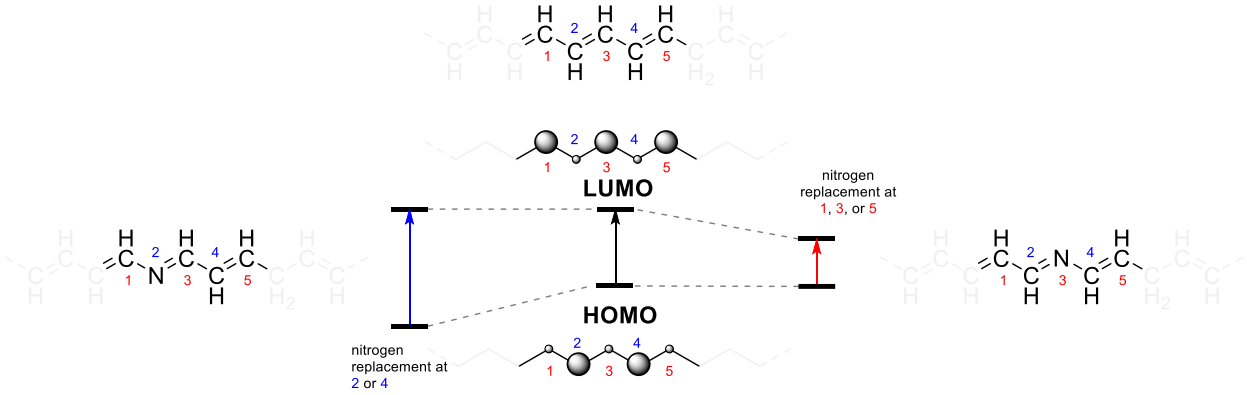

Figure 3: Square of LCAO coefficients (solid black circles) on polymethine dye and the spectral shifts as a result of perturbation by nitrogen replacement of methine(s).

In cases of more complex conjugated systems, such as D-A dyes with CT characteristics, DFT calculations can model FMO topologies with accuracies that depend on the choice of the functional[16-17]. The lack of a truly systematic approach for determining the appropriate functional is a current limitation of DFT[16-17]. For this reason, empirical evidence remains to be the gold standard to which DFT calculations are weighed against.

Here we show that D-A communication through the naphthalene wire occurs *via* a fixed conjugation pathway. We found that empirically substituting C-H with N in a naphthalene wire at positions C-1 and C-5 to give aza-analogues significantly perturbs donor/acceptor strengths. In contrast, when the substitution occurs at C-3 and C-7, the effect is relatively minimal. The distinction is particularly evident when comparing C-H to N substitution sites of equal proximity (e.g. C-1 *vs.* C-3) to the donor and/or acceptor,

indicating that effects of proximity are subordinate to specificity of the path. Using (TD)DTF calculations to predict empirical effects of electronegative perturbation at large-coefficient sites in the FMOs, we found that experimental results were consistent with theory in extreme cases, while milder cases were not consistent. By identifying the pathway for electron transport, this work vastly expands the understanding of the electronic nature of naphthalene in donor-acceptor the context. Furthermore, the analysis from this experimental perturbation method may be relevant to larger PAH systems that, in accordance to Clar's pi-sextet rule[18], inherently contain dissimilar pathways for potential conjugation.

Results and Discussion

Synthesis

To measure the perturbation caused by C-H to N substitution, six aza-analogues of naphthalene dye **ANCA** were synthesized (Figure 4a). The dialkylamine donor, in this case piperidine, and cyanoacrylate acceptor are common motifs in push-pull dyes[9]. **ANCA** was prepared by a previously described procedure[14]. The aza-analogues **QN1**, **QN2**, **NTD**, **iQN1**, **iQN2**, **iNTD** were synthesized (Scheme 1) *via* a PPh_3-catalyzed Knoevenagel condensation[19] between key aldehyde intermediates **3**, **6**, **9**, **12**, **15**, **18**, which were derived from commercially available substrates, and *2*-(*2*-(*2*-methoxyethoxy)ethoxy)ethyl *2*-cyanoacetate.

The full syntheses are described in the appendix. Key intermediates of **QN1** and **iQN1** were synthesized from the dihalide starting reagents **1** and **4** by direct substitution of the chloride with piperidine to give compounds **2** and **5** respectively. Compound **2** was directly formylated to afford **3** by lithiation with *n*-BuLi followed by a dimethylformamide (DMF) quench. Compound **5** was first converted to the vinyl intermediate *via* Suzuki-coupling with vinyl boronic acid pinacol ester, followed by oxidative cleavage using $OsO_4/NaIO_4$ to afford aldehyde **6**.

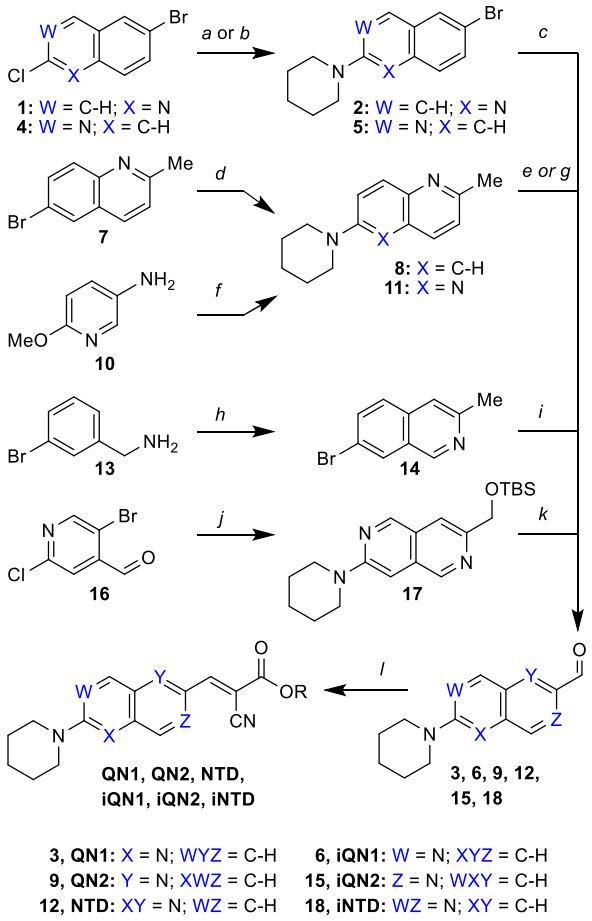

Scheme 1. Synthesis of analogues. (a) **1**, piperidine, DMSO (100% yield of **2**); (b) **4**, piperidine, DMSO (68% yield of **5**); (c) **2**, *n*-BuLi, DMF, THF (52% yield of **3**); (d) i. **5**, vinylboronic acid pinacol ester, $Pd(PPh_3)_4$, $NaHCO_3$, toluene, EtOH, H_2O; ii. 2,6-lutidine, $NaIO_4$, 1,4-dioxane, OsO_4 (56% yield of **6** over two steps); (d) **7**, piperidine, $Pd(OAc)_2$, CyJohnPhos, *t*-BuOK (78% yield of **8**); (e) **8**, SeO_2, 1,4-dioxane (44% yield of **9**); (f) i. **10**, acetaldehyde, HCl; ii. $POCl_3$; iii. piperidine, DMSO (21% yield of **11** over 3 steps); (g) SeO_2, 1,4-dioxane (95% yield of **12**); (h) i. **13**, 1,1-dimethoxyacetone, $NaBH(AcO)_3$, DCM; ii. chlorosulfonic acid (38% yield of **14**); (i) i. **14,** benzoyl peroxide, 1,2-dichloroethane, NBS; ii. KOAc, DMF; iii. NaOH, THF, MeOH, water; iv. MnO_2, DCM (62% yield of **15** over four steps); (j) i. **16**, *t*-butylamine, H_2O; ii. tert-butyldimethyl(prop-2-yn-1-yloxy)silane, zinc, $NiCl_2(dppp)$, ACN; iii. piperidine, ACN (16% yield of **17** over three steps); (k) i. **17**, THF, 2M HCl; ii. MnO_2, DCM (85% of **18** over two steps); (l) **3, 6, 9, 12, 15,** or **18**, 2-cyanoester, PPh_3 (56-93% yield of **QN1**, **iQN1**, **QN2**, **iQN2**, **NTD**, and **iNTD**).

Key intermediates of **QN2** and **NTD** were synthesized by the benzylic oxidation of **8** and **11**, respectively, using selenium(IV)oxide. Compound **8** was synthesized in one step *via* a Buchwald-Hartwig[20] coupling of compound **7** and piperidine. Compound **11** was synthesized over four steps; the reaction of **10** and acetaldehyde in concentrated hydrochloric acid (HCl) yielded the methyl naphthyridinone **10a** (Scheme 2), which was chlorinated with phosphorous oxychloride ($POCl_3$) to obtain **10b**; direct substitution of the chloride with piperidine afforded **11**.

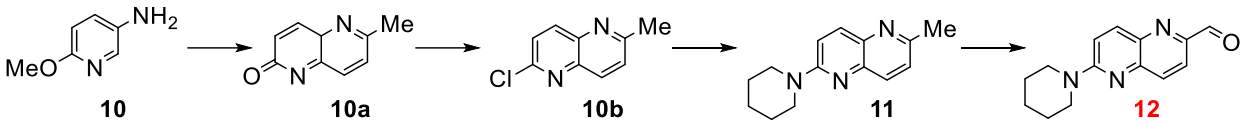

Scheme 2. Synthesis of NTD key intermediate

iQN2 key intermediate **15** was synthesized over nine steps (Scheme 3). Commercially-available **13** was combined with dimethyl glyoxal acetate in the presence of sodium tri(acetoxy)borohydride to yield compound **13a**, which cyclized to **14** after addition to concentrated chlorosulfonic acid. Compound **14** was brominated at the benzylic position with *n*-bromosuccinamide and benzoyl peroxide to give **14a**. The bromide was displaced with potassium acetate to yield **14b**, which was subsequently hydrolyzed to furnish **14c**. Oxidation of the alcohol with Dess-Martin periodinane afforded aldehyde **14d**. The aldehyde was protected with ethylene glycol under acidic conditions to afford **14e**. Using Buchwald-Hartwig conditions similar to those used in the conversion

of **7** to **8**, **14e** was converted to **14f** which, after deprotection, yielded key intermediate **15**.

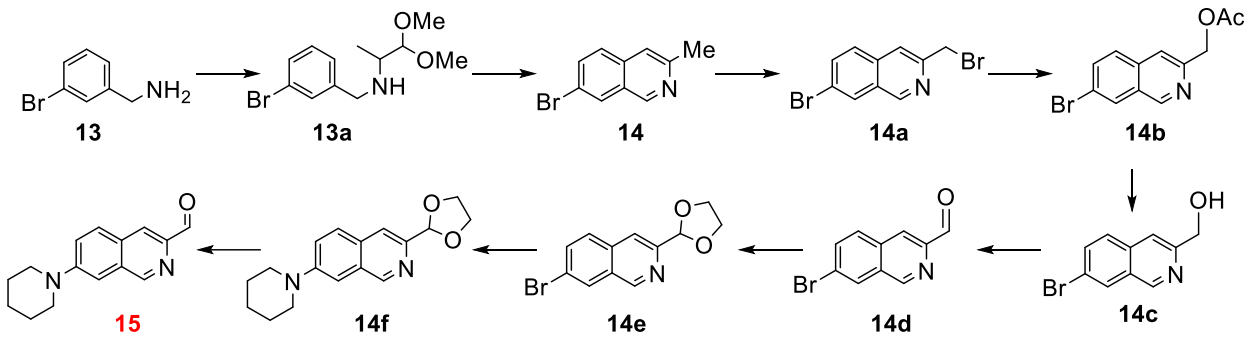

Scheme 3. Synthesis of iQN2 key intermediate

Lastly, **iNTD** key intermediate **18** was synthesized in five steps (Scheme 4). Addition of **16** to a solution of *t*-butylamine yielded compound **16a**. This was combined with tert-butyldimethyl(prop-2-yn-1-yloxy)silane, zinc, and nickel catalyst to produce **16b**. The piperidine was installed *via* direct substitution to give **17**, which was deprotected to produce **17b**. Finally, manganese dioxide oxidized the alcohol to yield key intermediate **18**.

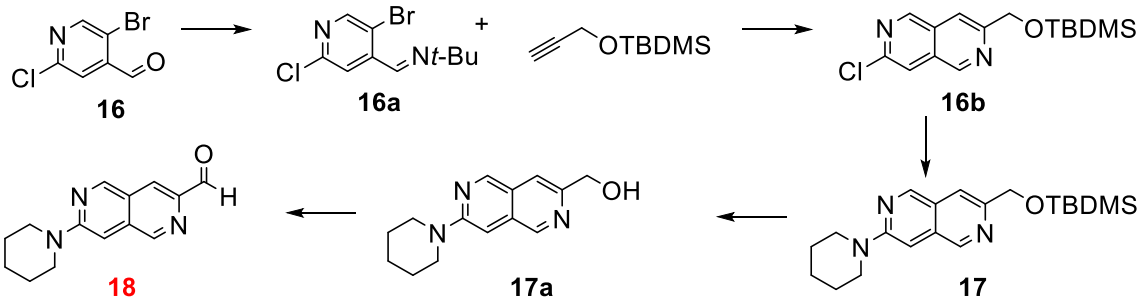

Scheme 4. Synthesis of iNTD key intermediate

Notable reactivity features of the syntheses provided clues to the conjugation path of the dyes. For example, despite being structurally similar, compounds **1** and **4** differ considerably in reactivity. Specifically, the S_NAr transformation of compound **1** to **2**

proceeded quantitatively after heating at 100°C for 1 hour, while the analogous conversion of **4** to **5** was low-yielding and required harsh conditions to proceed. Along the same lines, the methyl groups of intermediates **8** and **11** were easily oxidized to the respective aldehydes by treatment with selenium(IV)oxide under mild conditions, while the analogous methyl of **14** was completely unreactive to the same oxidant, even at extreme (decomposition) temperatures. These results indicate that reactions of isoquinolines **4** and **14** form less stable transition state intermediates than those of quinolines **1**, **8**, and **11**. Comparing 2-methylquinoline and 3-methylisoquinoline, *Mills* and *Smith* proposed that the enhanced reactivity of the former's benzylic hydrogens stemmed from its methyl being in conjugation with the nitrogen, a feature lacking in the latter[21]. The results of this study converged with other independent reactivity studies to suggest that positions C-1 and C-3 in naphthalene are fundamentally dissimilar; specifically, substituents at C-2 can communicate influentially with C-1 (and *vice versa*) but not C-3 [21-23]. The push-pull arrangement of **ANCA** raises a separate but related question: how does the donor (C-2 substituent) communicate with the acceptor (C-6 substituent) through naphthalene? The perturbation by nitrogen substitution at positions C-1, C-3, C-5, and C-7 (Figure 4b) in **ANCA** aims to reveal the pathway of D-A conjugation.

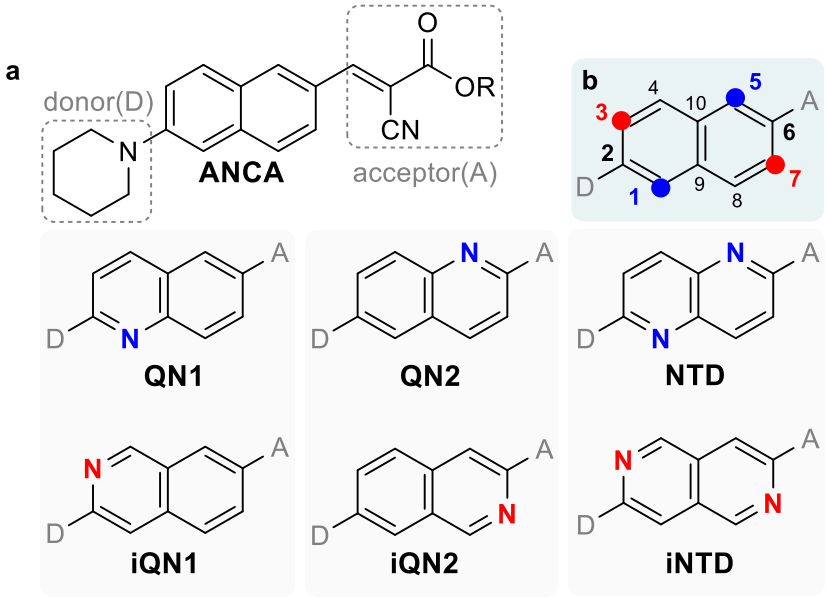

Figure 4: a) seven synthesized dyes. b) four substitution sites of ANCA highlighted.

Computational studies

The D-pi-A arrangement of **ANCA** and its aza-analogues suggests the possibility of multiple conjugation routes. As a starting point, we used density functional theory (DFT) at the B3LYP level to model the FMOs of the seven dyes (Figure 5). Since the effective conjugation of a molecule is governed by the frontier molecular orbital (FMO) topologies[8], DFT(B3LYP), which excels at calculating ground-state properties, is appropriate for this application. Compared to the formal definition of conjugation, which depends on bond-length alternation computed with Huckel MO theory, the localization patterns in the FMOs more accurately describe effective conjugation in complex systems such as polyenes or donor-acceptor dyes[8].

As typical of D-pi-A systems, the highest-occupied molecular orbital (HOMO) coefficients of the seven dyes are largely localized near the donor, while the lowest-

unoccupied molecular orbitals (LUMO) coefficients are largely localized near the acceptor. Furthermore, the localization patterns of the FMOs are very similar between the dyes, the LUMOs being nearly indistinguishable from each other. In the HOMOs, all dyes consistently have the largest coefficients at the donor nitrogen and C-1 (naphthalene's numbering). The largest coefficients in the LUMOs are on the acceptor substituent and C-5.

QN1 and **NTD** have nearly identical HOMO topologies that are significantly different from those of other dyes (including **ANCA**), i.e. in the coefficients of C-4, C-9, and C-10. The calculated FMO energies (Figure 6) show that all aza-analogues have decreased values of the HOMO and LUMO. This signifies that nitrogen-substitution stabilizes the FMOs. The most significant stabilization is seen when dyes contain nitrogen at C-1, C-5, or both. Specifically, when nitrogen is at C-1 (i.e. **QN1** and **NTD**), the HOMO is greatly stabilized. On the other hand, the LUMO is largely stabilized when nitrogen is at C-5 (i.e. **QN2** and **NTD**). The dyes **iQN1**, **iQN2**, and **iNTD** show only mild to moderate stabilization of the FMOs. These dyes are nitrogen-substituted at positions C-3 and/or C-7. Based on this qualitative picture, it would be reasonable to predict that **ANCA** is effectively conjugated along C-1 and C-5 and that nitrogen substitution at these positions will experimentally yield the greatest perturbations.

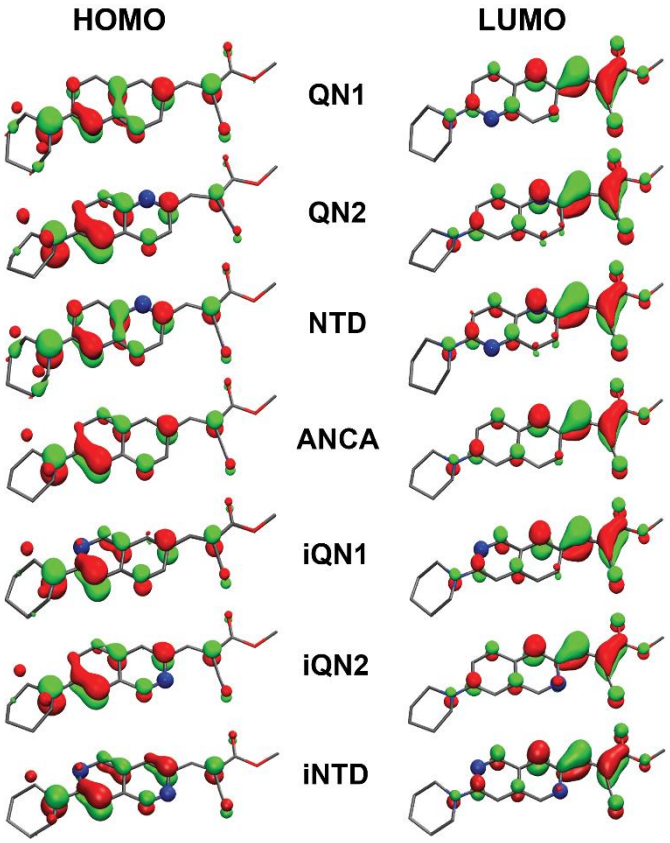

Figure 5: Frontier molecular orbitals of all dyes, ground-state optimized in acetonitrile, calculated with density functional theory (DFT) using the hybrid GGA functional B3LYP.

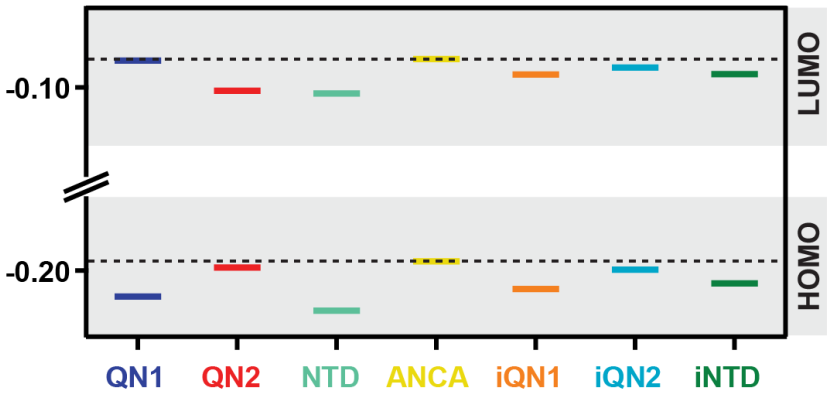

Figure 6: DFT calculated HOMO/LUMO energy levels for the seven dyes. Dotted line denotes the HOMO/LUMO levels of ANCA.

Photophysical studies

The experimental UV-vis spectra of all dyes (Figure 7) show the absorption max (λ_{max}) of reference dye **ANCA** at 434 nm, which is flanked at the extreme blue- and red-shifted regions by **QN1** (λ_{max} = 410 nm) and **QN2** (λ_{max} = 450 nm) respectively. This accounts for an overall λ_{max} range of 40 nm, where the maximum hypsochromic and bathochromic shifts are 24 nm and 16 nm, respectively. Dyes that deviate least are **iNTD** (λ_{max} = 434 nm) and **NTD** (λ_{max} = 430 nm), the former coinciding precisely with **ANCA** while the latter is blue-shifted by 4 nm. Moderate deviations are observed with **iQN1** (λ_{max} = 442 nm) and **iQN2** (λ_{max} = 424 nm), which are red-shifted by 8 nm and blue-shifted by 10 nm, respectively.

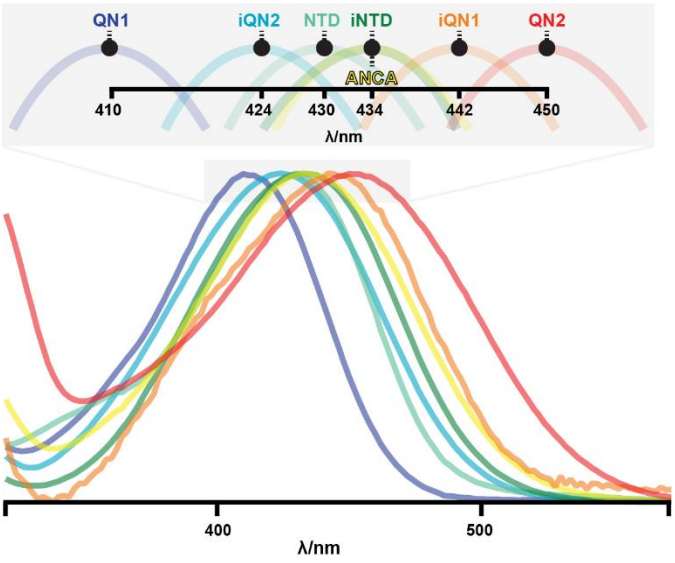

Figure 7: Normalized experimental UV-vis spectra of the seven dyes in acetonitrile. Expanded view (above) is simulated to scale

The computed spectra (Figure 8) qualitatively replicate the experimental λ_{max} trend of the blue- and red-shifted extremes, i.e., **QN1** and **QN2** respectively. However, the λ_{max}

order of **iQN1** and **iQN2** is reversed when compared to experimental spectra. Moreover, the computed results underestimate the magnitude of changes in λ_{max} (*rel.* to $\lambda_{(\mathbf{ANCA})max}$) of **iQN1** and **iQN2** while overestimating the λ_{max} changes of **NTD** and **iNTD.** All computed λ_{max} values of individual dyes are greater than the respective experimental λ_{max} values, and the computational λ_{max} range (76 nm) overestimates of the experimental range by 36 nm.

The extreme shifts in opposite directions for **QN1** and **QN2** can be explained by the locations of nitrogen-substitution relative to the donor and acceptor. The nitrogen is an internal electron-withdrawing substituent[24], which depletes the donor and strengthens the acceptor to an extent that is related to the proximity [25]. Since the source of pi-deficiency (i.e. nitrogen) is adjacent to the donor in **QN1**, the depletion effect on the donor surpasses the strengthening effect on the acceptor, resulting in a blue shift. Conversely, the "acceptor-side" nitrogen in **QN2** causes a red shift. The proximity theory also explains the negligible shifts of **iNTD** and **NTD**, since these dyes contain both "donor-side" and "acceptor-side" nitrogens. However, the explanation breaks down for isoquinolines **iQN1** and **iQN2**. Containing a "donor-side" nitrogen, **iQN1** was expected to undergo a blue-shift to a similar extent as **QN1**, instead of the observed *red-shift*. Analogously, **iQN2**, which contains the "acceptor-side" nitrogen, defied expectations by displaying a *blue-shift.* These anomalies suggest that the proximity effect is secondary to the specificity of nitrogen location along a certain path. Namely, nitrogen-substitution at C-1 and C-5 resulted in large shifts that obeyed the proximity theory, while substitution at C-3 and C-7 produced small shifts.

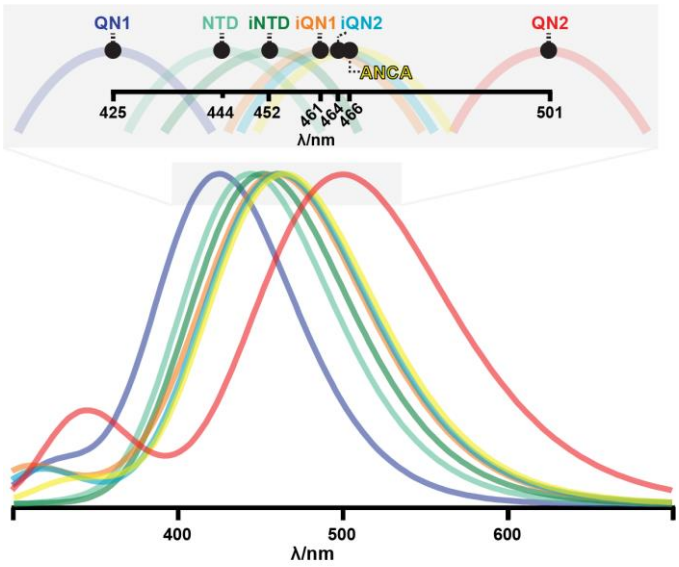

Figure 8: Normalized TDDFT-calculated UV-vis spectra of the seven dyes in acetonitrile. Expanded view (above) is simulated to scale

Electrochemical studies

Measurements to confirm nitrogen-substitution effects on donor and acceptor strengths can be obtained by looking at the ionization potential (IP) and electron affinity (EA) of each dye. Using cyclic voltammetry (CV) experiments (Figure 9), we obtain approximations of oxidation and reduction potentials, which are directly related to IP and EA [26-27]. Moreover, IP and EA are related to the HOMO and LUMO, respectively [28]. It should be noted that these relations are approximate and more rigorous conversion factors are required to truly use them interchangeably[29]. Values obtained (Table 1) are estimated onset potentials, which are sufficient for qualitative analysis [30]. Perturbations as a result of nitrogen-substitution are measured by comparing the onset potentials

(E_{red}^{onset}, E_{ox}^{onset}) of the six aza-dyes against the onset potentials of **ANCA**. Accordingly, the largest onset oxidation potential change (δE_{ox}^{onset}) and onset reduction potential change (δE_{red}^{onset}) are both observed with **NTD**. Therefore, the total change ($\delta E_{total}^{onset} = \delta E_{ox}^{onset} + \delta E_{red}^{onset}$) is also the largest with **NTD**, making it the most perturbed dye. This is not evident in the UV-vis absorption spectra, which show **NTD** being among the least perturbed in terms of λ_{max}. However, the CV and UV-vis data are in fact consistent, because the perturbation increases both HOMO and LUMO energies concomitantly, thus causing the energy gap to remain relatively unchanged. Similarly, **iNTD** shows moderate but well-balanced perturbation in both E_{red}^{onset} *and* E_{ox}^{onset}, which is reflected in the zero-shift of its λ_{max} relative to **ANCA**. When only a large δE_{ox}^{onset} is present (i.e. the case of **QN1**), the UV-vis spectrum displays a large blue-shift. On the other hand, a large δE_{red}^{onset} in the absence of a large δE_{ox}^{onset} (i.e. **QN2**) consistently displays a large red-shift. Of the six aza-dyes, **iQN1** and **iQN2** show the smallest perturbations in terms of δE_{total}^{onset} values, with largely similar values of δE_{ox}^{onset} and δE_{red}^{onset}. This explains the moderate shifts in λ_{max}. However, because of the closeness in values, no rationalization can be made for the reversal in expected blue- and red-shift order for these two dyes. Nonetheless, comparing δE_{total}^{onset} values of **QN1**, **QN2**, and **NTD** to those of their respective isomers (**iQN1**, **iQN2**, and **iNTD**) clearly shows that C-1/C-5 substitutions lead much larger overall perturbations than C-3/C-7 substitutions. In the extreme case, **QN1** is 21-fold more perturbed than **iQN1** when comparing δE_{total}^{onset} values. Even in the mildest scenario, **NTD** is more than 2-fold more perturbed than **iNTD**.

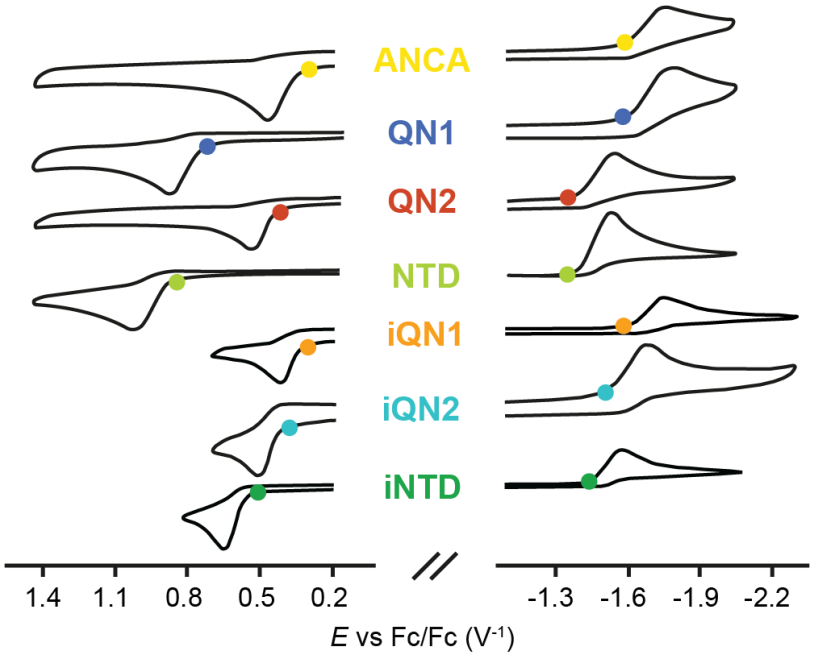

Figure 9: Cyclic voltammograms of dyes investigated in this study. (n-Bu_4NPF_6 0.1M in acetonitrile, 100 mVs-1, vs. Fc+/Fc).

Table 1: Estimated cyclic voltammetry onset potential values and differences (δ) in values with respect to ANCA potentials

Dye	**E_{ox}^{onset}** (V)	**E_{red}^{onset}** (V)	**δE_{ox}^{onset}** † (V)	**δE_{red}^{onset}** ‡ (V)	**δE_{total}** § (V)
ANCA	0.34	-1.58	**-**	**-**	**-**
QN1	0.76	-1.58	***0.42***	0	***0.42***
QN2	0.42	-1.34	0.08	***0.24***	***0.32***
NTD	0.85	-1.33	***0.51***	***0.25***	***0.76***
iQN1	0.34	-1.56	0	0.02	0.02
iQN2	0.40	-1.51	0.06	0.07	0.13
iNTD	0.50	-1.42	0.16	0.16	0.32

† Difference values $\delta E_{ox}^{onset} = E_{ox}^{onset} - E_{(ANCA)ox}^{onset}$

‡ Difference values $\delta E_{red}^{onset} = E_{red}^{onset} - E_{(ANCA)red}^{onset}$

§ Sum of differences $\delta E_{total} = \delta E_{ox}^{onset} + \delta E_{red}^{onset}$

These data empirically point to the ground-state localization of FMO electron density existing along C-1 and C-5. Moreover, because IP and EA are associated with donor and acceptor strengths, respectively, these results imply that perturbation along the conjugated path drastically affects donor and acceptor strengths, while substitution outside the path (i.e. C-3 and C-7) has a minimal effect on D and A. The reversal of expected order of perturbation in λ_{max} for **iQN1** and **iQN2** indicates that the proximity effect is only relevant when the substitution occurs inside the conjugation path (i.e. the case of **QN1**, **QN2**, and **NTD**). As a whole, the standard deviation for E_{ox}^{onset} (σ = 0.2) values is

two-fold greater than that of E_{red}^{onset} (σ = 0.1), signifying that donor strength is more sensitive than acceptor strength to the effects of C-H to N substitution.

Conclusion

The determination of the conjugated pathway in push-pull naphthalene has direct implications in the design of naphthalene dyes. Particularly, **ANCA**[14, 31] and related fluorescent dyes such as PRODAN[32] and FDDNP[33] can be rationally modified with the consideration that certain sites produce the greatest spectral shifts. Although the phenomena of fluorescence may be more complicated to examine, the understanding of how changes in structure affect the optical gap and the HOMO-LUMO energies is a prerequisite. The results of this study pose some unanswered questions about the effects of perturbation outside of the proposed pathway. These questions may in the future be answered using newer models. While some discrepancies between theory and experiment still exist, the use of modern computational methods such as (TD)DFT proves to be an indispensable complement to empirical results for the study of more complex systems. It is in fact the active attempt to reconcile these conflicts that have historically led to an evolution of how conjugation is perceived.

The Thesis is currently being prepared for submission for publication of the material. Nguyen, Kevin; Melaimi, Mohand; Cirera, Jordi. The Thesis author was the primary investigator and author of this material.

Appendix

Knoevenagel condensation

General procedure A

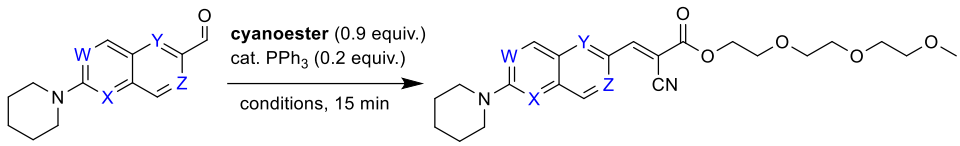

A mixture of **aldehyde** (1 equiv.), **cyanoester** [2-(2-(2-methoxyethoxy)ethoxy)ethyl 2-cyanoacetate] (0.9 equiv.), and PPh_3 (0.2 equiv.) was heated to reflux in absolute ethanol or with microwave radiation (neat) to 95°C. After cooling to room temperature, the mixture was purified by silica gel column chromatography (or preparative TLC) to afford the cyanoacrylate dye, which appears (when visualized with 365 nm UV light) as a fluorescent color that is red-shifted from the fluorescence of the precursor aldehyde (e.g. **Figure S1**).

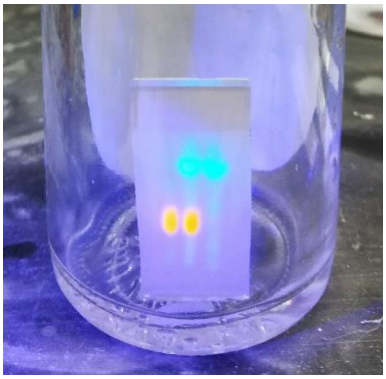

Figure 10: Developing TLC plate of **QN2** (left spot), **aldehyde 9** (right spot), and co-spot (middle) illuminated by handheld 365 nm UV light.

Synthetic scheme for preparation of aldehydes 3, 6, 9, 12, 15, 18

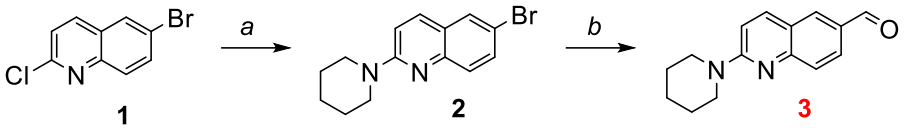

a) Compound **1** (1 equiv.), piperidine (5 equiv.), DMSO, 100°C, 1 h (100% yield of Compound **2**)

b) Compound **2**, *n*-BuLi (1.2 eq., 2.2 N hexanes), THF, –78 °C, 1 h; then DMF (2 equiv.) –78 °C, 1 h; then 1M HCl, r.t., 1h (52% yield of Compound **3**)

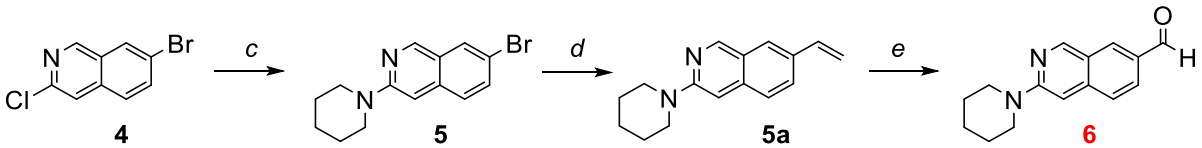

c) Compound **4** (1 equiv.), piperidine (5 equiv.) DMSO, 150°C, 12 h (68% yield of Compound **5**)

d) Compound **5** (1 equiv.), vinylboronic acid pinacol ester (2 equiv.), $Pd(PPh_3)_4$ (0.1 equiv.), sodium bicarbonate (1.3 equiv.), toluene, ethanol, water, 70°C, 20 h (68% yield of Compound **5a**)

e) Compound **5a** (1 equiv.), 2,6-lutidine (2 equiv.), and $NaIO_4$ (4 equiv.), OsO_4 (4% in water; 0.002 equiv.), 1,4-dioxane (5 mL), rt, 4 h (76% yield of Compound **6**)

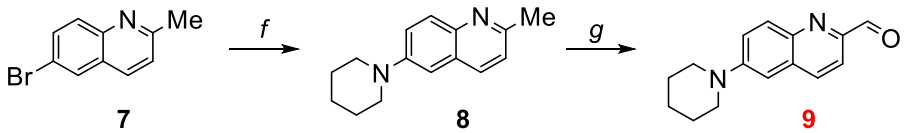

f) Compound **7** (1 equiv.), piperidine (1.3 equiv.), $Pd(OAc)_2$ (0.1 equiv.), CyJohnPhos (0.2 equiv.), *t*-BuOK (1.3 equiv.), 120°C, 19 h, (78% yield of Compound **8**)

g) Compound **8** (1 equiv.), SeO_2 (2 equiv.), 1,4-dioxane, 0.25 h MW (44% yield of Compound **9**)

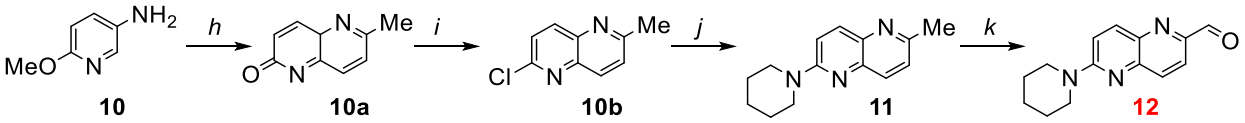

10 **10a** **10b** **11** **12**

h) Compound **10** (1 equiv.), acetaldehyde (4 equiv.), conc. HCl, 0°, 1 h, then 100°C, 1 h (32% yield of Compound **10a**)

i) Compound **10a** (1 equiv.), $POCl_3$ (neat excess), 100°C, 2 h (67% yield of **Compound 10b**)

j) Compound **10b** (1 equiv.), piperidine (5 equiv.), DMSO, 100°C, 1 h (100% yield of Compound **11**)

k) Compound **11** (1 equiv.) SeO_2 (1.5 equiv.), 1,4-dioxane, reflux, 2 h (95% yield of Compound **12**)

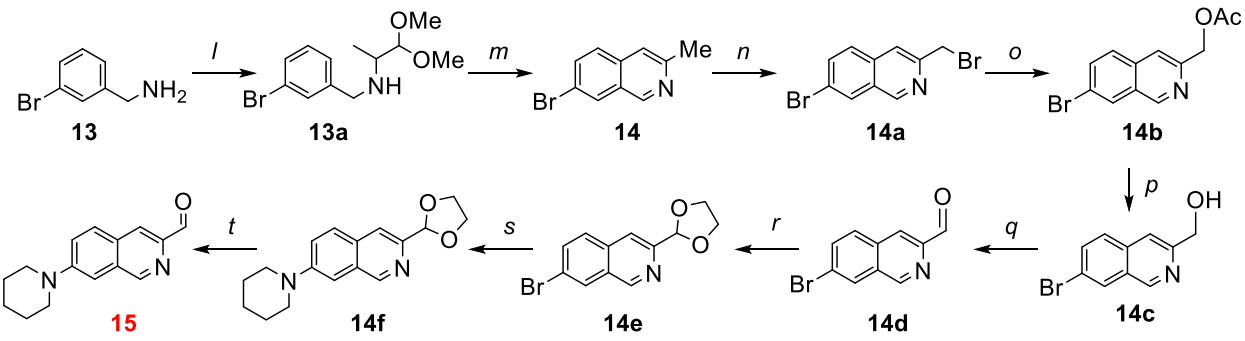

l) Compound **13** (1 equiv.), methyl glyoxal 1,1-dimethyl acetate (1 equiv.), $NaBH(AcO)_3$ (1.5 equiv.), DCM, rt, 16 h (100% yield of **Compound 13a**)

m) Compound **13a** (1 equiv.), chlorosulfonic acid (10 equiv.), 100°C, 1 h (38% yield of Compound **14**)

n) Compound **14** (1 equiv.), benzoyl peroxide (70% in water, 0.1 equiv.), 1,2-dichloroethane, *N*-bromosuccinimide (1.1 equiv.), 50°C, 20 h (66% yield of **Compound 14a**)

o) Compound **14a** (1 equiv.), KOAc (3 equiv.), DMF, 70°C, 2 h (100% yield of **Compound 14b**)

p) Compound **14b** (1 equiv.), THF, MeOH, 2N NaOH, reflux, 2 h **(100% yield of Compound 14c**)

q) Compound **14c** (1 equiv.), DMP (1.2 equiv.), DCM, rt, 4 h (72% yield of **Compound 14d**)

r) Compound **14d** (1 equiv.), ethylene glycol (1.5 equiv.), *p*-tolunesulfonic acid (0.1 equiv.), toluene, 24 h (92% yield of **Compound 14e**)

s) Compound **14e** (1 equiv.), $Pd(OAc)_2$ (0.1 equiv.), CyJohnPhos (0.2 equiv.), piperidine (1.3 equiv.), and *t*-BuOK (1.3 equiv.), toluene, reflux, 12 h (49% yield of **Compound 14f**)

t) Compound **14f** (1 equiv.), 1N HCl, THF, 16 h (100% yield of **Compound 15**)

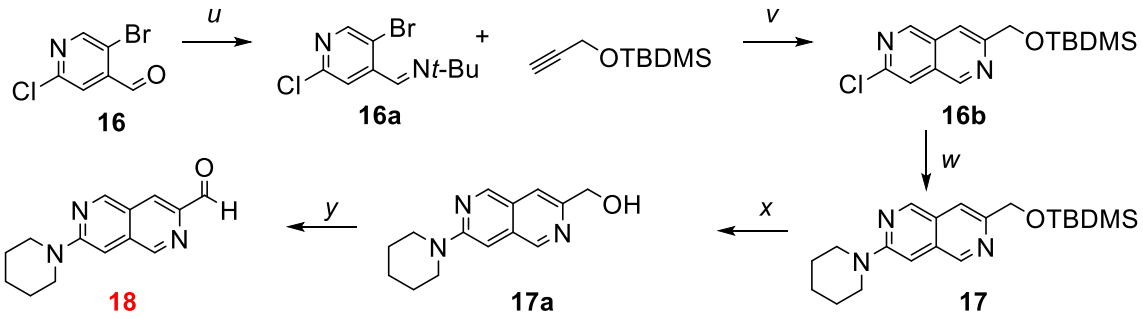

u) Compound **16** (1 equiv.), *t*-butylamine (4.75 equiv.), water, rt, 12 h (74% yield of Compound **16a**)

v) Compound **16a** (1 equiv.), tert-butyldimethyl(prop-2-yn-1-yloxy)silane (1.53 equiv.), zinc (2.05 equiv.), and $NiCl_2$(dppp) (0.05 equiv.), acetonitrile, 70°C, 1 h (42% yield of Compound **16b**)

w) Compound **16b** (1 equiv.), piperidine (5 equiv.), acetonitrile (5 mL), 130°C, 12 h (53% yield of Compound **17**)

x) Compound **17** (1 equiv.), THF, 2M HCl, rt, 12 h (85% yield of **Compound 17a**)

y) Compound **17a** (1 equiv.), MnO_2 (20 equiv.), DCM (91% yield of **Compound 18**)

Experimental procedures and characterization data

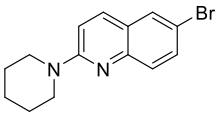

Compound **2**: A mixture of commercially-available compound **1** (250 mg, 1 mmol, 1 equiv.) and piperidine (0.48 mL, 5 equiv.) in DMSO (1 mL) was heated to 100°C in a capped vial for 1 h. After cooling to room temperature, the reaction was poured into ice water (5 mL) and rinsed twice with ethyl acetate (10 mL). The organic layer was separated and washed three times with ice water (15 mL). The washed organic layer was dried with sodium sulfate concentrated *in vacuo* to afford a brownish-white solid (282 mg, 100% yield).

R_f = 0.44 (1:9 EtOAc:hexanes)

^{1}H NMR (400 MHz, Chloroform-*d*): δ 10.18 (s, 1H), 8.32 (d, *J* = 1.8 Hz, 1H), 8.22 – 8.18 (m, 1H), 8.15 – 8.10 (m, 2H), 7.65 – 7.60 (m, 1H).

^{13}C NMR (101 MHz, Chloroform-*d*): δ 191.30, 151.26, 145.34, 139.59, 134.77, 133.14, 130.16, 128.37, 127.38, 126.70.

HRMS (ESI-TOF) calc'd for $C_{14}H_{16}BrN_2$ $[M+H]^+$: 291.0491; found 291.0490.

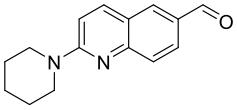

Compound **3**: A solution of compound **2** (122 mg, 0.42 mmol, 1 equiv.) in dry THF (2 mL) under argon was cooled to -78°C. Then *n*-BuLi (2.2M in hexanes; 0.23 mL, 0.5 mmol, 1.2 equiv.) was added via syringe over a period of 0.5 h, causing a color change of the solution from pale yellow to dark brown. Dry DMF was subsequently added dropwise over a period of 10 minutes, causing the solution to lighten in color. The reaction was allowed to slowly warm to room temperature, after which 1N HCl was added portion-wise until acidic. The reaction was basified with saturated $NaHCO_3$ solution and extracted with ethyl acetate. After concentrating *in vacuo,* the crude product was subjected to flash chromatography and eluted with 20% ethyl acetate in hexanes. The solvent was removed *in vacuo* to afford a brownish-orange solid (52 mg, 52% yield).

R_f = 0.56 (1:1 EtOAc:hexanes)

^{1}H NMR (500 MHz, Chloroform-*d*): δ 10.00 (s, 1H), 8.04 (d, *J* = 1.9 Hz, 1H), 7.98 (dd, *J* = 8.7, 2.0 Hz, 1H), 7.91 (dd, *J* = 9.2, 0.7 Hz, 1H), 7.66 (d, *J* = 8.7 Hz, 1H), 7.02 (d, *J* = 9.3 Hz, 1H), 3.81 – 3.78 (m, 4H), 1.75 – 1.67 (m, 6H).

^{13}C NMR (126 MHz, Chloroform-*d*): δ 191.44, 158.41, 152.20, 138.33, 132.97, 130.24, 127.74, 127.07, 121.67, 110.29, 45.96, 25.88, 24.79.

HRMS (ESI-TOF) calc'd for $C_{15}H_{17}N_2O$ $[M+H]^+$: 241.1335; found 241.1333.

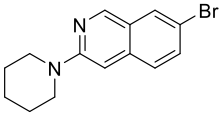

Compound **5:** A mixture of commercially-available compound **4** (225 mg, 0.9 mmol, 1 equiv.) and piperidine (5 equiv.) in ACN (2 mL) was heated at 135°C for 16 h in a sealed pressure tube. After cooling to room temperature, the reaction was poured into water (10 mL). The resulting yellow-brown precipitate was

isolated by vacuum filtration. After washing with water, the solid was recrystallized from ethanol to give a light yellow-green powder (183 mg, 68% yield).

R_f = 0.37 (1:9 EtOAc:hexanes).

^{1}H NMR (400 MHz, Chloroform-*d*): δ 8.83 (s, 1H), 7.88 (s, *J* = 1.9 Hz, 1H), 7.50 (d, *J* = 8.9, 1H), 7.41 (d, *J* = 8.9 Hz, 1H), 6.70 (s, 1H), 3.57 (t, *J* = 4.9 Hz, 4H), 1.77 – 1.63 (m, 6H).

^{13}C NMR (75 MHz, Chloroform-*d*) δ 157.27, 150.08, 137.39, 133.37, 129.53, 126.90, 123.90, 115.42, 98.27, 77.45, 77.03, 76.61, 47.07, 25.50, 24.71.

HRMS (ESI-TOF) calc'd for $C_{14}H_{16}BrN_2$ $[M+H]^+$: 291.0491; found 291.0494.

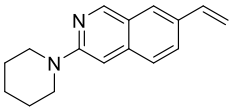

Compound **5a:** To a degassed mixture of compound **5** (87 mg, 0.3 mmol, 1 equiv.), vinylboronic acid pinacol ester (0.1 mL, 0.6 mmol, 2 equiv.), sodium bicarbonate (41 mg, 0.4 mmol, 1.3 equiv.), toluene (2 mL), ethanol (1 mL), and water (1 mL) under argon was added $Pd(PPh_3)_4$ (34 mg, 0.03 mmol, 0.1 equiv.) in one portion. The reaction was heated to 70°C with vigorous stirring for 20 h. After cooling to room temperature, the reaction was diluted with water and extracted with ethyl acetate. The organic layer was concentrated *in vacuo* and the crude was purified by flash chromatography to afford a bright yellow solid (54 mg, 76% yield).

R_f = 0.31 (1:9 EtOAc:hexanes).

^{1}H NMR (400 MHz, Chloroform-*d*): δ 8.89 (s, 1H), 7.66 – 7.62 (d, *J* = 7.2 Hz 2H), 7.50 (d, *J* = 9.2 Hz, 1H), 6.80 (dd, *J* = 17.6, 10.9 Hz, 1H), 6.73 (s, 1H), 5.77 (d, *J* = 17.6 Hz, 1H), 5.26 (d, *J* = 10.9 Hz, 1H), 3.58 (t, *J* = 5.2 Hz, 4H), 1.77 – 1.64 (m, 6H).

^{13}C NMR (101 MHz, Chloroform-*d*): δ 157.48, 151.48, 138.90, 136.73, 132.41, 127.62, 126.13, 125.69, 123.34, 113.11, 98.99, 47.45, 25.78, 24.97.

HRMS (ESI-TOF) calc'd for $C_{16}H_{19}N_2$ $[M+H]^+$: 239.1543; found 239.1545.

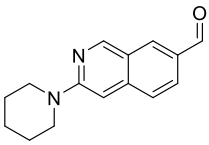

Compound **6:** To a mixture of compound **5a** (53 mg, 0.22 mmol, 1 equiv.), 2,6-lutidine (47 mg, 0.44 mmol, 2 equiv.), and $NaIO_4$ (190 mg, 0.88 mmol, 4 equiv.) in 1,4-dioxane (5 mL) was added OsO_4 (4% in water; 28 µL, 4.4 µmol) at 0°C. The reaction was warmed to room temperature and stirred for 4 h. Water (5 mL) was added, and the mixture was extracted twice with ethyl acetate (10 mL). The organic layer was dried with sodium sulfate and concentrated *in vacuo.* The crude was purified with flash chromatography to give a yellowish-brown solid (32 mg, 60% yield).

R_f = 0.20 (1:9 EtOAc:hexanes).

^{1}H NMR (400 MHz, Chloroform-*d*): δ 9.98 (s, 1H), 9.00 (s, 1H), 8.19 (s, 1H), 7.89 (d, *J* = 8.7, 1H), 7.53 (d, *J* = 8.7 Hz, 1H), 6.72 (s, 1H), 3.69 (m, 4H), 1.72 – 1.68 (m, 6H).

^{13}C NMR (101 MHz, Chloroform-*d*): δ 191.21, 158.57, 153.45, 142.37, 135.54, 131.42, 126.98, 126.15, 121.67, 97.96, 46.76, 25.73, 24.93.

HRMS (ESI-TOF) calc'd for $C_{15}H_{17}N_2O$ $[M+H]^+$: 241.1335; found 241.1337.

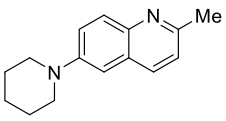

Compound **8:** To dry and degassed toluene (6 mL), $Pd(OAc)_2$ (30 mg, 0.135 mmol) and CyJohnPhos (95 mg, 0.27 mmol) was added in one portion. After stirring for 30 min, commercially-available compound **7** (600 mg, 2.7 mmol), piperidine (276 mg, 3.54 mmol), and *t*-BuOK (366 mg (3.54 mmol) was added.

The reaction flask was evacuated with argon, sealed, and brought to 120° C. After stirring for 19 h, the reaction was cooled to room temperature. The crude mixture concentrated under reduced pressure and purified by silica gel chromatography (EtOAc:hexanes gradient 1:9 to 1:2). The fractions were concentrated *in vacuo* to give a yellow solid (78% yield).

R_f = 0.30 (1:9 EtOAc:hexanes).

^{1}H NMR (400 MHz, Chloroform-*d*): δ 7.86 (d, J= 9.2 Hz, 2H), 7.46 (dd, J= 6.4 Hz, 2.8 Hz 1H), 7.17 (d, J= 8.4), 7.0 (d, J= 2.8 Hz), 3.24 (t, J= 5.2 Hz, 4H), 2.68 (s, 3H), 1.75 (m, 4H), 1.61 (m, 2H).

^{13}C NMR (101 MHz, Chloroform-*d*): δ 155.6, 149.6, 143.2, 134.9, 129.0, 127.5, 123.2, 122.0, 109.3, 50.7, 25.8, 25.0, 24.2.

HRMS (ESI-TOF) calc'd for $C_{15}H_{19}N_2$ $[M+H]^+$: 227.1543; found 227.1542.

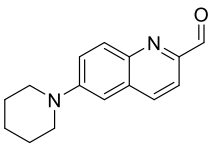

Compound **9:** To a microwave vial, compound **8** (250 mg, 1.1 mmol) and SeO_2 (246 mg, 2.2 mmol) was added. The mixture was diluted with 1,4-dioxane (2.5 mL) and sealed. The reaction was subjected to microwave irradiation for 15 minutes until completion, as indicated by TLC. After cooling to room temperature, the black selenium was filtered out with a pad of Celite. The remaining crude mixture was concentrated and purified by silica gel chromatography (gradient of 100% hexanes to EtOAc:hexanes 2:3). The fractions were concentrated to give yellow crystals (44% yield).

R_f = 0.35 (2:8 EtOAc:hexanes).

^{1}H NMR (400 MHz, Chloroform-*d*): δ 8.03 (t, J= 8.4 Hz, 2H), 7.91 (d, J= 8.8 Hz, 1H), 7.56 (dd, J= 6.4 Hz, 2.6 Hz, 1H), 6.99 (d, J=2.8, 1H), 3.41 (m, 4H), 1.74 (m, 4H), 1.67 (m, 2.08).

^{13}C NMR (101 MHz, Chloroform-*d*): 193.5, 151.4, 149.5, 142.7, 134.7, 132.1, 131.0, 122.9, 118.0, 107.2, 49.4, 25.5, 24.2.

HRMS (ESI-TOF) calc'd for $C_{15}H_{17}N_2O$ $[M+H]^+$: 241.1335; found 241.3333.

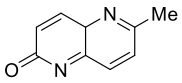

Compound **10a:** Following literature preparation[34], a solution of commercially-available compound **10** (786 mg, 6.3 mmol, 1 equiv.) in conc. HCl (5 mL) was cooled to 0°C before acetaldehyde (1.5 mL, 27 mmol, 4.3 equiv.) was added dropwise. The reaction was stirred at this temperature for 1 h and before heating to reflux for an additional 1 h. After cooling to room temperature, the brown solid was filtered off and washed with water. The filtrate was basified with sat. $NaHCO_3$ and twice extracted with DCM (10 mL). The organic layer was dried with sodium sulfate. Then hexanes was slowly added to precipitate a white solid, which after filtration afforded pure product (323 mg, 32% yield).

R_f = 0.62 (1:1 EtOAc:hexanes).

^{1}H NMR (400 MHz, Chloroform-*d*): δ 7.99 (d, *J* = 9.7 Hz, 1H), 7.70 (d, *J* = 8.4 Hz, 1H), 7.30 (d, *J* = 8.4 Hz, 1H), 6.89 (d, *J* = 9.7 Hz, 1H), 2.63 (s, 6H).

^{13}C NMR (126 MHz, Chloroform-*d*): δ 164.30, 154.58, 142.35, 136.76, 132.88, 125.31, 124.86, 124.45, 24.34.

HRMS (ESI-TOF) calc'd for $C_9H_9N_2O$ $[M+H]^+$: 161.1709; found 161.0709.

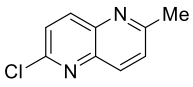

Compound **10b:** Adapted from literature preparation[34], a suspension compound **10a** (300 mg, 2 mmol, 1 equiv.) in $POCl_3$ (2 mL) was heated to 100°C for 2 h. The reaction was cooled to room temperature, then slowly poured onto ice. After allowing the ice to melt, the mixture was washed with DCM (10 mL). The aqueous layer was basified with 2N NaOH and extracted three times with DCM (15 mL). The organic layer was dried with sodium sulfate and concentrated *in vacuo* to give a brownish-white solid (67%, 241 mg).

R_f = 0.32 (1:1 EtOAc:hexanes).

^{1}H NMR (400 MHz, Chloroform-*d*): δ 8.24 (dd, *J* = 8.7, 0.8 Hz, 1H), 8.18 (d, *J* = 8.7 Hz, 1H), 7.56 (d, *J* = 8.7 Hz, 1H), 7.52 (d, *J* = 8.7 Hz, 1H), 2.76 (s, 3H).

^{13}C NMR (126 MHz, Chloroform-*d*): δ 160.36, 150.47, 142.26, 141.72, 139.12, 136.75, 126.41, 125.99, 25.01.

HRMS (ESI-TOF) calc'd for $C_9H_8ClN_2$ $[M+H]^+$: 179.0370; found 179.0371.

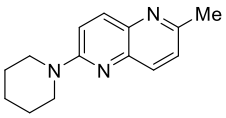

Compound **11:** A mixture of compound **10b** (200 mg, 1.1 mmol, 1 equiv.) and piperidine (5 equiv.) in DMSO (1 mL) was heated to 100°C in a capped vial for 1 h. After cooling to room temperature, the reaction was poured into ice water (5 mL) and rinsed twice with ethyl acetate (10 mL). The organic layer was separated and washed three times with ice water (15 mL). The washed organic layer was dried with sodium sulfate concentrated *in vacuo* to afford a light brown oil (254 mg, 100% yield).

R_f = 0.44 (1:1 EtOAc:hexanes).

^{1}H NMR (400 MHz, Chloroform-*d*): δ 7.98 (d, *J* = 9.4, 1H), 7.85 (d, *J* = 8.6 Hz, 1H), 7.29 (d, *J* = 8.6 Hz, 1H), 7.16 (d, *J* = 9.4 Hz, 1H), 3.71 (dd, *J* = 5.1, 2.8 Hz, 4H), 2.65 (s, 3H), 1.73 – 1.62 (m, 6H).

^{13}C NMR (101 MHz, Chloroform-*d*): δ 157.29, 154.37, 142.14, 139.21, 137.65, 134.48, 125.13, 113.14, 46.51, 25.97, 24.97, 24.76.

HRMS (ESI-TOF) calc'd for $C_{14}H_{18}N_3$ $[M+H]^+$: 228.1495; found 228.1495.

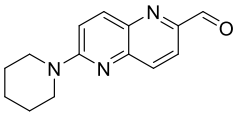

Compound **12:** A mixture of compound **11** (227 mg, 1 mmol, 1 equiv.) and SeO_2 (167 mg, 1.5 mmol, 1.5 equiv) in 1,4-dioxane was heated to reflux for 2 h. The reaction was cooled to room temperature, diluted with ethyl acetate, and filtered through Celite. The crude was subjected to flash chromatography and eluted with 30% ethyl acetate in hexanes. The solvent was removed *in vacuo* to afford a light yellow solid (229 mg, 95% yield).

R_f = 0.44 (1:1 EtOAc:hexanes).

^{1}H NMR (300 MHz, Chloroform-*d*): δ 10.11 (s, 1H), 8.08 (m, *J* = 13.7, 9.1 Hz, 2H), 7.96 (d, *J* = 8.7 Hz, 1H), 7.28 (d, *J* = 9.0 Hz, 1H), 3.83 (t, *J* = 5.0 Hz, 4H), 1.80 – 1.62 (m, 6H).

^{13}C NMR (126 MHz, Chloroform-*d*): δ 192.87, 157.82, 148.18, 146.20, 139.64, 138.70, 133.97, 121.57, 113.89, 46.13, 25.90, 24.70.

HRMS (ESI-TOF) calc'd for $C_{14}H_{16}N_3O$ $[M+H]^+$: 242.1288; found 242.1290.

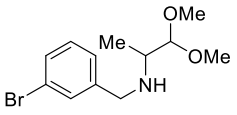

Compound **13a**: Following literature preparation[35]**, c**ommercially-available compound **13** (2.00 g, 11 mmol, 1 equiv.) and methyl glyoxal 1,1-dimethyl acetate (1.27g, 11 mmol, 1 equiv.) in DCM (60 mL) was cooled to 0°C. Then $NaBH(AcO)_3$ (3.42 g, 16 mmol, 1.5 equiv.) was added portion-wise. The mixture was

warmed to room temperature and stirred for 16 h. The reaction was poured into a sat. $NaHCO_3$ solution (120 mL) and the organic layer was separated. The aqueous layer was extracted twice with DCM (60 mL) and the combined organic layers were dried with sodium sulfate and concentrated *in vacuo* to give a turbid pale yellow oil (3.1g, 100% yield).

R_f = 0.27 (1:9 EtOAc:hexanes).

^{1}H NMR (400 MHz, Chloroform-*d*): δ 7.49 (s, 1H), 7.39 – 7.35 (d, *J* = 8.0 Hz, 1H), 7.25 (d, *J* = 8.0 Hz, 1H), 7.18 (m, 1H), 4.14 (d, *J* = 6.2 Hz, 1H), 3.86 (d, *J* = 13.5 Hz, 1H), 3.68 (d, *J* = 13.4 Hz, 1H), 3.38 (d, *J* = 8.4 Hz, 6H), 2.81 (m, 1H), 1.72 (s, 1H), 1.09 (d, *J* = 6.4 Hz, 3H).

^{13}C NMR (101 MHz, Chloroform-*d*): δ 143.24, 131.36, 130.18, 126.91, 122.76, 108.16, 55.06, 55.01, 53.89, 50.83, 15.27.

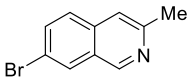

Compound **14:** Following literature preparation[35], compound **13a** (500 mg, 1 equiv.) was slowly added dropwise to ice-cold chlorosulfonic acid (2.5 g, 10 equiv.) and stirred at 0°C for 0.5 h. The reaction was subsequently warmed to room temperature and then heated at 100°C for an additional 1 h. After cooling to 0°C, the reaction mixture was added very slowly into an ice-cold solution of 2N NaOH. The pH was adjusted to basic with additional 2N NaOH. The white precipitate was vacuum filtered and washed with water to give a mixture of regioisomers (1:0.17) of product to 8-bromo-3-methylisoquinoline (217 mg combined). The mixture was recrystallized from methanol and water to give pure product as a tannish-white solid (38% yield).

R_f = 0.43 (1:1 EtOAc:hexanes).

^{1}H NMR (300 MHz, Chloroform-*d*): δ 9.10 (s, 1H), 8.13 – 8.03 (s, 1H), 7.70 (dd, *J* = 8.8, 2.0 Hz, 1H), 7.60 (d, *J* = 8.8 Hz, 1H), 7.45 (s, 1H), 2.68 (s, 3H).

^{13}C NMR (126 MHz, Chloroform-*d*): δ 152.31, 150.85, 134.94, 133.76, 129.60, 127.72, 127.69, 119.68, 118.33, 24.27.

HRMS (ESI-TOF) calc'd for $C_{10}H_9BrN$ $[M+H]^+$: 221.9913; found 221.9916.

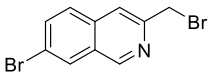

Compound **14a:** To a suspension of compound **14** (150 mg, 0.65 mmol, 1 equiv.) and benzoyl peroxide (70% in water; 23 mg, 0.065 mmol, 0.1 equiv.) in 1,2-dichloroethane (20 mL) was added *N*-bromosuccinimide (129 mg, 0.65 mmol, 1.1 equiv.). The reaction was stirred at 50°C and irradiated with a 60W incandescent light for 20 h. After cooling to room temperature, the solid was filtered off and washed with DCM. The solution was concentrated *in vacuo* and purified with flash chromatography with a gradient of 1:9 ethyl acetate/hexanes to 3:7 ethyl acetate/hexanes. Removal of solvent *in vacou* afforded a white-brown solid (129 mg, 66% yield).

R_f = 0.32 (1:1 EtOAc:hexanes).

^{1}H NMR (400 MHz, Chloroform-*d*): δ 9.17 (s, 1H), 8.14 (d, *J* = 1.9 Hz, 1H), 7.78 (dd, *J* = 8.7, 1.9 Hz, 1H), 7.74 (s, 1H), 7.69 (d, *J* = 8.7 Hz, 1H), 4.72 (s, 2H).

^{13}C NMR (101 MHz, Chloroform-*d*): δ 152.03, 150.84, 134.88, 134.61, 130.03, 128.57, 121.79, 119.79, 90.43, 34.57.

HRMS (ESI-TOF) calc'd for $C_{10}H_8Br_2N$ $[M+H]^+$: 299.9018; found 299.9017.

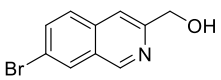

Compound **14c**: A mixture of compound **14a** (1 equiv.) and potassium acetate (2 equiv.) in DMF (amount) was stirred at 70°C for 2 h. After

cooling to room temperature, the reaction was diluted with water and extracted with ethyl acetate. The organic layer was dried with sodium sulfate and concentrated *in vacuo* to give a white-brown solid (compound **14b**), which was used in the next step without further purification. R_f = 0.41 (1:1 EtOAc/Hex). A solution of (7-bromoisoquinolin-3-yl)methyl acetate in THF, MeOH, and 2N NaOH was stirred at reflux for 2 h. After cooling to room temperature, the mixture was partitioned between ethyl acetate and water. The organic layer was dried with sodium sulfate and concentrated *in vacuo* to give an off-white solid (100% yield over two steps).

R_f = 0.02 (1:1 EtOAc:hexanes)

^{1}H NMR (400 MHz, Chloroform-*d*): δ 9.15 (s, 1H), 8.13 (d, *J* = 1.9 Hz, 1H), 7.76 (dd, *J* = 8.8, 1.9 Hz, 1H), 7.69 (d, *J* = 8.8 Hz, 1H), 7.64 (s, 1H), 4.91 (s, 2H), 3.37 (s, 1H).

^{13}C NMR (126 MHz, Chloroform-*d*): δ 153.44, 150.89, 134.80, 134.24, 129.78, 128.78, 128.27, 120.64, 116.50, 64.88.

HRMS (ESI-TOF) calc'd for $C_{10}H_9BrNO$ $[M+H]^+$: 237.9862; found 237.9863.

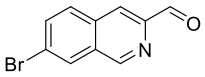

Compound **14d**: To a room-temperature solution of compound **14c** (1 equiv.) in DCM was added Dess-Martin periodinane (1.2 equiv.) in one portion. The reaction was stirred for 4 h. Saturated sodium thiosulfate was added and the reaction was stirred for an additional 0.5 h. The mixture was poured into saturated $NaHCO_3$. The organic layer was separated and the aqueous layer was extracted twice with DCM. The combined organic layers were concentrated *in vacuo* to give an off-white solid, which was used in the next step without further purification (72% yield).

R_f = 0.62 (1:1 EtOAc:hexanes).

^{1}H NMR (400 MHz, Chloroform-d): δ 10.26 (s, 1H), 9.31 (s, 1H), 8.36 (s, 1H), 8.25 (s, 1H), 7.91 – 7.87 (m, 2H).

^{13}C NMR (101 MHz, Chloroform-d): δ 193.07, 152.09, 147.11, 135.05, 133.76, 131.25, 130.20, 130.07, 124.38, 121.22.

HRMS (ESI-TOF) calc'd for $C_{10}H_7BrNO$ $[M+H]^+$: 235.9706; found 235.9706.

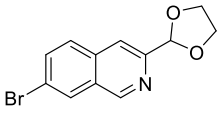

Compound **14e**: A solution of compound **14d** (1 equiv.), ethylene glycol (1.5 equiv.), and *p*-tolunesulfonic acid (0.1 equiv.) in toluene was stirred at reflux for 24 h. The reaction was cooled to room temperature and partitioned between ethyl acetate and water. The aqueous layer was basified with sat. $NaHCO_3$ and extracted with ethyl acetate. The combined organic layers were dried with sodium sulfate and concentrated *in vacuo* to give an off-white solid, which was used in the next step without further purification (96% yield).

R_f = 0.38 (1:1 EtOAc:hexanes).

^{1}H NMR (500 MHz, Chloroform-*d*): δ 9.18 (s, 1H), 8.13 (s, 1H), 7.85 (s, 1H), 7.75 (dd, *J* = 8.7, 1.9 Hz, 1H), 7.71 (d, *J* = 8.7 Hz, 1H), 6.03 (s, 1H), 4.25 – 4.18 (m, 2H), 4.16 – 4.08 (m, 2H).

^{13}C NMR (126 MHz, Chloroform-d): δ 151.52, 150.74, 134.42, 134.21, 129.76, 129.48, 128.75, 121.45, 117.42, 103.44, 65.65.

HRMS (ESI-TOF) calc'd for $C_{12}H_{11}BrNO_2$ $[M+H]^+$: 279.9968; found 279.9967.

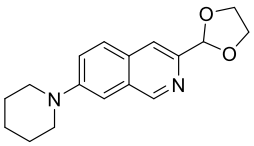

Compound **14f**: To dry and degassed toluene (6 mL), $Pd(OAc)_2$ (4 mg, 0.018 mmol, 0.1 equiv.) and CyJohnPhos (13 mg, 0.036 mmol, 0.2 equiv.) was added and stirred for 15 min before compound **14e** (50 mg, 0.18 mmol, 1 equiv.), piperidine (23 µL, 0.23 mmol, 1.3 equiv.), and *t*-BuOK (26 mg 0.23 mmol, 1.3 equiv.) was added. The reaction flask was evacuated with argon, sealed, and brought to 110° C. After stirring for 12 h, the reaction was cooled to room temperature. The crude mixture was concentrated and purified by silica gel chromatography (1:4 EtOAc:hexanes to 7:3 EtOAc:hexanes, slow gradient). Removal of solvent yielded a clear oil that solidified upon standing into white disk crystals (25 mg, 49% yield).

R_f = 0.17 (1:1 EtOAc:hexanes).

^{1}H NMR (500 MHz, Chloroform-*d*): δ 9.09 (s, 1H), 7.73 (s, 1H), 7.69 (d, *J* = 9.0 Hz, 1H), 7.48 (dd, *J* = 9.1, 2.5 Hz, 1H), 7.18 (d, *J* = 2.4 Hz, 1H), 6.01 (s, 1H), 4.27 – 4.08 (m, 4H), 3.33 – 3.26 (m, 4H), 1.80 – 1.71 (m, 4H), 1.68 – 1.58 (m, 2H).

^{13}C NMR (126 MHz, Chloroform-*d*): δ 151.13, 150.97, 146.97, 130.26, 130.23, 127.54, 124.23, 117.45, 108.60, 103.77, 65.44, 50.21, 25.58, 24.13.

HRMS (ESI-TOF) calc'd for $C_{17}H_{21}N_2O_2$ [M+H]: 285.1598; found 285.1596.

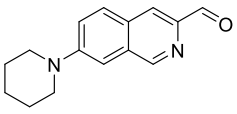

Compound **15**: A solution of compound **14f** (1 equiv.) in THF and 1N HCl was stirred at room temperature for 16 h. The reaction was poured in sat. $NaHCO_3$ and extracted with ethyl acetate. The organic layer was concentrated *in vacuo* to give a light yellow solid, which was used in the final step without further purification.

R_f = 0.50 (1:1 EtOAc:hexanes).

^{1}H NMR (300 MHz, Chloroform-*d*): δ 10.19 (s, 1H), 9.13 (s, 1H), 8.24 (s, 1H), 7.85 (d, *J* = 9.2 Hz, 1H), 7.55 (dd, *J* = 9.2, 2.6 Hz, 1H), 7.23 (s, 1H), 3.44 (t, *J* = 5.3 Hz, 4H), 1.82 – 1.69 (m, 6H).

^{13}C NMR (126 MHz, Chloroform-*d*): δ 193.13, 152.47, 151.30, 144.54, 132.82, 129.56, 128.46, 123.31, 122.00, 107.55, 49.39, 25.46, 24.27.

HRMS (ESI-TOF) calc'd for $C_{15}H_{17}N_2O$ $[M+H]^+$: 241.1335; found 241.1338.

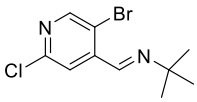

Compound **16a**: To a mixture of commercially-available compound **16** (500 mg, 2.26 mmol, 1 equiv.) in water (1 mL) was added *t*-butylamine (1.13 mL, 10.77 mmol, 4.75 equiv.). The reaction was stirred at room temperature for 12 hours, after which it was concentrated *in vacuo*. The residue was partitioned between ethyl acetate and water. The organic layer was dried with sodium sulfate and concentrated *in vacuo* to give a clear-white solid (460 mg, 74% yield).

R_f = 0.84 (1:1 EtOAc:hexanes).

^{1}H NMR (400 MHz, Chloroform-*d*): δ 8.51 (s, 1H), 8.45 (s, 1H), 7.90 (s, 1H), 1.32 (s, 9H).

^{13}C NMR (75 MHz, Chloroform-*d*): δ 152.07, 151.59, 150.84, 144.72, 122.80, 120.55, 59.14, 29.37.

HRMS (ESI-TOF) calc'd for $C_{10}H_{13}BrClN_2$ $[M+H]^+$: 274.9945; found 274.9946.

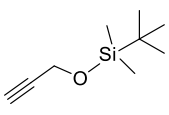

tert-butyldimethyl(prop-2-yn-1-yloxy)silane: To a solution of commercially-available propyn-2-ol (2 g, 33 mmol, 1 equiv.) and *1H-*

imidazole (4.5 g, 67 mmol, 2 equiv.) in DCM (100 mL) was added *tert*-Butyl(chloro)dimethylsilane (5.5 g, 37 mmol, 1.1 equiv.) portion-wise at 0°C. The reaction was warmed to room temperature and stirred for 4 h. Aqueous saturated NH_4Cl was added. The organic layer was separated and washed twice with water, dried with sodium sulfate, and concentrated *in vacuo* to give a clear oil that was used in the next step without further purification (5.7 g, 100% yield).

^{1}H NMR (400 MHz, Chloroform-*d*): δ 4.32 (d, *J* = 2.2 Hz, 2H), 1.01 – 0.80 (s, 9H), 0.24 – 0.07 (s, 6H).

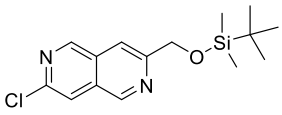

Compound **16b**: A mixture of compound **16a** (370 mg, 1.34 mmol, 1 equiv.), tert-butyldimethyl(prop-2-yn-1-yloxy)silane (0.42 mL, 2.05 mmol, 1.53 equiv.), zinc (180 mg, 2.76 mmol, 2.05 equiv.), and $NiCl_2$(dppp) (38 mg, 0.07 mmol, 0.05 equiv.) in acetonitrile (8 mL) was stirred at 70°C for 1 h under argon. After cooling to room temperature, the reaction was diluted with DCM, filtered through Celite, and concentrated *in vacuo*. The crude was purified by flash chromatography with 10% ethyl acetate in hexanes. Evaporation of the solvent afforded a yellowish-white solid (200 mg, 42% yield).

R_f = 0.2 (1:9 EtOAc:hexanes).

^{1}H NMR (300 MHz, Chloroform-*d*): δ 9.15 (s, 1H), 9.11 (s, 1H), 7.88 (s, 1H), 7.78 (s, 1H), 4.98 (s, 1H), 0.97 (s, 9H), 0.15 (s, 6H).

^{13}C NMR (75 MHz, Chloroform-*d*): δ 157.36, 152.06, 150.09, 146.30, 130.97, 129.69, 118.91, 114.08, 65.68, 25.96, 18.43, -5.34.

HRMS (ESI-TOF) calc'd for $C_{15}H_{22}ClN_2OSi$ $[M+H]^+$: 309.1184; found 309.1187.

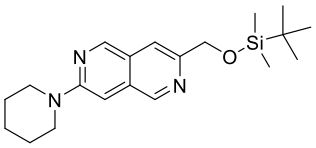

Compound **17**: A solution of compound **16b** (200 mg, 0.65 mmol, 1 equiv.), piperidine (0.32 mL, 3.25 mmol, 5 equiv.), and acetonitrile (5 mL) was heated in a sealed tube at 130°C for 12 h. After cooling to room temperature, the reaction was partitioned between water and ethyl acetate. The organic layer was dried with sodium sulfate and concentrated *in vacuo* to give a yellow-green solid (123 mg, 53% yield).

R_f = 0.2 (1:9 EtOAc:hexanes).

^{1}H NMR (300 MHz, Chloroform-*d*): δ 9.00 (s, 1H), 8.99 (s, 1H), 7.69 (s, 1H), 6.83 (s, 1H), 4.96 (s, 2H), 3.61 (d, *J* = 5.5 Hz, 4H), 1.73 (t, *J* = 3.9 Hz, 6H), 1.02 (s, 9H), 0.19 (s, 6H).

^{13}C NMR (75 MHz, Chloroform-*d*): δ 157.71, 151.76, 150.42, 150.03, 132.74, 124.77, 114.49, 97.07, 65.90, 47.07, 26.03, 25.46, 24.67, 18.51, -5.27.

HRMS (ESI-TOF) calc'd for $C_{20}H_{32}N_3OSi$ $[M+H]^+$: 358.2309; found 358.2312.

.

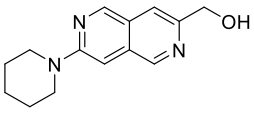

Compound **17a**: A solution of compound **17** (60 mg, 1 equiv.) in THF (2 mL) and aqueous HCl (2M, 1 mL) was stirred at room temperature for 12 h. Aqueous NaOH (2M, 1 mL) was added dropwise until pH neutral, and the mixture was extracted three times with ethyl acetate (15 mL). The organic layer was dried with sodium sulfate and concentrated *in vacuo* to give a yellow-green residue (85% yield).

R_f = 0.2 (1:1 EtOAc:hexanes).

^{1}H NMR (500 MHz, Chloroform-*d*): δ 9.02 (s, 1H), 8.96 (s, 1H), 7.54 (s, 1H), 6.81 (d, *J* = 2.7 Hz, 1H), 4.85 (s, 2H), 3.62 (s, 4H), 1.70 (s, 6H).

^{13}C NMR (126 MHz, Chloroform-*d*): δ 157.80, 150.43, 149.74, 133.06, 124.35, 115.69, 115.68, 96.90, 64.99, 46.94, 25.44, 24.64.

HRMS (ESI-TOF) calc'd for $C_{14}H_{18}N_3O$ $[M+H]^+$: 244.1444; found 244.1447.

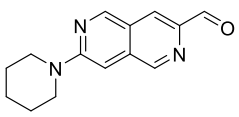

Compound **18:** To a 0.1M solution of **17a** (1 equiv.) in DCM was added MnO_2 (20 equiv.) at room temperature. After stirring for 24 hours, the reaction was filtered through Celite and concentrated *in vacuo*. The crude was purified by silica gel flash chromatography using 3:5 EtOAc:hexanes as the eluent. Concentration of the fractions resulted in a pale yellow solid (91% yield).

R_f = 0.52 (1:1 EtOAc:hexanes)

^{1}H NMR (500 MHz, Chloroform-d): δ 10.11 (s, 1H), 9.07 (s, 2H), 8.23 (s, 1H), 6.81 (1, 2H), 3.75 (m, 4H), 1.72 (m, 6H).

^{13}C NMR (126 MHz, Chloroform-d): δ 192.21, 158.70, 153.06, 151.12, 144.08, 135.95, 122.23, 121.90, 96.10, 46.39, 25.49, 24.63.

HRMS (ESI-TOF) calc'd for $C_{14}H_{16}N_3O$ $[M+H]^+$: 242.1288; found 242.1290.

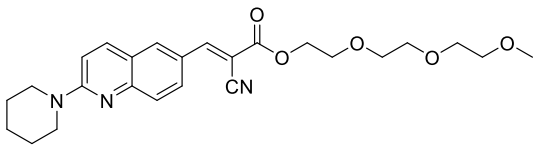

QN1: Following General Procedure A with Compound **3** on a 0.21 mmol scale dissolved in EtOH and heated to reflux for 1 h. After cooling to room temperature, the solvent was evaporated. The crude mixture was diluted in DCM and purified by preparative TLC with 100% EtOAc as the developing solvent to afford bright-yellow crystals (87% yield).

R_f = 0.22 (1:1 EtOAc:hexanes).

^{1}H NMR (400 MHz, Chloroform-*d*): δ 8.28 (s, 1H), 8.22 (s, 1H), 8.14 (d, *J* = 8.8 Hz, 1H), 7.87 (d, *J* = 9.3 Hz, 1H), 7.63 (d, *J* = 8.8 Hz, 1H), 7.01 (d, *J* = 9.3 Hz, 1H), 4.47 (s, 2H), 3.83 (s, 6H), 3.73 (s, 2H), 3.68 (s, 4H), 3.55 (s, 2H), 3.37 (s, 3H), 1.68 (s, 6H).

^{13}C NMR (101 MHz, Chloroform-*d*): δ 163.59, 158.59, 155.29, 151.79, 138.46, 133.40, 131.01, 127.36, 124.90, 122.31, 116.61, 110.67, 98.90, 72.16, 71.07, 70.89, 70.82, 69.04, 65.68, 59.29, 46.21, 26.13, 24.99.

HRMS (ESI-TOF) calc'd for $C_{25}H_{31}N_3O_5$ $[M+Na]^+$: 476.2156; found 476.2159.

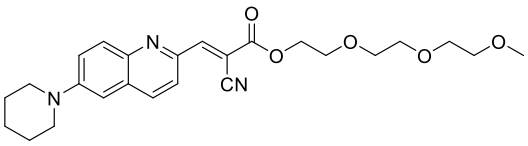

QN2: Following General Procedure A with Compound **9** on a 0.14 mmol scale, neat, and subjected to microwave radiation (Biotage Initiator™) for 15 min at 95°C. The crude mixture was diluted in DCM and purified by preparative TLC with 100% EtOAc as the developing solvent to afford a dark-red semisolid (93% yield).

R_f = 0.27 (1:1 EtOAc:hexanes).

^{1}H NMR (400 MHz, Chloroform-*d*): δ 8.40 (s, 1H), 7.98 (d, *J* = 7.5 Hz, 3H), 7.52 (d, *J* = 12.3 Hz, 1H), 6.94 (s, 1H), 4.48 (s, 2H), 3.83 (s, 2H), 3.73 (s, 2H), 3.67 (s, 4H), 3.56 (s, 2H), 3.41 (s, 4H), 3.35 (s, 3H), 1.73 (s, 4H), 1.68 (s, 2H).

^{13}C NMR (101 MHz, Chloroform-*d*): δ 154.91, 151.58, 146.05, 134.51, 131.43, 131.01, 123.28, 122.92, 115.57, 107.02, 72.15, 71.07, 70.88, 70.81, 68.96, 65.95, 59.27, 49.64, 25.74, 24.52.

HRMS (ESI-TOF) calc'd for $C_{25}H_{31}N_3O_5$ $[M+Na]^+$: 476.2156, found 476.2155.

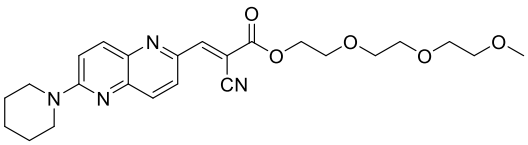

NTD: Following General Procedure A with Compound **12** on a 0.35 mmol scale in EtOH and heated to reflux for 1 h. The crude mixture was diluted in DCM and purified by preparative TLC with 100% EtOAc as the developing solvent to afford a yellow-green solid (91% yield).

R_f = 0.18 (1:1 EtOAc:hexanes).

^{1}H NMR (400 MHz, Chloroform-*d*): δ 8.37 (d, *J* = 2.0 Hz, 1H), 8.06 (dd, *J* = 10.4, 8.4 Hz, 2H), 7.91 (d, *J* = 8.7 Hz, 1H), 7.24 (s, 1H), 4.49 (t, *J* = 4.7 Hz, 2H), 3.83 (d, *J* = 5.0 Hz, 6H), 3.76 – 3.72 (m, 2H), 3.68 (td, *J* = 5.6, 2.9 Hz, 4H), 3.58 – 3.53 (m, 2H), 3.37 (d, *J* = 2.1 Hz, 3H), 1.75 – 1.68 (m, 6H).

^{13}C NMR (101 MHz, Chloroform-*d*): δ 162.93, 157.96, 154.07, 145.50, 144.65, 140.68, 138.91, 133.61, 126.88, 115.53, 114.42, 103.91, 72.16, 71.08, 70.89, 70.82, 68.97, 65.95, 59.28, 46.40, 26.16, 24.91.

HRMS (ESI-TOF) calc'd for $C_{24}H_{30}N_4O_5$ $[M+Na]^+$: 477.2108; found 477.2117.

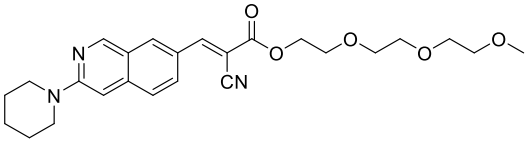

iQN1: Following General Procedure A with Compound **6** on a 0.31 mmol scale in EtOH and heated to reflux for 1 h. The crude mixture was diluted in DCM and purified by preparative TLC with 100% EtOAc as the developing solvent to afford a red solid (87% yield).

R_f = 0.53 (neat EtOAc).

^{1}H NMR (400 MHz, Chloroform-*d*): δ 8.94 (s, 1H), 8.22 (dd, *J* = 20.3, 10.3 Hz, 3H), 7.52 (d, *J* = 8.9 Hz, 1H), 6.70 (s, 1H), 4.47 (s, 2H), 3.83 (s, 2H), 3.69 (s, 10H), 3.56 (s, 2H), 3.37 (d, *J* = 4.2 Hz, 3H), 1.70 (s, 6H).

^{13}C NMR (101 MHz, Chloroform-*d*): δ 163.47, 158.34, 154.79, 153.83, 141.31, 135.82, 129.45, 126.23, 125.73, 121.96, 116.52, 99.28, 97.72, 72.16, 71.06, 70.89, 70.82, 69.02, 65.75, 59.29, 46.70, 25.77, 24.93.

HRMS (ESI-TOF) calc'd for $C_{25}H_{31}N_3O_5$ $[M+Na]^+$: 476.2156; found 476.2160.

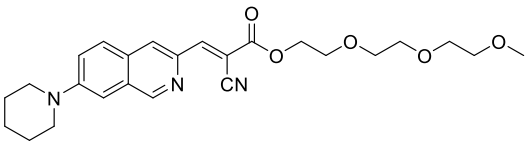

iQN2: Following General Procedure A with Compound **15** on a 0.13 mmol scale in EtOH and heated to reflux for 1 h. The crude mixture was diluted in DCM and purified by preparative TLC with 100% EtOAc as the developing solvent to afford a red solid that turns darker upon standing (56% yield).

R_f = 0.44 (neat EtOAc).

^{1}H NMR (400 MHz, Chloroform-*d*): δ 9.12 (s, 1H), 8.35 (s, 1H), 8.11 (s, 1H), 7.77 (d, *J* = 9.1 Hz, 1H), 7.49 (dd, *J* = 9.2, 2.5 Hz, 1H), 7.16 (d, *J* = 2.4 Hz, 1H), 4.50 – 4.46 (m, 2H), 3.84 (dd, *J* = 5.7, 4.1 Hz, 2H), 3.76 – 3.71 (m, 2H), 3.68 (ddd, *J* = 9.5, 4.3, 2.0 Hz, 4H), 3.58 – 3.54 (m, 2H), 3.44 (t, *J* = 5.3 Hz, 4H), 3.37 (s, 3H), 1.79 – 1.66 (m, 6H).

^{13}C NMR (101 MHz, Chloroform-*d*): δ 163.46, 154.67, 152.72, 151.75, 140.97, 132.00, 129.42, 128.47, 126.77, 123.02, 116.02, 108.16, 101.70, 72.16, 71.09, 70.89, 70.81, 69.00, 65.80, 59.28, 49.49, 25.69, 24.49.

HRMS (ESI-TOF) calc'd for $C_{25}H_{31}N_3O_5$ $[M+H]^+$: 454.2336; found 454.2337

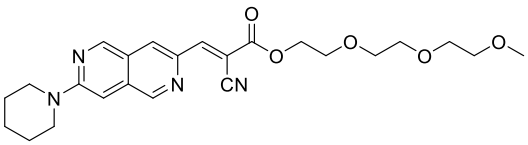

iNTD: Following General Procedure A with Compound **18** on a 0.22 mmol scale in EtOH and heated to reflux for 1 h. The crude mixture was diluted in DCM and purified by preparative TLC with 100% EtOAc as the developing solvent to afford a red solid that turns darker upon standing (66% yield).

R_f = 0.47 (neat EtOAc).

^{1}H NMR (400 MHz, Chloroform-*d*): δ 9.07 (s, 1H), 8.98 (s, 1H), 8.30 (s, 1H), 8.07 (s, 1H), 6.80 (s, 1H), 4.48 (s, 2H), 3.83 (s, 2H), 3.74 (s, 6H), 3.68 (s, 4H), 3.55 (s, 2H), 3.37 (s, 3H), 1.72 (s, 6H).

^{13}C NMR (126 MHz, Chloroform-*d*): δ 163.16, 158.66, 153.40, 152.46, 151.31, 140.19, 134.88, 126.20, 122.18, 115.69, 101.57, 96.78, 71.93, 70.86, 70.66, 70.59, 68.77, 65.64, 59.08, 46.38, 25.54, 24.62.

HRMS (ESI-TOF) calc'd for $C_{24}H_{30}N_4O_5$ $[M+Na]^+$: 477.2108; found 477.2105.

Spectral Data (1H and 13C NMR)

1.66
1.67
3.69
3.70
3.72
6.95
6.97
7.53
7.54
7.54
7.68
7.68
7.70
7.73
Br
N
N
5.85
3.89
1.00
1.77
1.78
f1 (ppm)

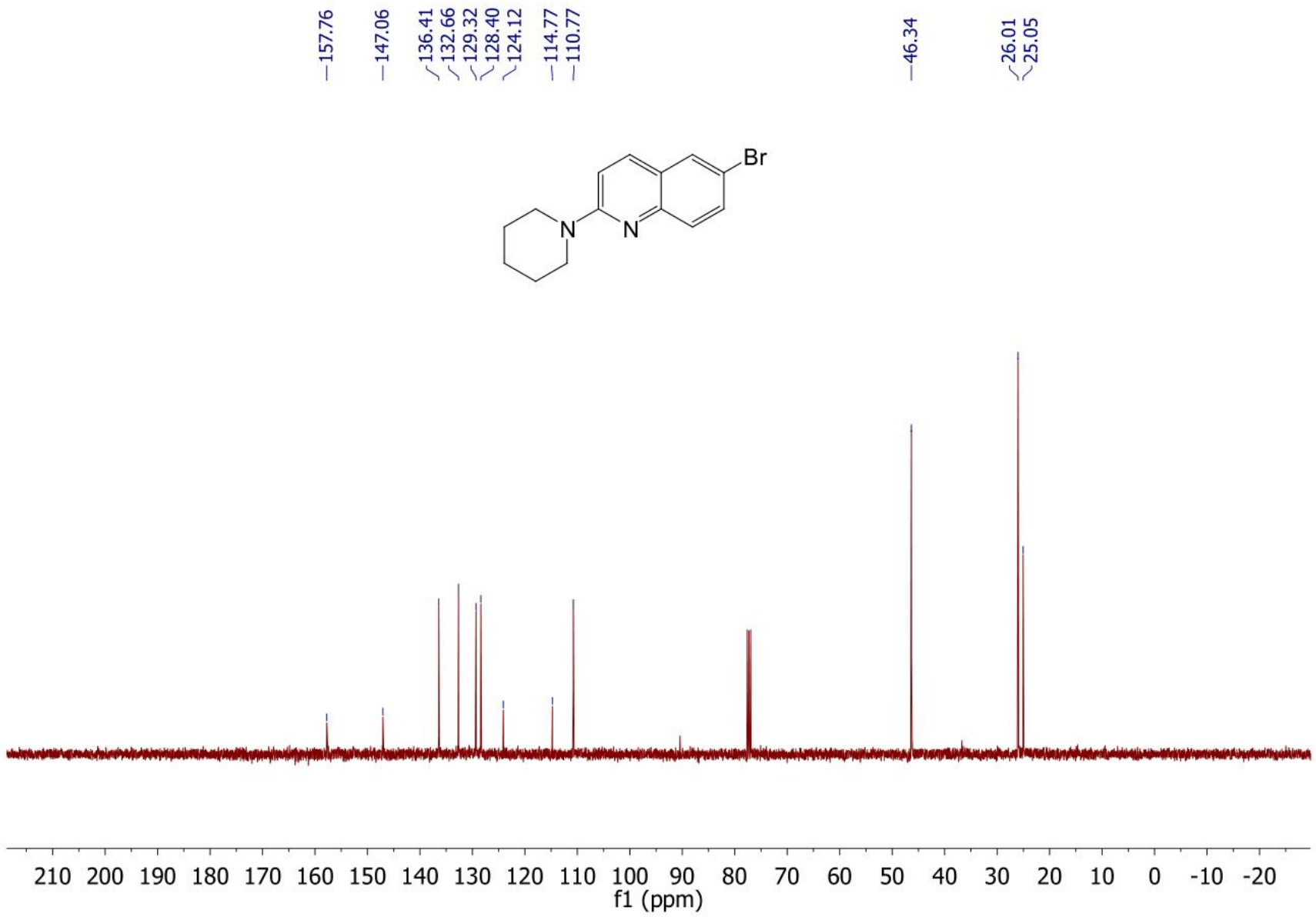
157.76
147.06
136.41
132.66
129.32
128.40
124.12
114.77
110.77
46.34
26.01
25.05
Br
N
N
210 200 190 180 170 160 150 140 130 120 110 100 90 80 70 60 50 40 30 20 10 0 -10 -20
f1 (ppm)

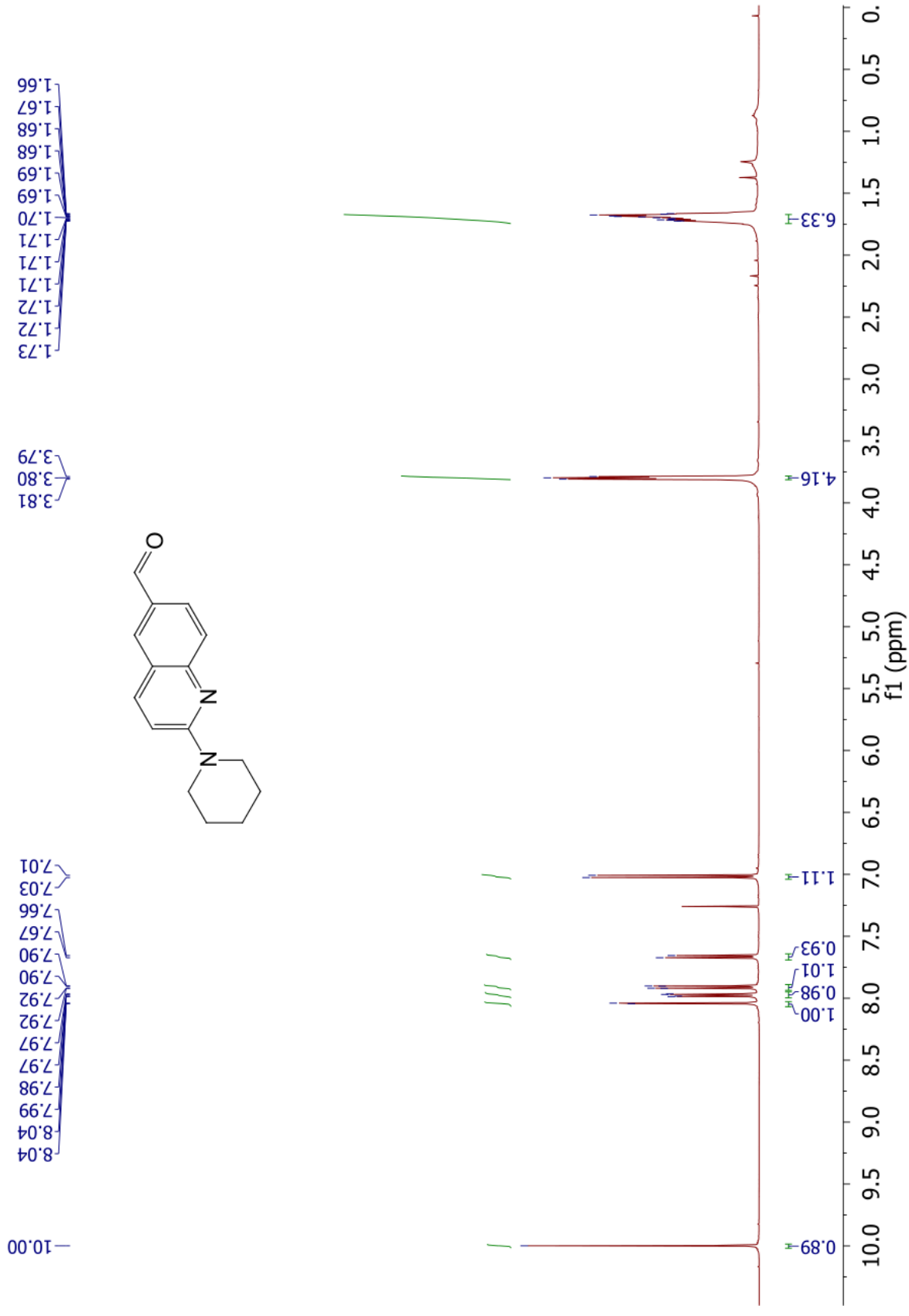
10.00
8.04
8.04
7.99
7.98
7.97
7.97
7.92
7.92
7.90
7.90
7.67
7.66
7.03
7.01
3.81
3.80
3.79
1.73
1.72
1.72
1.71
1.71
1.71
1.70
1.69
1.69
1.68
1.68
1.67
1.66
O
N
N
0.89
1.11
4.16
6.33
1.00
0.98
1.01
0.93
10.0
9.5
9.0
8.5
8.0
7.5
7.0
6.5
6.0
5.5
5.0
4.5
4.0
3.5
3.0
2.5
2.0
1.5
1.0
0.5
0.
f1 (ppm)

191.44
158.41
152.20
138.33
132.97
130.24
127.74
127.07
121.67
110.29
45.96
25.88
24.79
O
N
N
f1 (ppm)

8.28
8.22
8.16
8.13
7.88
7.86
7.64
7.62
7.02
7.00
4.47
3.83
3.73
3.68
3.55
3.37
1.68
O
O
O
O
O
O
O
CH3
N
N
6.15
2.84
2.00
4.15
2.26
6.17
2.05
1.12
1.00
1.07
1.08
1.03
1.11
f1 (ppm)

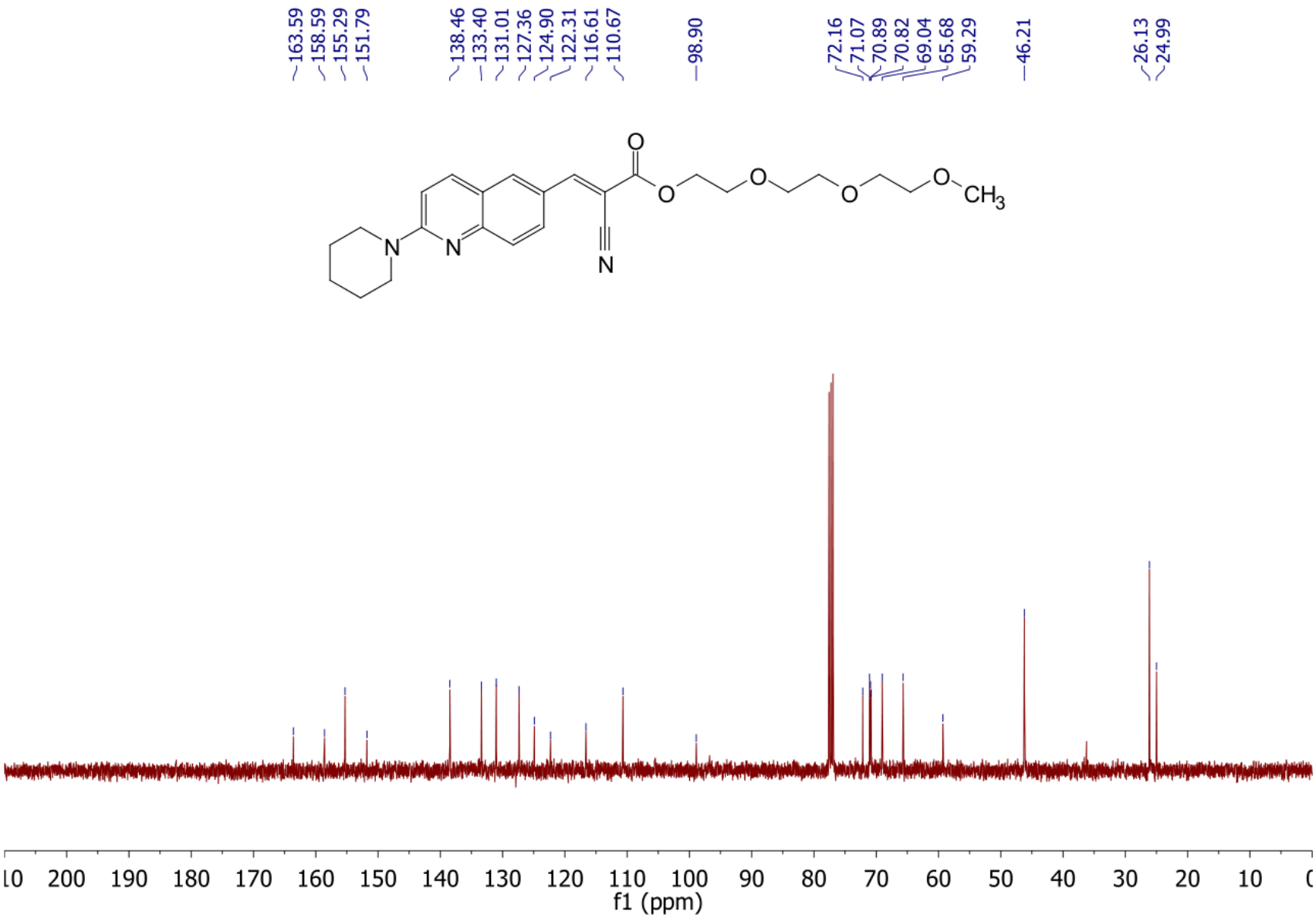
163.59
158.59
155.29
151.79
138.46
133.40
131.01
127.36
124.90
122.31
116.61
110.67
98.90
72.16
71.07
70.89
70.82
69.04
65.68
59.29
46.21
26.13
24.99
O
O
O
O
O
CH3
N
N
N
f1 (ppm)

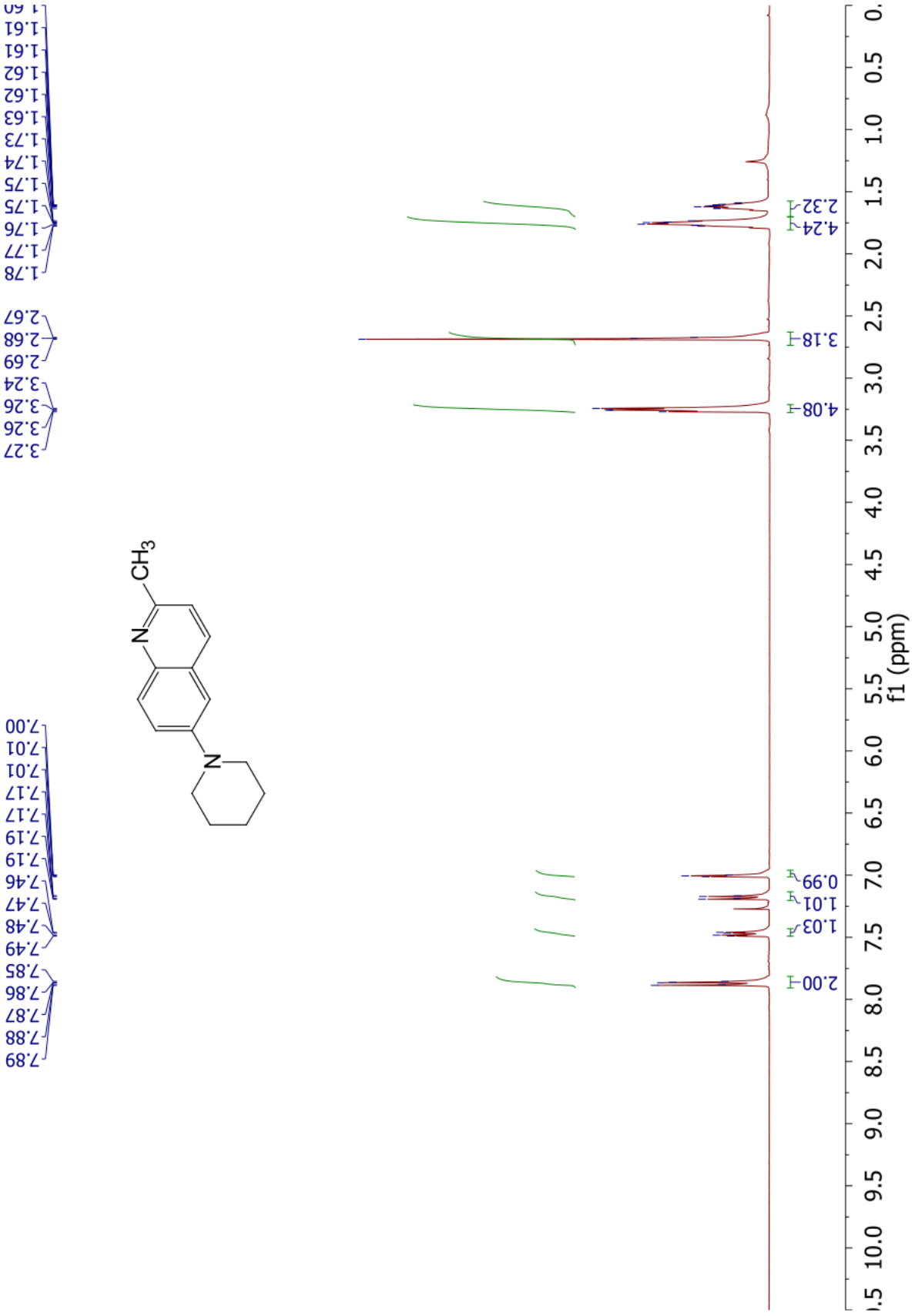
7.89
7.88
7.87
7.86
7.85
7.49
7.48
7.47
7.46
7.19
7.19
7.17
7.17
7.01
7.01
7.00
3.27
3.26
3.26
3.24
2.69
2.68
2.67
1.78
1.77
1.76
1.75
1.75
1.74
1.73
1.63
1.62
1.62
1.61
1.61
1.60
CH3
N
N
2.00
1.03
1.01
0.99
4.08
3.18
4.24
2.32
f1 (ppm)

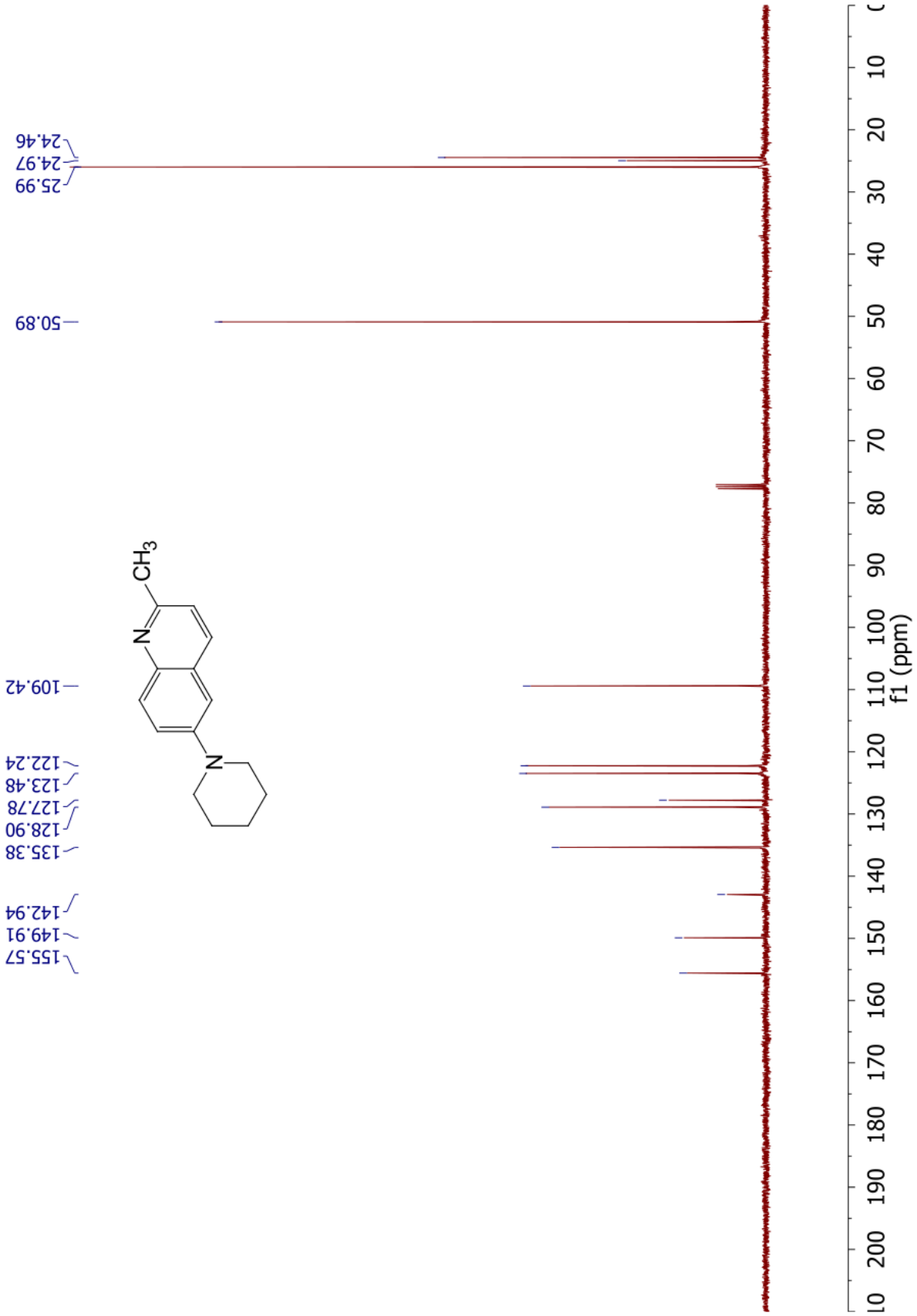
24.46
24.97
25.99
50.89
109.42
122.24
123.48
127.78
128.90
135.38
142.94
149.91
155.57
CH3
N
N
f1 (ppm)

10.13
10.13
8.05
8.03
8.03
8.01
8.01
7.92
7.90
7.58
7.57
7.56
7.55
7.00
7.00
3.43
3.41
3.40
1.78
1.77
1.76
1.75
1.75
1.74
1.73
1.73
1.72
1.70
1.70
1.69
1.68
1.68
1.67
1.67
1.66
O
N
N
0.74
2.00
0.93
1.09
1.11
4.34
4.15
2.22
f1 (ppm)

193.82
151.73
149.79
142.96
135.01
132.35
131.31
123.17
118.27
107.49
49.74
25.75
24.52
O
N
N
f1 (ppm)

8.40
7.99
7.97
7.54
7.51
6.94
4.48
3.83
3.73
3.67
3.56
3.41
3.35
1.73
1.68
0.93
2.85
1.06
1.00
2.00
2.04
3.91
2.01
4.04
0.03
2.90
4.34
2.04
f1 (ppm)

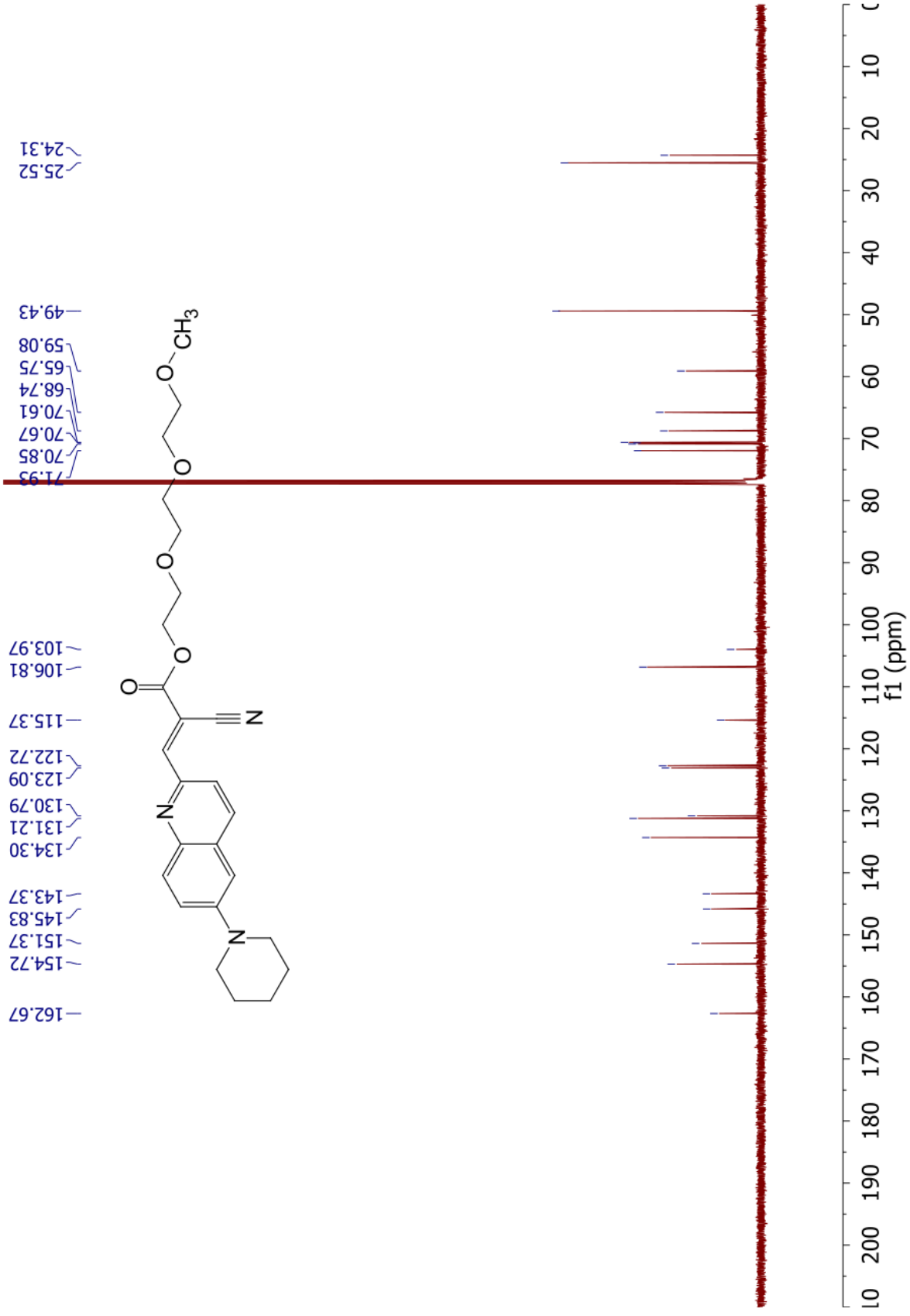
24.31
25.52
49.43
59.08
65.75
68.74
70.61
70.67
70.85
71.93
103.97
106.81
115.37
122.72
123.09
130.79
131.21
134.30
143.37
145.83
151.37
154.72
162.67
O
CH3
N
f1 (ppm)

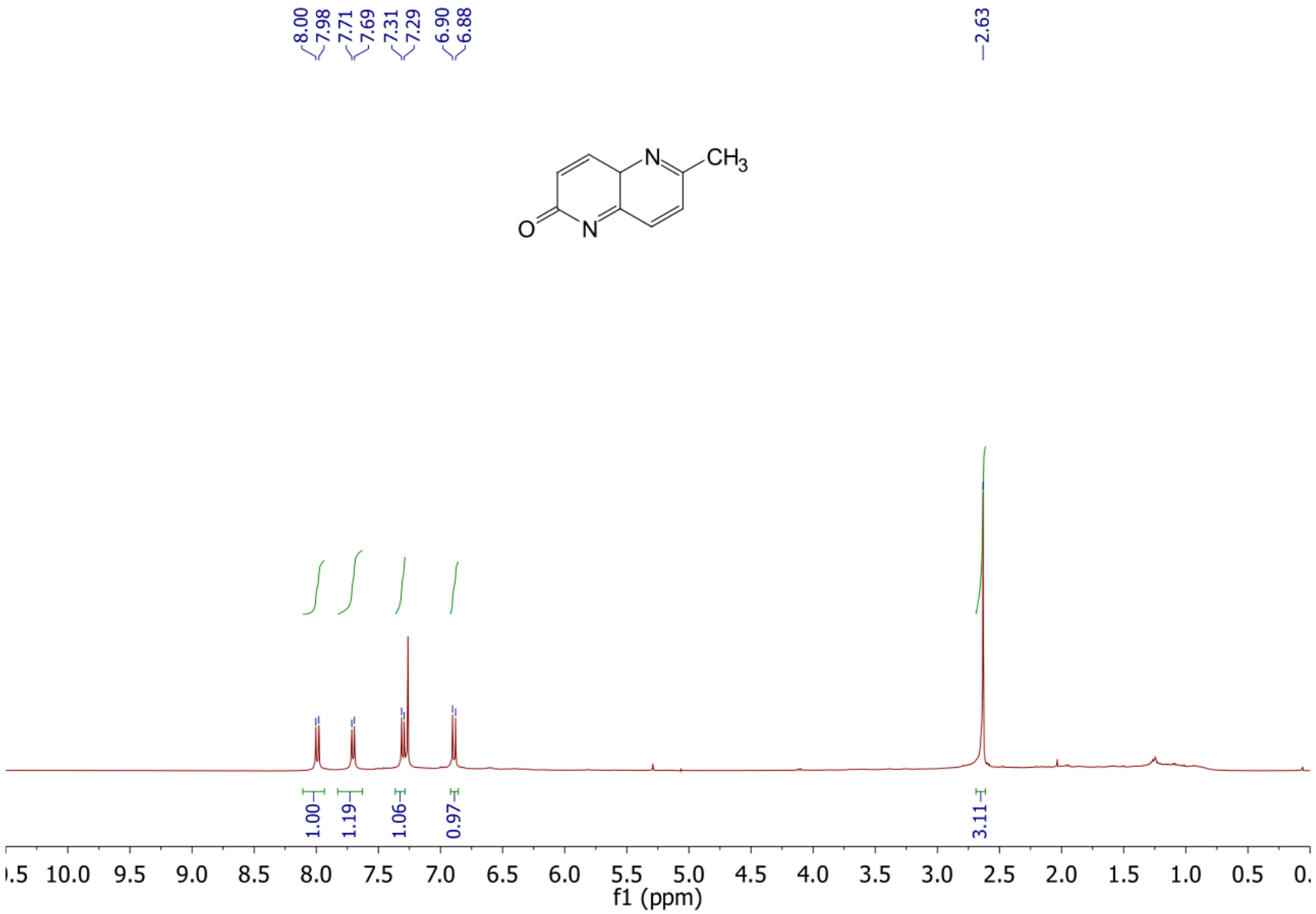
8.00
7.98
7.71
7.69
7.31
7.29
6.90
6.88
2.63
N
CH3
O
N
1.00
1.19
1.06
0.97
3.11
f1 (ppm)

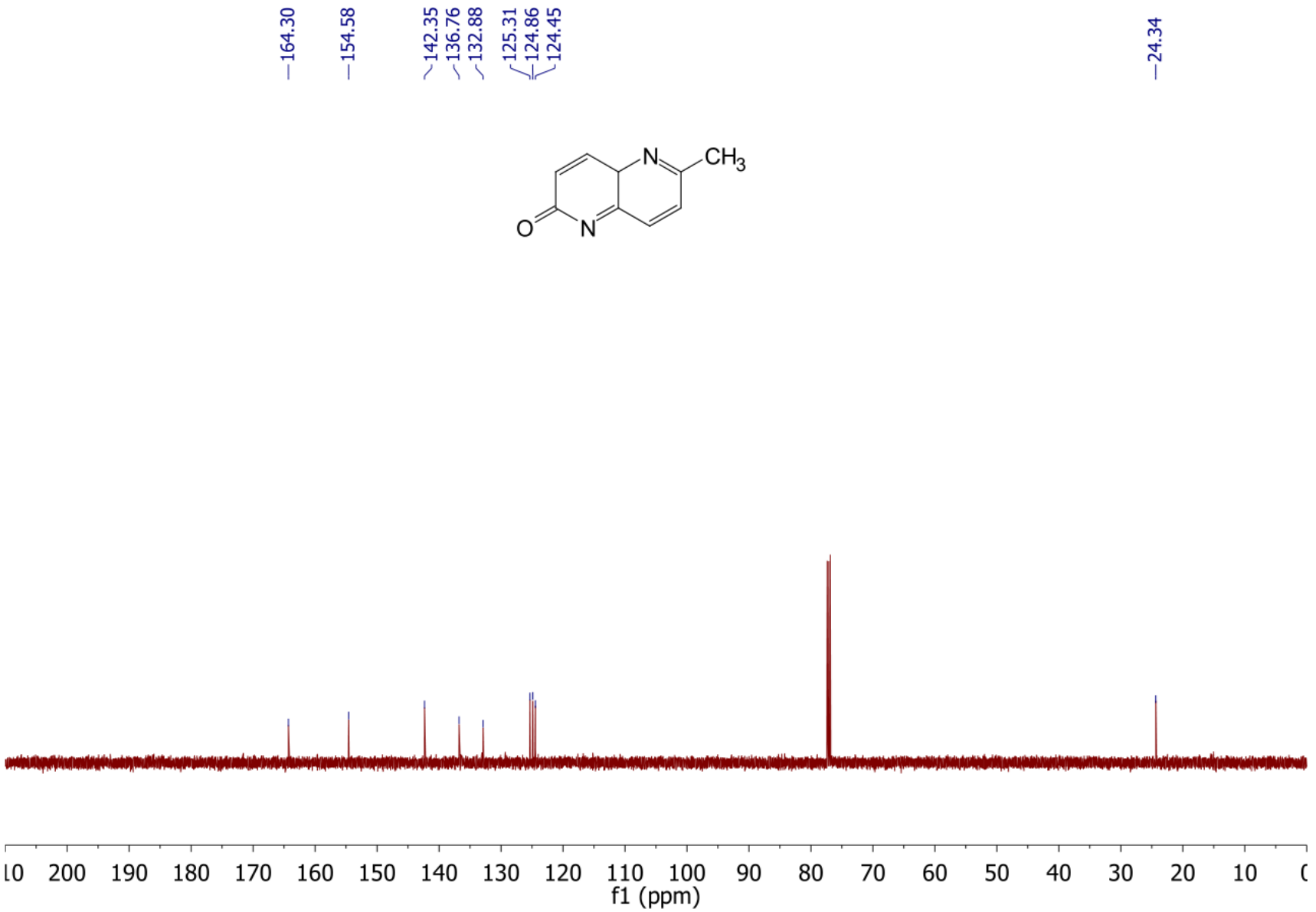
164.30
154.58
142.35
136.76
132.88
125.31
124.86
124.45
24.34
N
CH3
O
N
f1 (ppm)

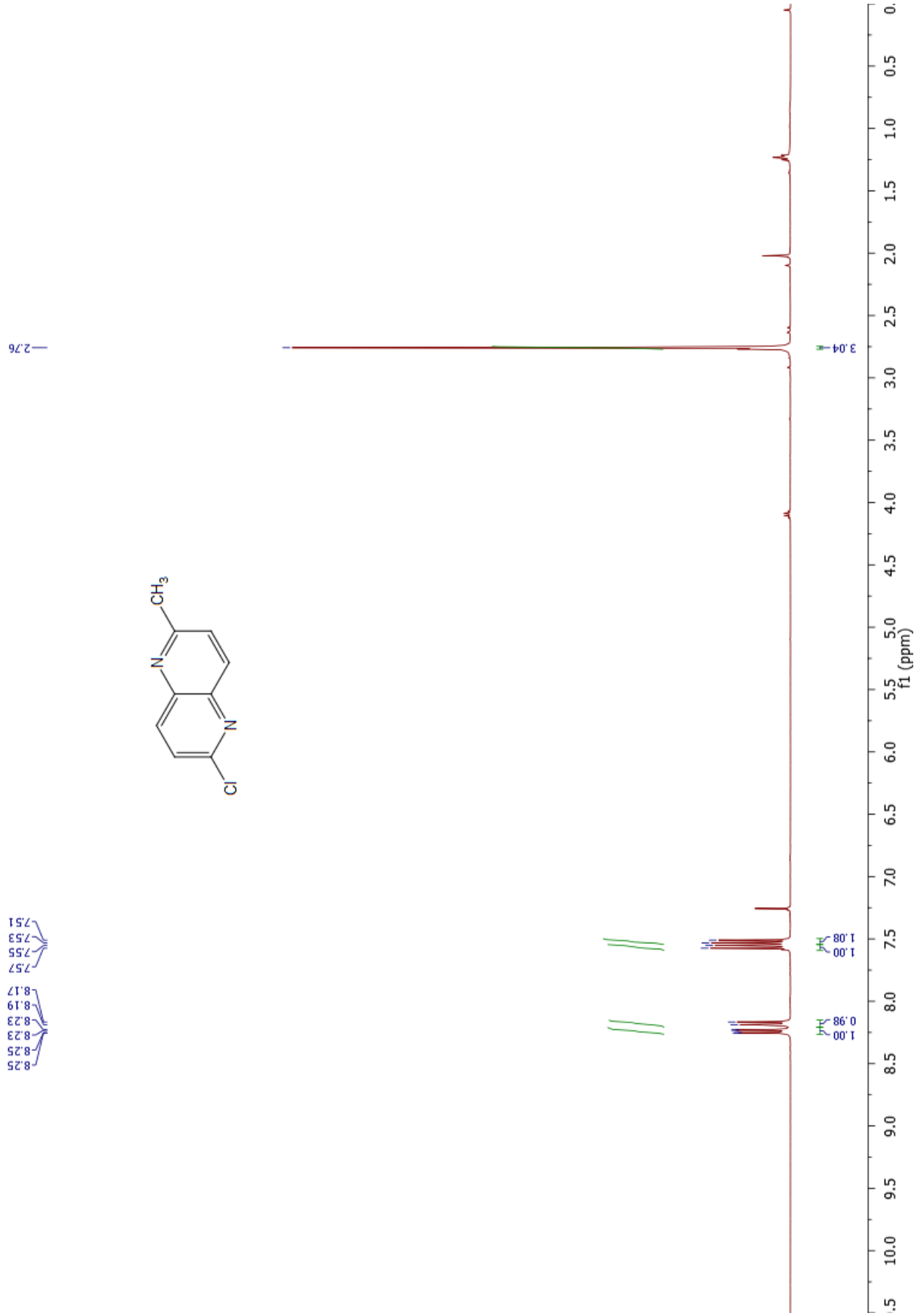
2.76
7.51
7.53
7.55
7.57
8.17
8.19
8.23
8.23
8.25
8.25
3.04
1.08
1.00
0.98
1.00
CH3
N
N
Cl
f1 (ppm)

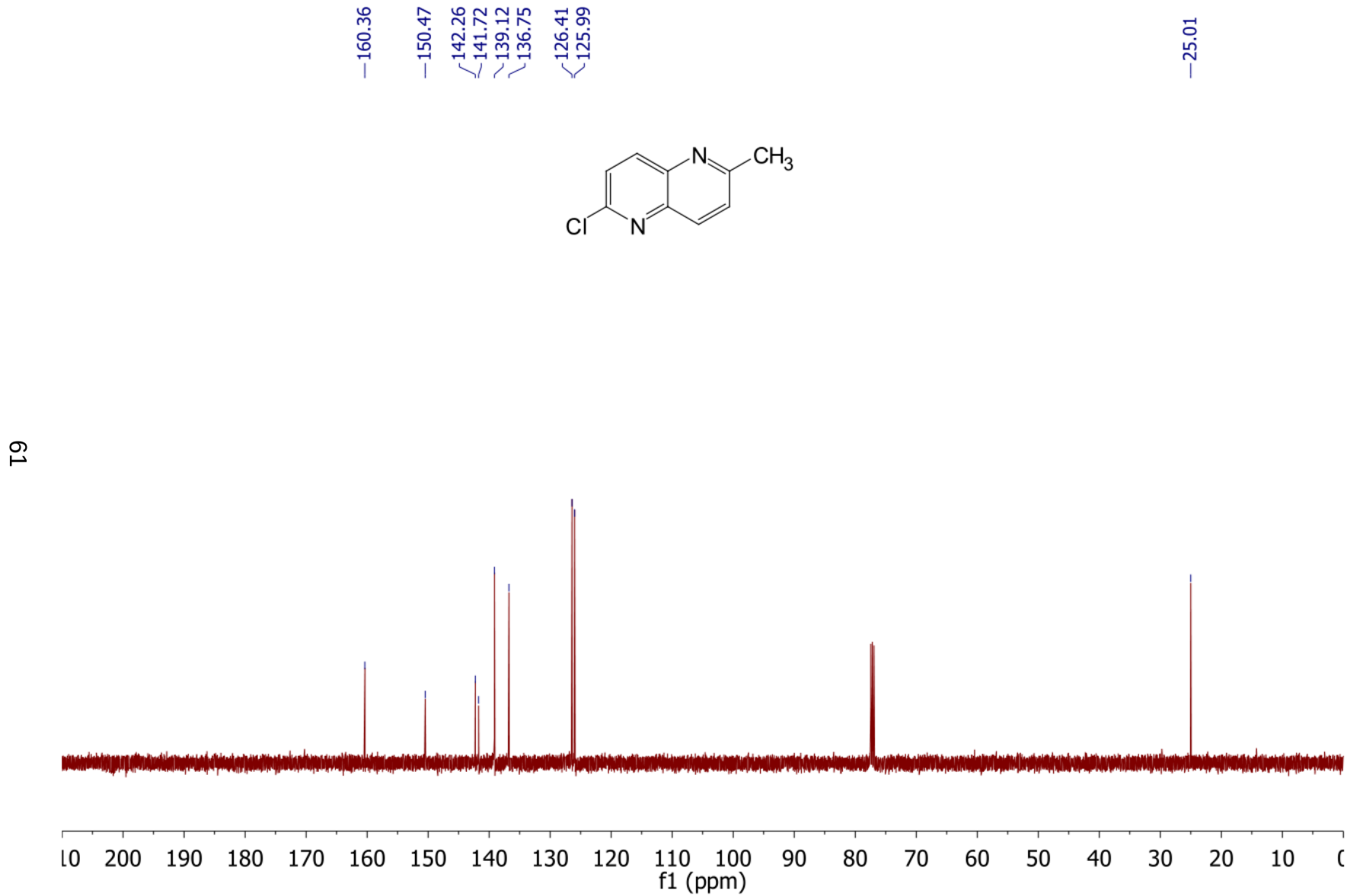
160.36
150.47
142.26
141.72
139.12
136.75
126.41
125.99
25.01
N
CH3
Cl
N
f1 (ppm)

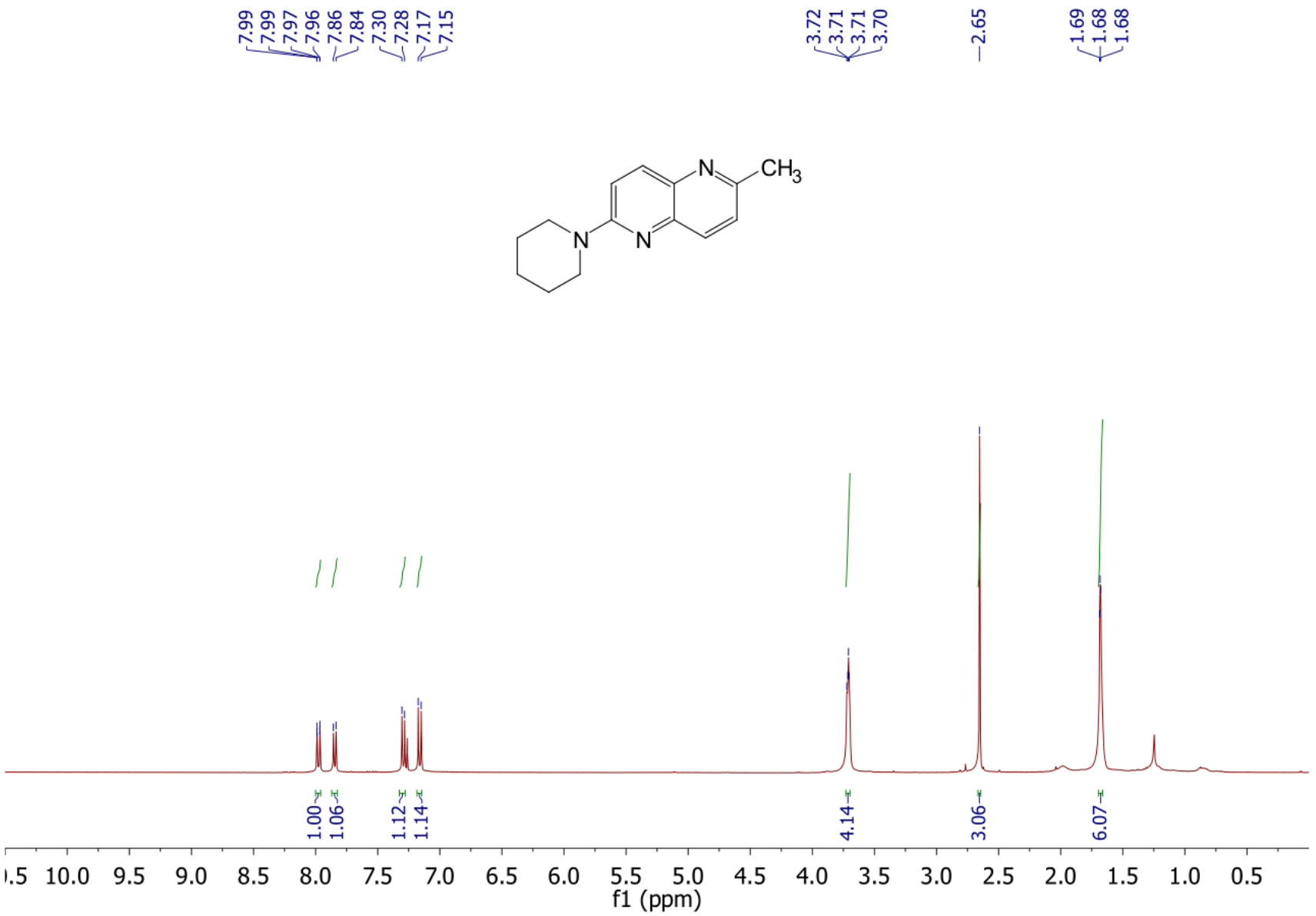
7.99
7.99
7.97
7.96
7.86
7.84
7.30
7.28
7.17
7.15
3.72
3.71
3.71
3.70
2.65
1.69
1.68
1.68
N
CH3
N
N
1.00
1.06
1.12
1.14
4.14
3.06
6.07
f1 (ppm)

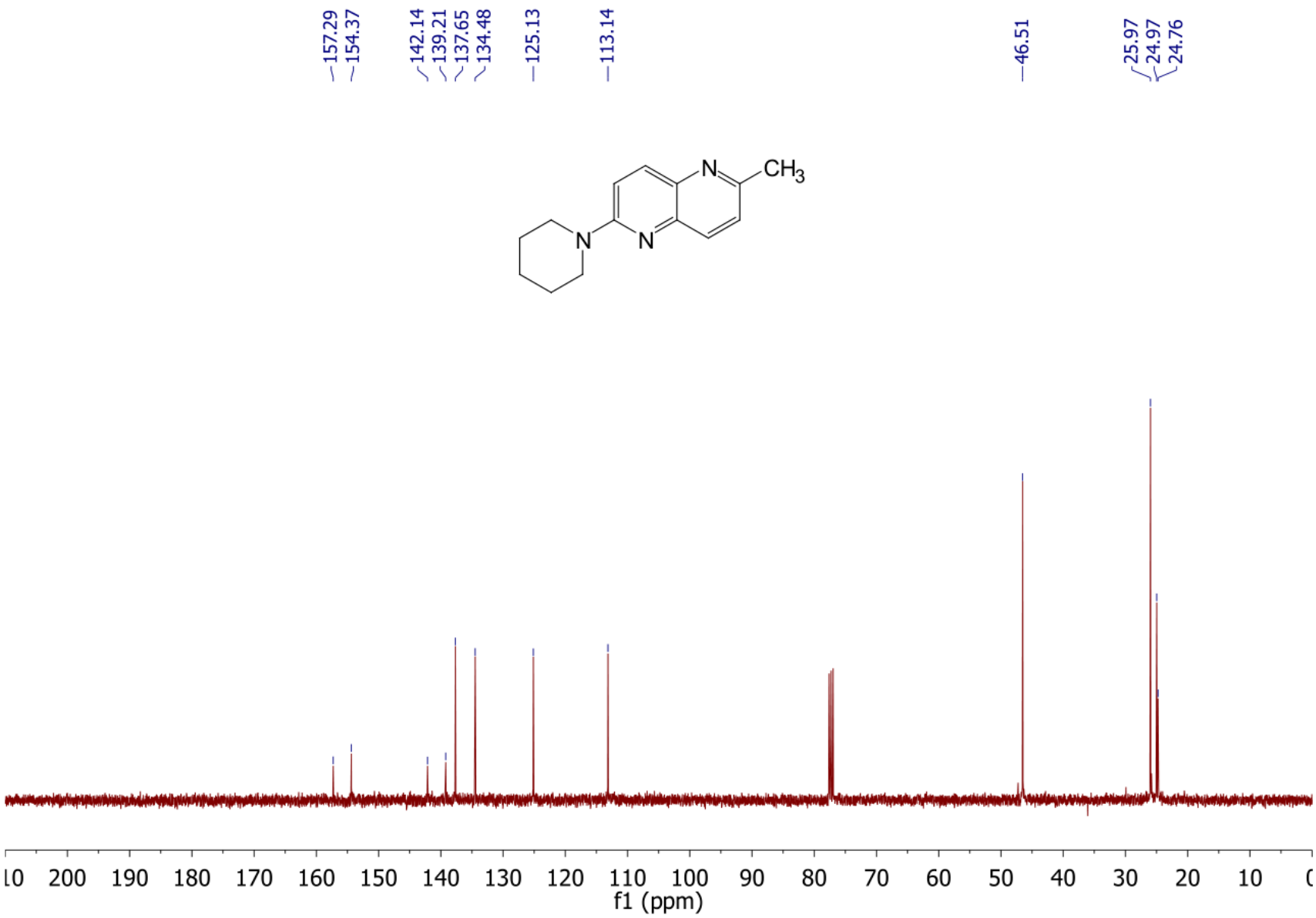
157.29
154.37
142.14
139.21
137.65
134.48
125.13
113.14
46.51
25.97
24.97
24.76
N
CH3
N
N
f1 (ppm)

10.11
8.12
8.09
8.07
8.04
7.97
7.94
7.28
3.85
3.83
3.82
1.73
1.72
1.70
1.00
1.99
1.02
1.08
4.15
6.35
f1 (ppm)

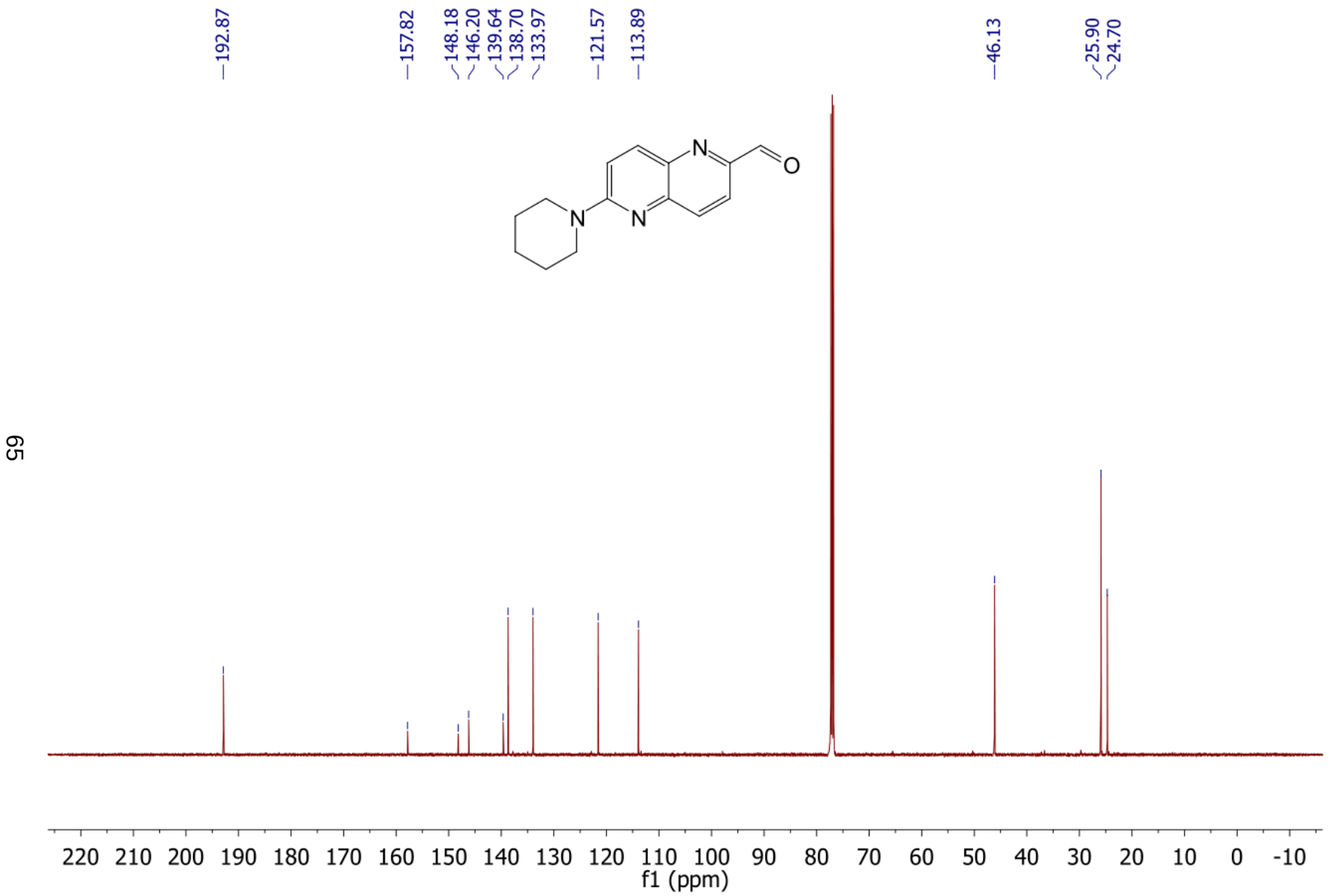
192.87
157.82
148.18
146.20
139.64
138.70
133.97
121.57
113.89
46.13
25.90
24.70
N
O
N
N
220 210 200 190 180 170 160 150 140 130 120 110 100 90 80 70 60 50 40 30 20 10 0 -10
f1 (ppm)

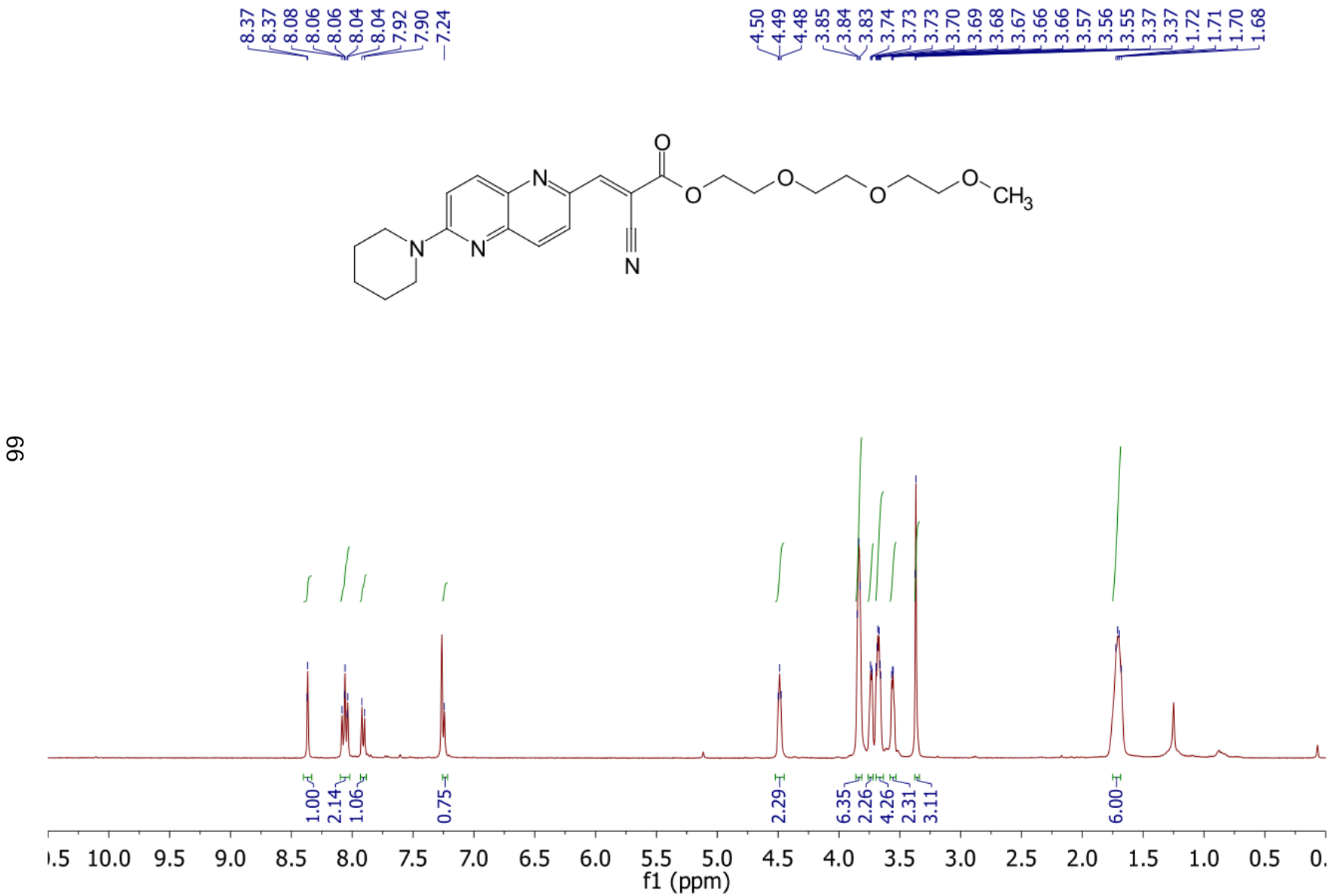
8.37
8.37
8.08
8.06
8.06
8.04
8.04
7.92
7.90
7.24
4.50
4.49
4.48
3.85
3.84
3.83
3.74
3.73
3.73
3.70
3.69
3.68
3.67
3.66
3.66
3.57
3.56
3.55
3.37
3.37
1.72
1.71
1.70
1.68
O
N
O
O
O
O
CH3
N
N
N
1.00
2.14
1.06
0.75
2.29
6.35
2.26
4.26
2.31
3.11
6.00
10.0
9.5
9.0
8.5
8.0
7.5
7.0
6.5
6.0
5.5
5.0
4.5
4.0
3.5
3.0
2.5
2.0
1.5
1.0
0.5
f1 (ppm)

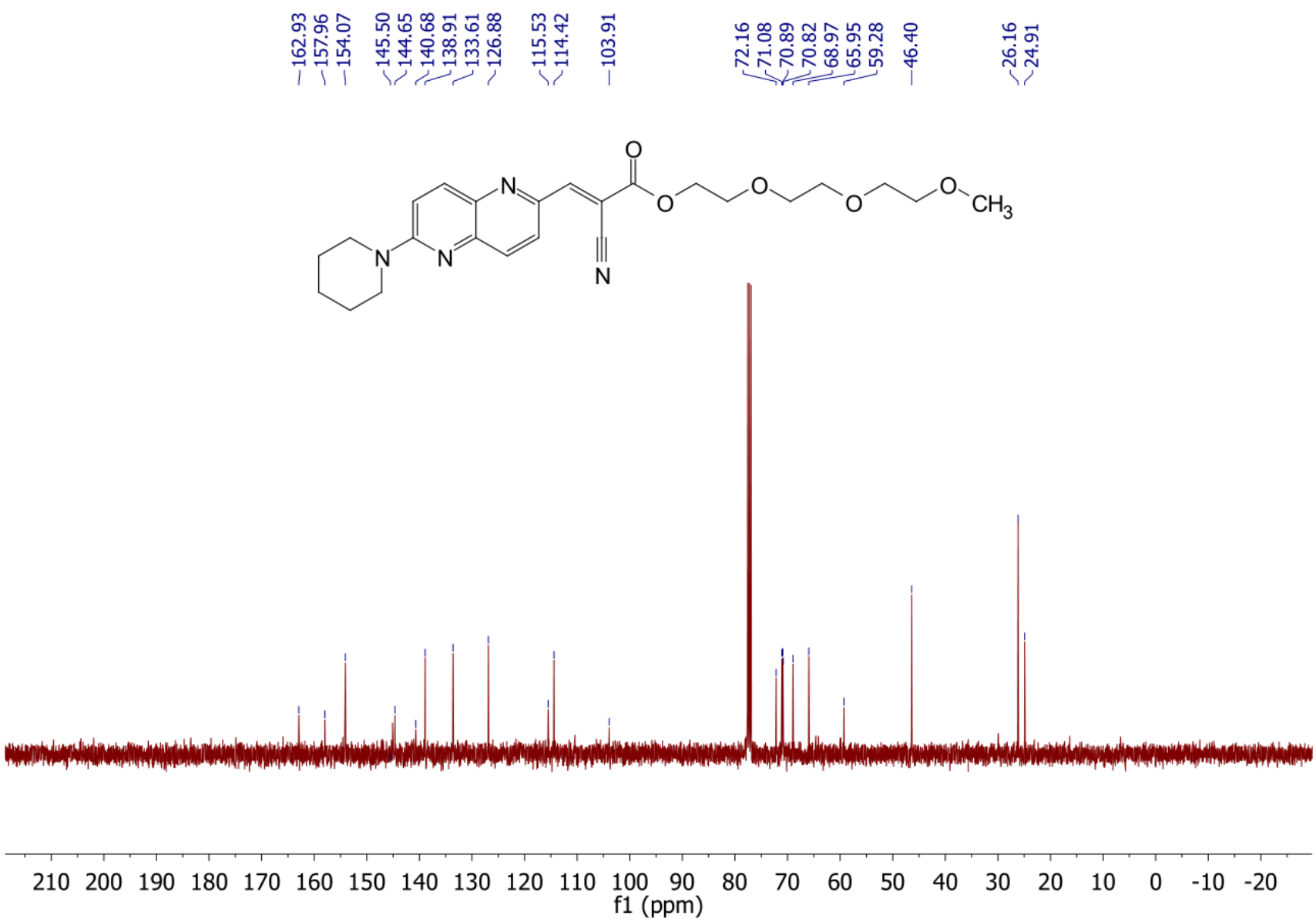
162.93
157.96
154.07
145.50
144.65
140.68
138.91
133.61
126.88
115.53
114.42
103.91
72.16
71.08
70.89
70.82
68.97
65.95
59.28
46.40
26.16
24.91
O
N
O
O
O
O
CH3
N
N
N
210 200 190 180 170 160 150 140 130 120 110 100 90 80 70 60 50 40 30 20 10 0 -10 -20
f1 (ppm)

8.83
7.89
7.88
7.51
7.51
7.51
7.49
7.49
7.48
7.42
7.40
6.70
3.59
3.57
3.56
1.72
1.71
1.70
1.69
Br
N
N
6.39
4.15
1.00
1.00
0.94
0.88
0.94
f1 (ppm)

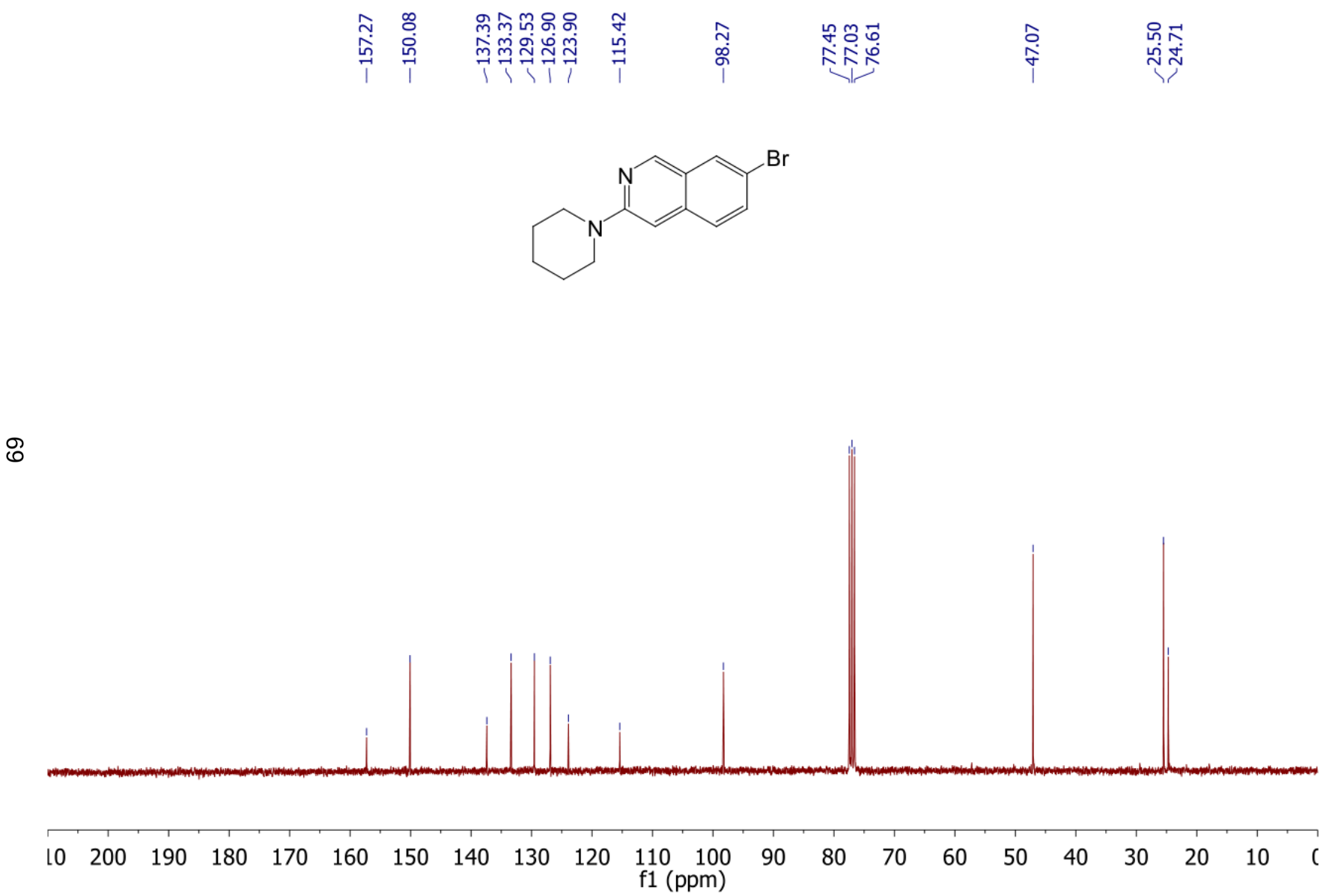
157.27
150.08
137.39
133.37
129.53
126.90
123.90
115.42
98.27
77.45
77.03
76.61
47.07
25.50
24.71
Br
N
N
69
f1 (ppm)

8.89
7.65
7.65
7.63
7.63
7.52
7.49
6.84
6.81
6.79
6.77
6.73
5.80
5.75
5.27
5.25
3.59
3.58
3.57
1.73
1.72
1.71
1.70
1.69
1.68
1.67
CH2
N
N
0.93
2.02
1.00
1.10
1.02
1.09
1.05
4.41
6.49
f1 (ppm)

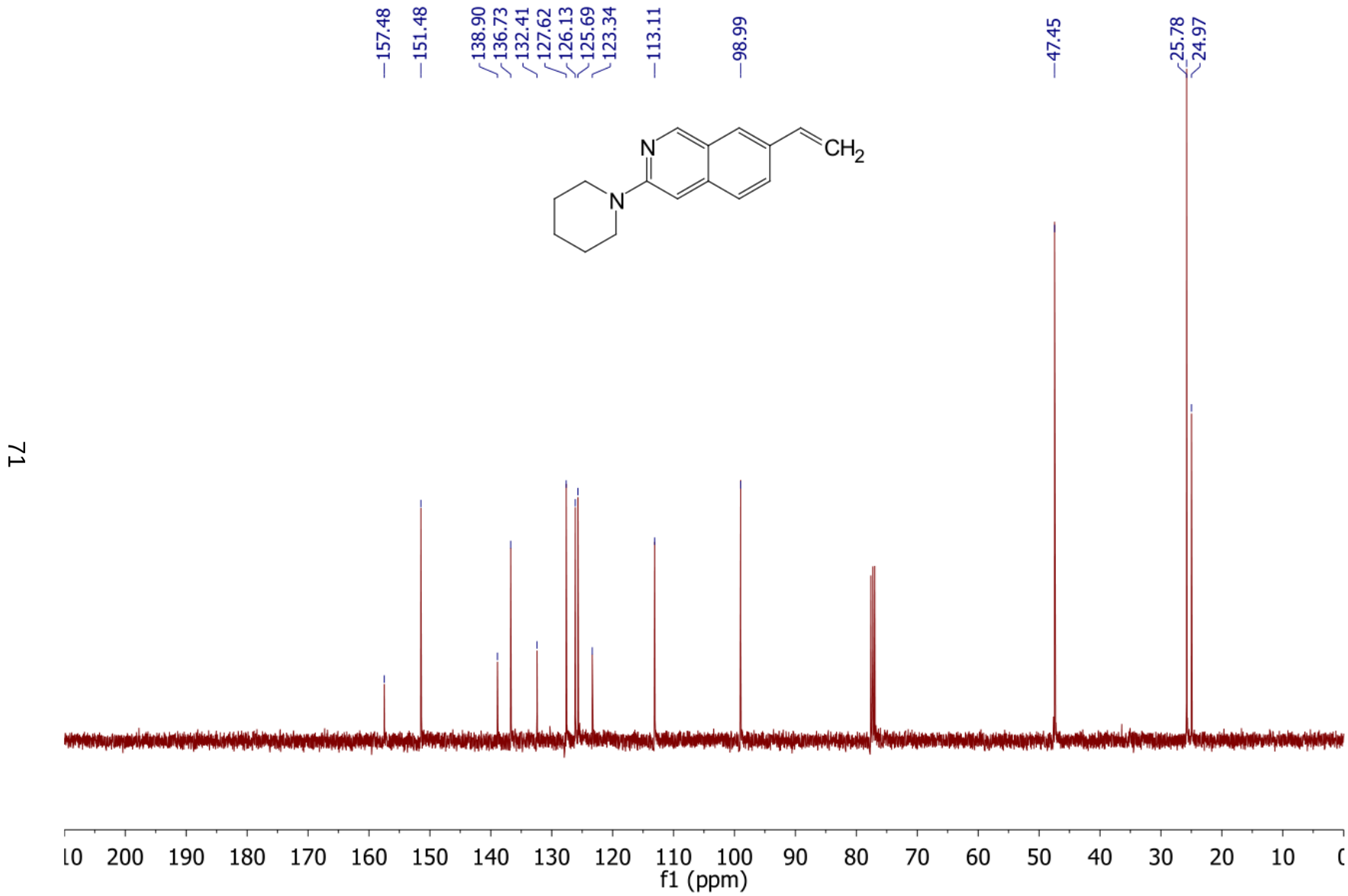
157.48
151.48
138.90
136.73
132.41
127.62
126.13
125.69
123.34
113.11
98.99
47.45
25.78
24.97
N
N
CH2
f1 (ppm)

71

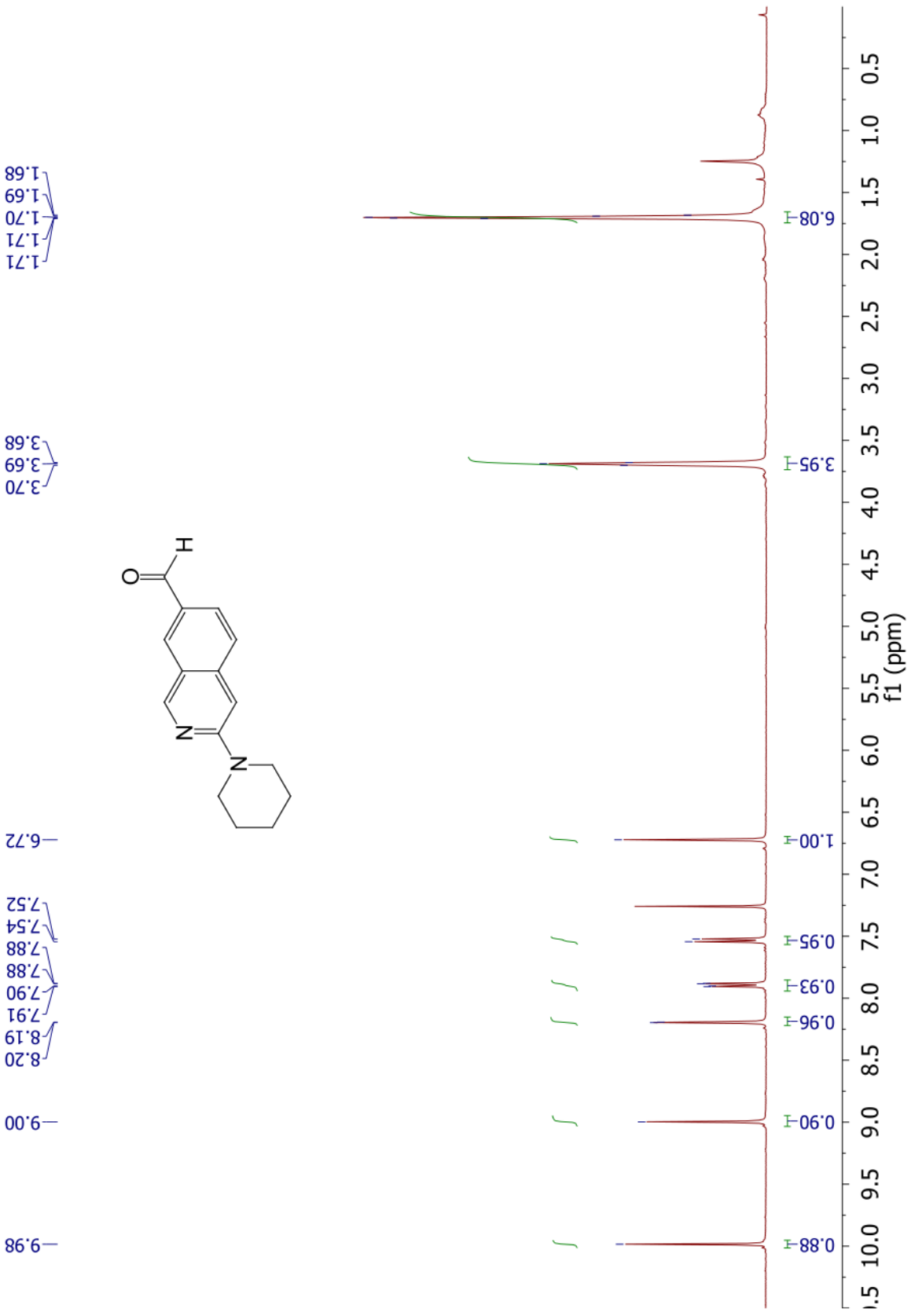
9.98
9.00
8.20
8.19
7.91
7.90
7.88
7.88
7.54
7.52
6.72
3.70
3.69
3.68
1.71
1.71
1.70
1.69
1.68
0.88
0.90
0.96
0.93
0.95
1.00
3.95
6.08
f1 (ppm)

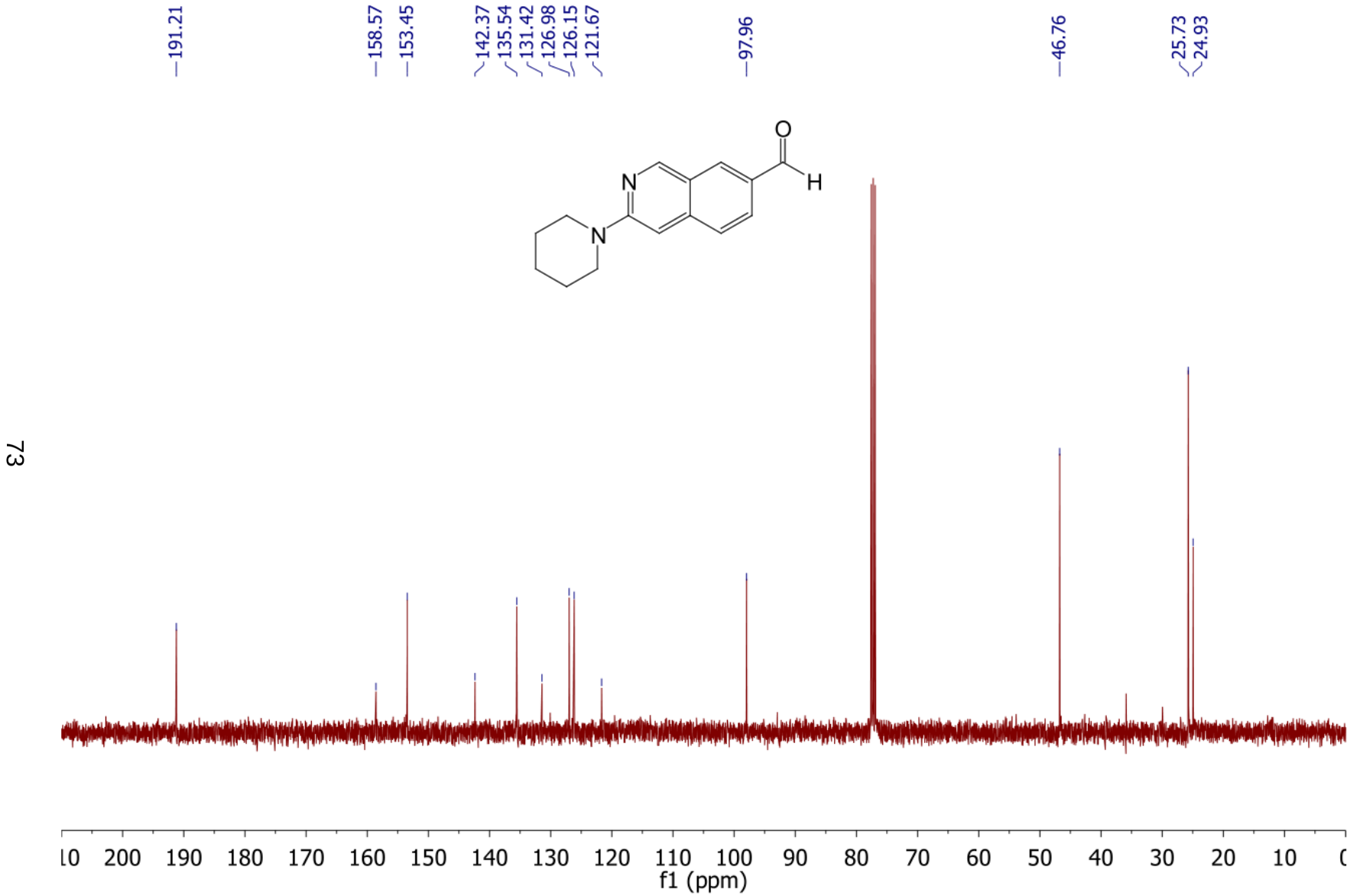
191.21
158.57
153.45
142.37
135.54
131.42
126.98
126.15
121.67
97.96
46.76
25.73
24.93
O
H
N
N
f1 (ppm)

O
O
O
O
O
O
O
CH3
N
N
N
6.27
3.05
9.81
2.05
2.03
1.01
1.05
2.87
1.00
11.5
10.5
9.5
8.5
7.5
6.5
5.5
4.5
3.5
2.5
1.5
0.5
-0.5
-1.5
f1 (ppm)

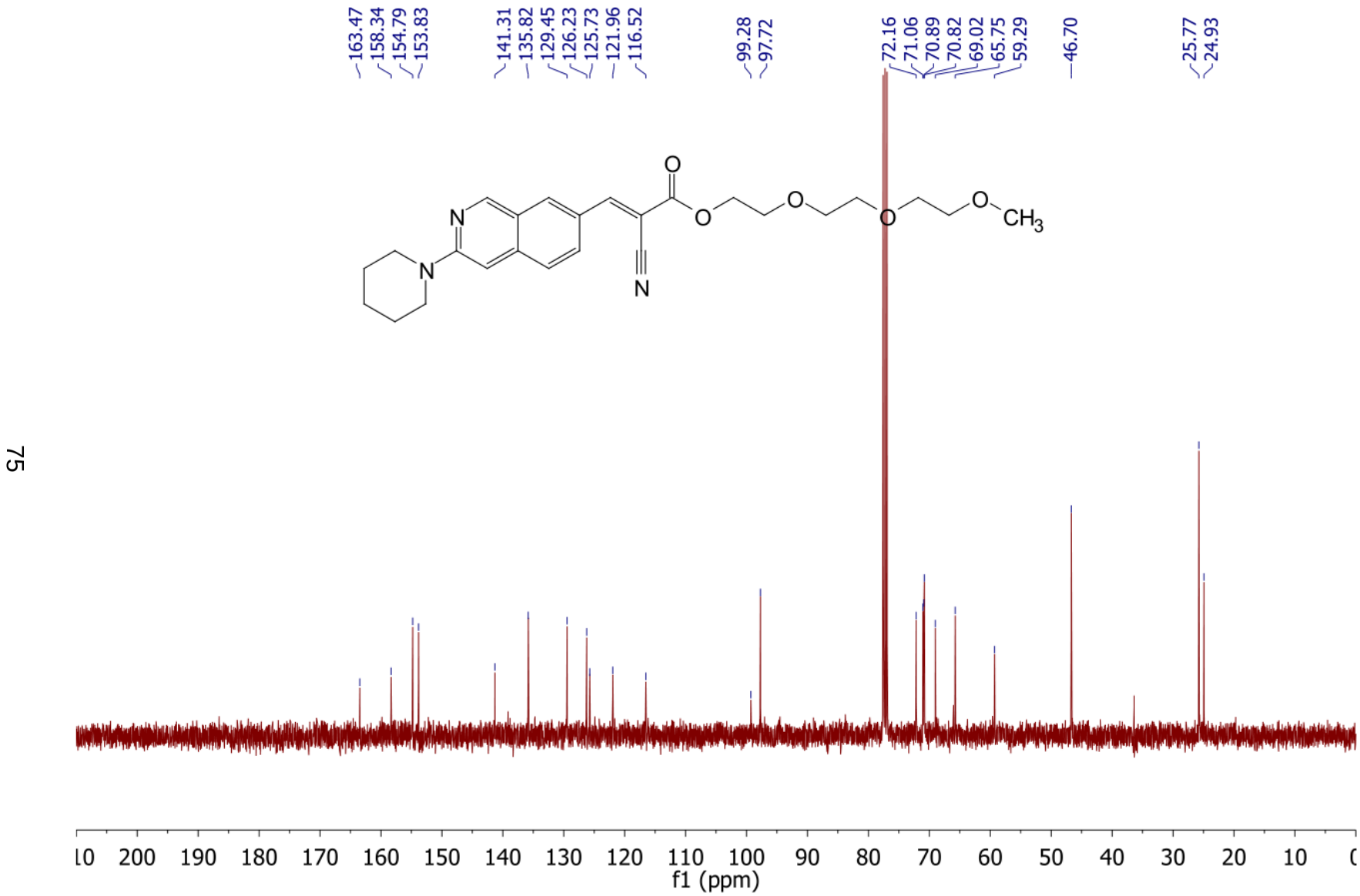
163.47
158.34
154.79
153.83
141.31
135.82
129.45
126.23
125.73
121.96
116.52
99.28
97.72
72.16
71.06
70.89
70.82
69.02
65.75
59.29
46.70
25.77
24.93
O
N
N
O
O
O
O
CH3
N
f1 (ppm)

f1 (ppm)
0.5
1.0
1.5
2.0
2.5
3.0
3.5
4.0
4.5
5.0
5.5
6.0
6.5
7.0
7.5
8.0
8.5
9.0
9.5
10.0
3.24
1.12
1.06
6.02
1.12
1.11
0.95
1.00
0.95
0.89
0.97
1.08
1.08
1.10
1.10
1.72
2.80
2.81
2.82
2.83
3.37
3.38
3.39
3.40
3.67
3.70
3.84
3.87
4.13
4.13
4.14
4.14
7.18
7.18
7.20
7.20
7.24
7.35
7.36
7.36
7.36
7.37
7.37
7.38
7.38
7.38
7.38
7.49
7.49
7.50
CH3
O
CH3
O
NH
H3C
Br

15.27
50.83
53.89
55.01
55.06
108.16
122.76
126.91
130.18
131.36
143.24
CH3
O
CH3
O
H3C
NH
Br
f1 (ppm)

2.68
9.10
8.08
8.08
8.08
7.72
7.71
7.69
7.68
7.62
7.59
7.45
CH3
N
Br
3.06
1.00
0.99
1.02
1.06
1.01
10.0
9.5
9.0
8.5
8.0
7.5
7.0
6.5
6.0
5.5
5.0
4.5
4.0
3.5
3.0
2.5
2.0
1.5
1.0
0.5
0.
f1 (ppm)

24.27
118.33
119.68
127.69
127.72
129.60
133.76
134.94
150.85
152.31
CH3
N
Br
f1 (ppm)

9.15
8.11
7.77
7.74
7.72
7.67
7.65
4.71
Br
N
Br
1.02
1.00
3.16
2.17
f1 (ppm)

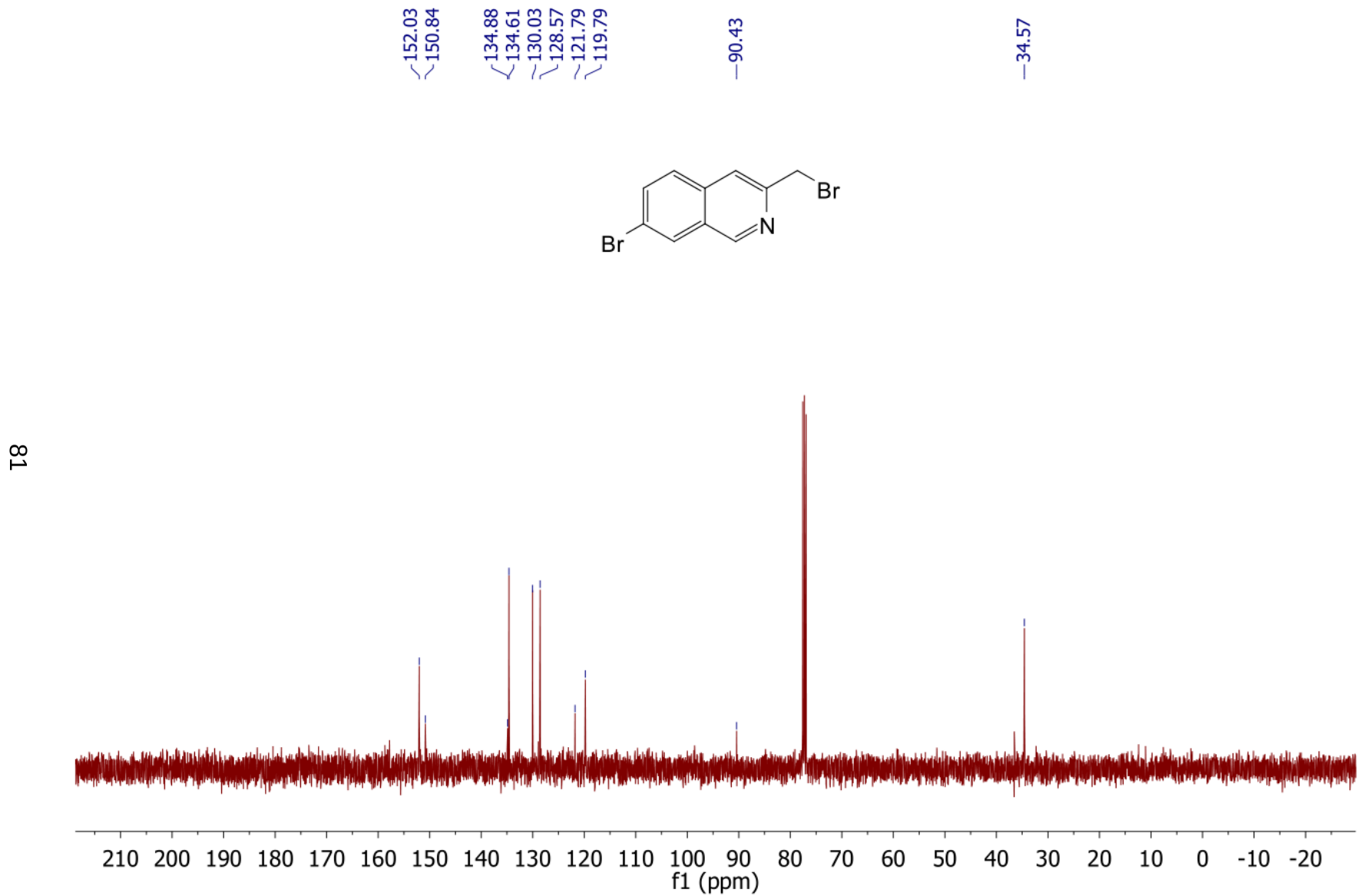
152.03
150.84
134.88
134.61
130.03
128.57
121.79
119.79
90.43
34.57
Br
Br
N
210 200 190 180 170 160 150 140 130 120 110 100 90 80 70 60 50 40 30 20 10 0 -10 -20
f1 (ppm)

9.15
8.14
8.13
8.13
7.78
7.77
7.75
7.75
7.70
7.68
7.64
4.91
1.68
OH
N
Br
1.00
0.92
2.80
2.09
1.08
f1 (ppm)

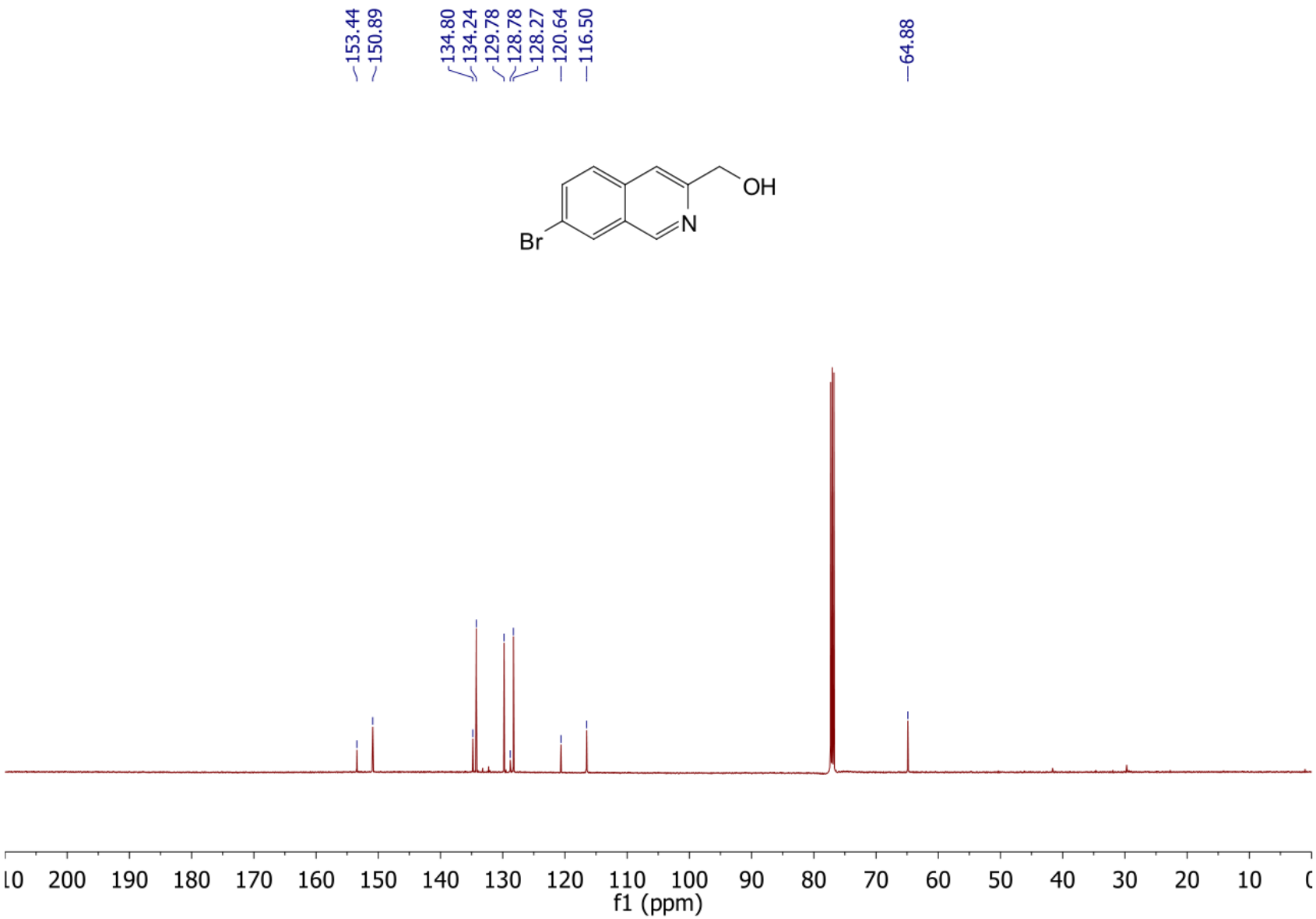
153.44
150.89
134.80
134.24
129.78
128.78
128.27
120.64
116.50
64.88
OH
N
Br
f1 (ppm)

10.26
9.31
8.36
8.25
7.90
1.00
1.13
1.06
1.06
1.96
f1 (ppm)
O
N
Br

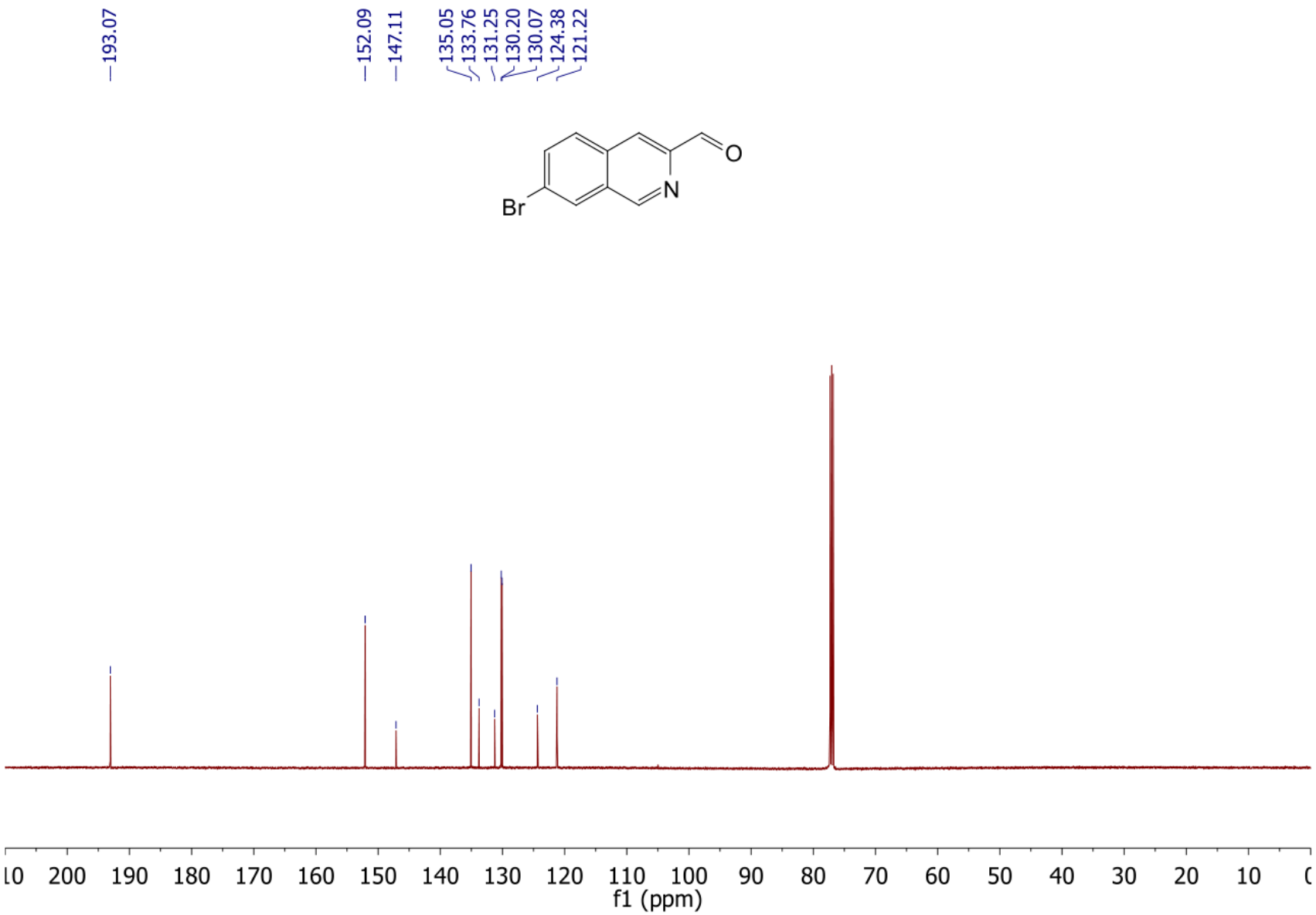
193.07
152.09
147.11
135.05
133.76
131.25
130.20
130.07
124.38
121.22
O
N
Br
f1 (ppm)

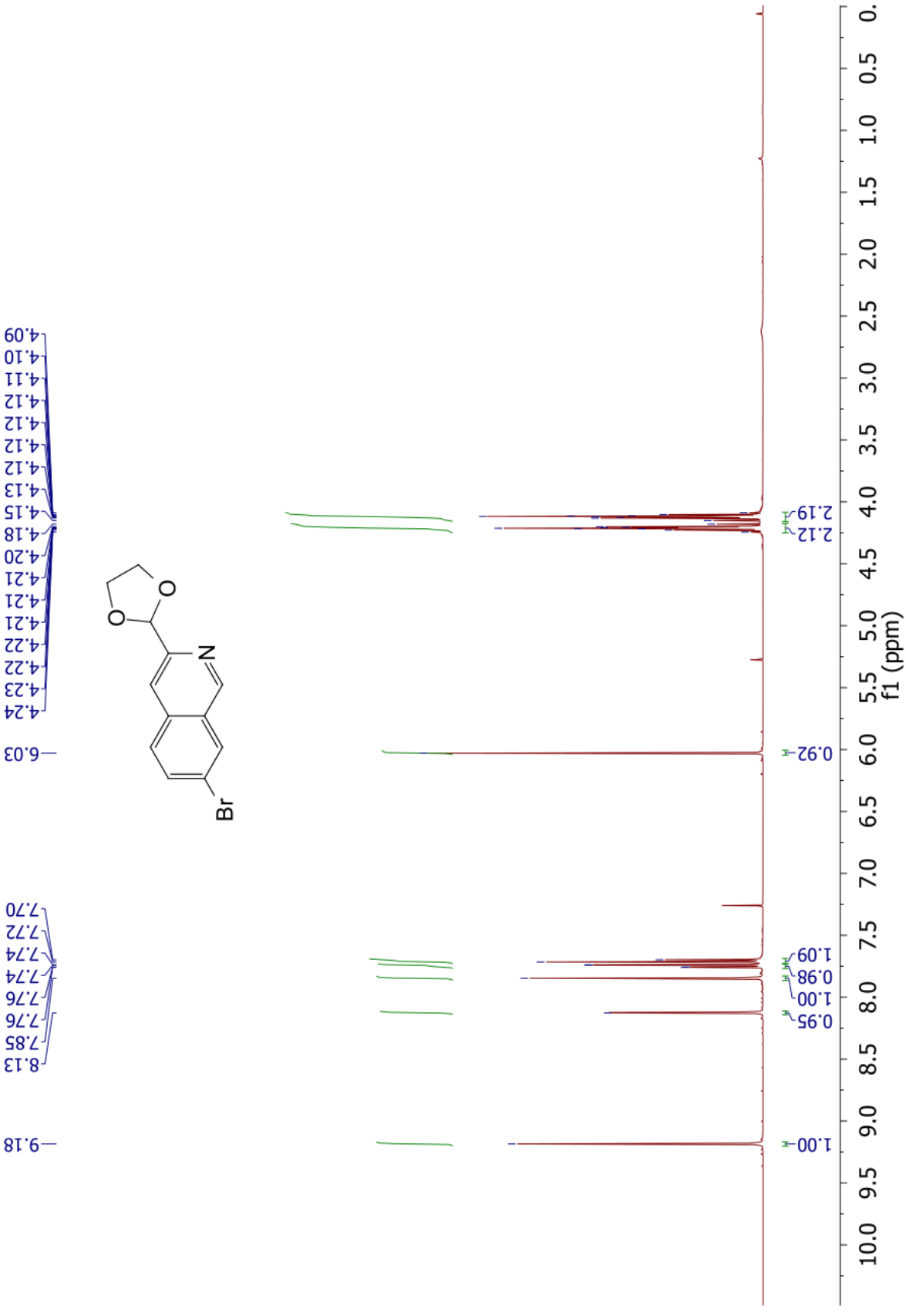
9.18
8.13
7.85
7.76
7.76
7.74
7.74
7.72
7.70
6.03
4.24
4.23
4.22
4.22
4.21
4.21
4.21
4.20
4.18
4.15
4.13
4.12
4.12
4.12
4.12
4.11
4.10
4.09
1.00
0.95
1.00
0.98
1.09
0.92
2.12
2.19
f1 (ppm)
Br
N
O
O

65.65
103.44
117.42
121.45
128.75
129.48
129.76
134.21
134.42
150.74
151.52
O
O
N
Br
f1 (ppm)

1.62
1.62
1.62
1.63
1.64
1.64
1.65
1.65
1.73
1.73
1.74
1.74
1.75
1.76
1.76
1.77
3.28
3.30
3.31
4.10
4.11
4.11
4.11
4.12
4.12
4.22
4.22
4.23
4.23
4.23
4.24
6.01
7.18
7.18
7.47
7.47
7.49
7.49
7.68
7.70
7.73
9.09
2.21
4.09
4.45
4.31
0.89
1.15
1.14
1.10
1.00
1.00
f1 (ppm)

24.13
25.58
50.21
65.44
103.77
108.60
117.45
124.23
127.54
130.23
130.26
146.97
150.97
151.13
O
O
N
N
f1 (ppm)

10.19
9.13
8.24
7.87
7.84
7.57
7.56
7.54
7.53
7.23
3.46
3.44
3.42
1.77
1.76
1.74
1.72
1.71
1.69
1.00
1.09
1.05
0.99
1.06
1.04
4.29
6.07
f1 (ppm)

193.13
152.47
151.30
144.54
132.82
129.56
128.46
123.31
122.00
107.55
49.39
25.46
24.27
O
H
N
N
f1 (ppm)

O
O
O
O
O
O
O
CH3
N
N
N
6.29
2.75
3.91
1.99
4.20
2.02
1.98
2.01
1.16
1.07
1.03
1.21
1.07
1.00
10.0
9.5
9.0
8.5
8.0
7.5
7.0
6.5
6.0
5.5
5.0
4.5
4.0
3.5
3.0
2.5
2.0
1.5
1.0
0.5
f1 (ppm)

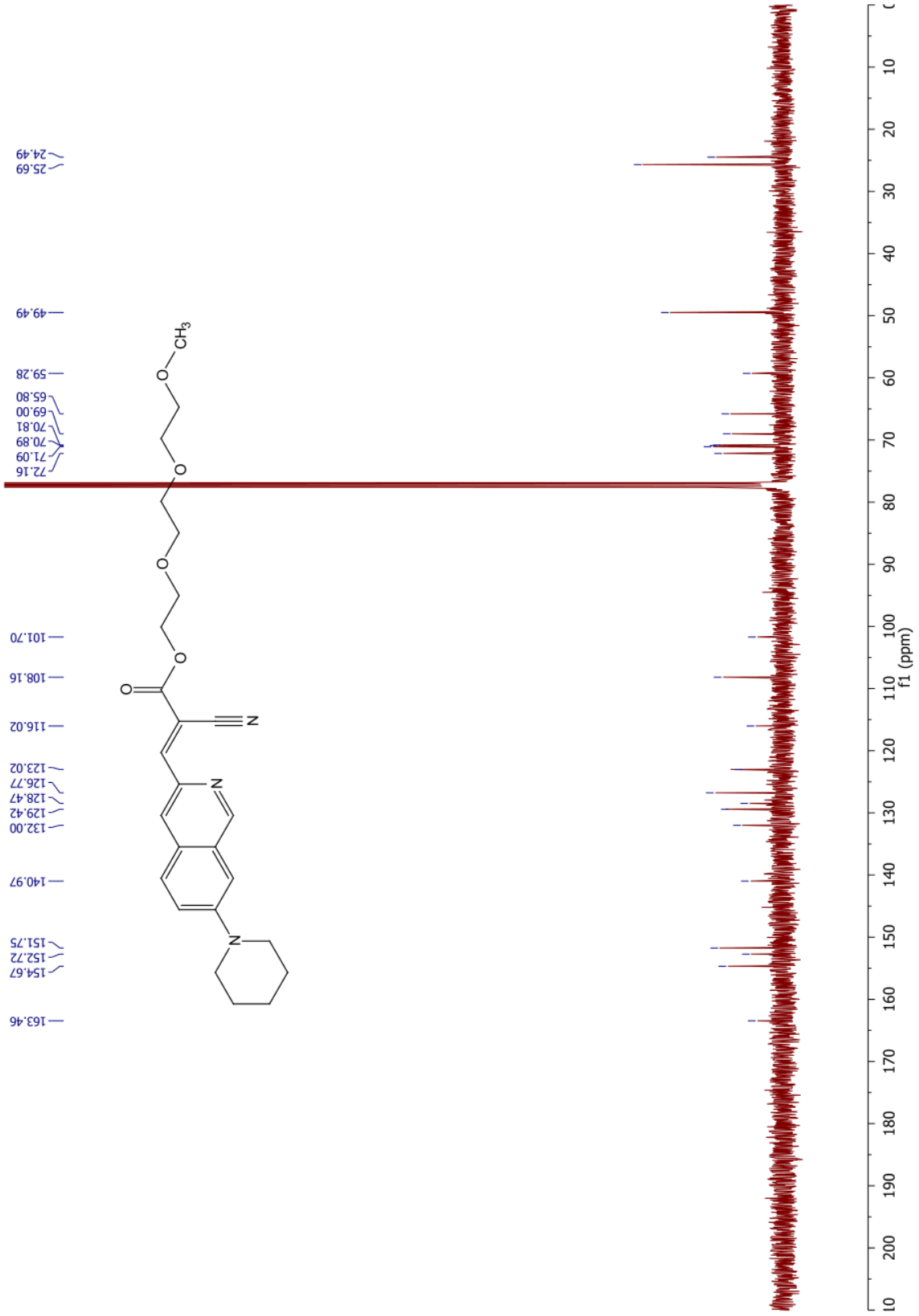
24.49
25.69
49.49
59.28
65.80
69.00
70.81
70.89
71.09
72.16
101.70
108.16
116.02
123.02
126.77
128.47
129.42
132.00
140.97
151.75
152.72
154.67
163.46
O
O
O
O
O
O
CH3
N
N
N
10
20
30
40
50
60
70
80
90
100
110
120
130
140
150
160
170
180
190
200
f1 (ppm)

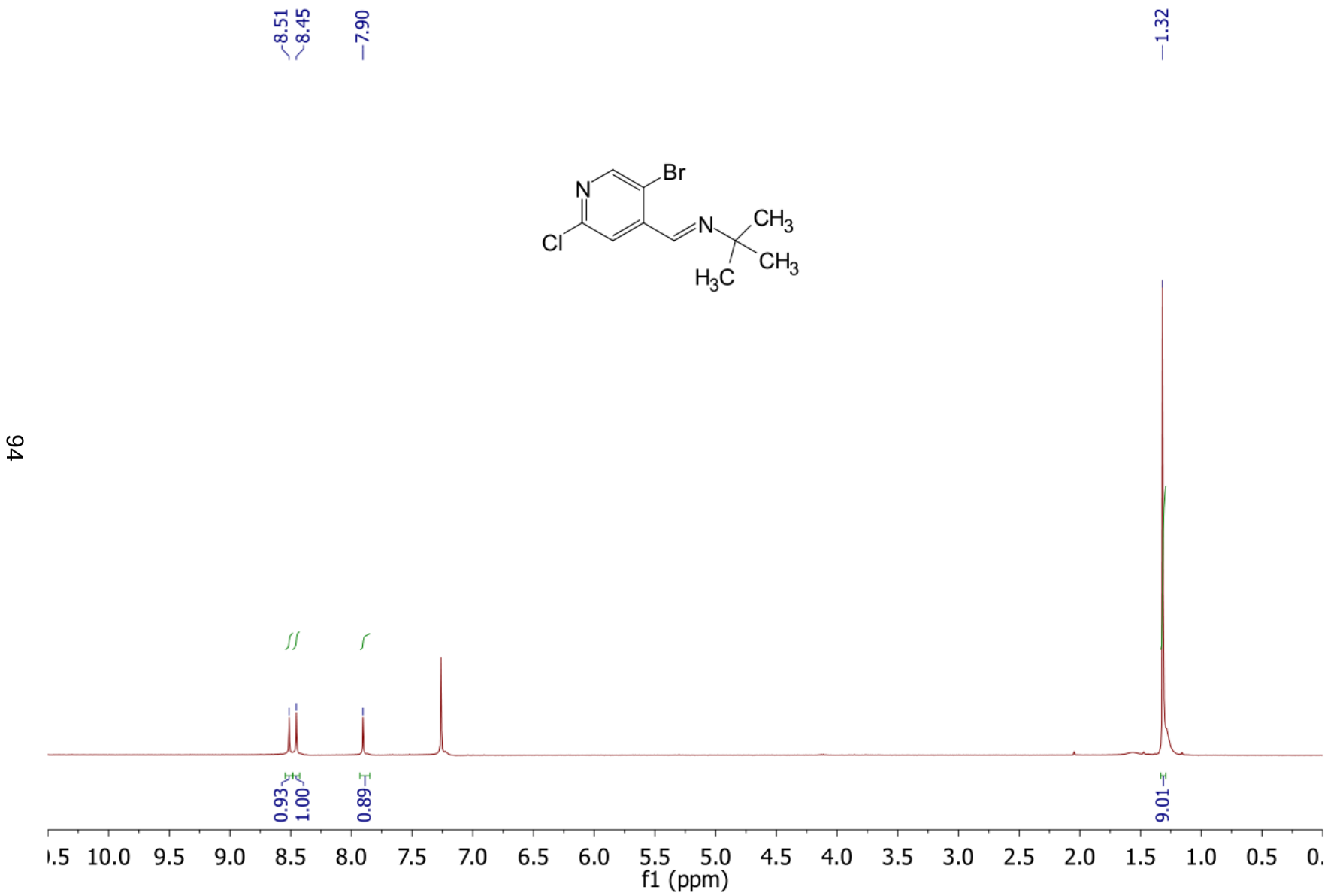
8.51
8.45
7.90
1.32
Br
N
Cl
N
CH3
CH3
H3C
0.93
1.00
0.89
9.01
10.0
9.5
9.0
8.5
8.0
7.5
7.0
6.5
6.0
5.5
5.0
4.5
4.0
3.5
3.0
2.5
2.0
1.5
1.0
0.5
f1 (ppm)

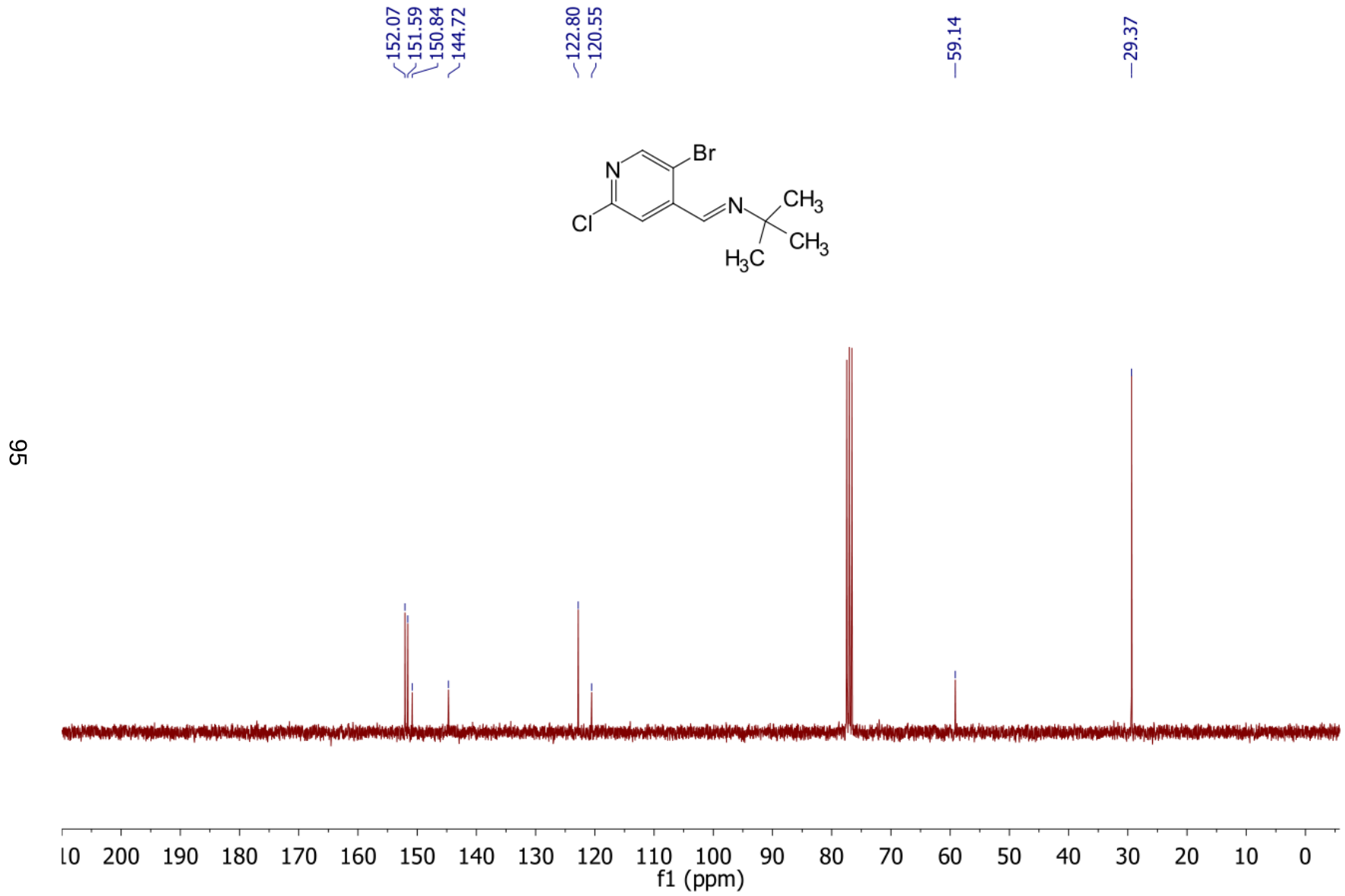
152.07
151.59
150.84
144.72
122.80
120.55
59.14
29.37
Br
N
Cl
N
CH3
CH3
H3C
f1 (ppm)

9.15
9.11
7.88
7.78
4.98
0.97
0.15
1.00
1.00
1.03
1.01
2.07
9.05
6.02
f1 (ppm)
CH3
CH3
CH3
CH3
Si
O
N
N
Cl

157.36
152.06
150.09
146.30
130.97
129.69
118.91
114.08
65.68
25.96
18.43
-5.34
f1 (ppm)

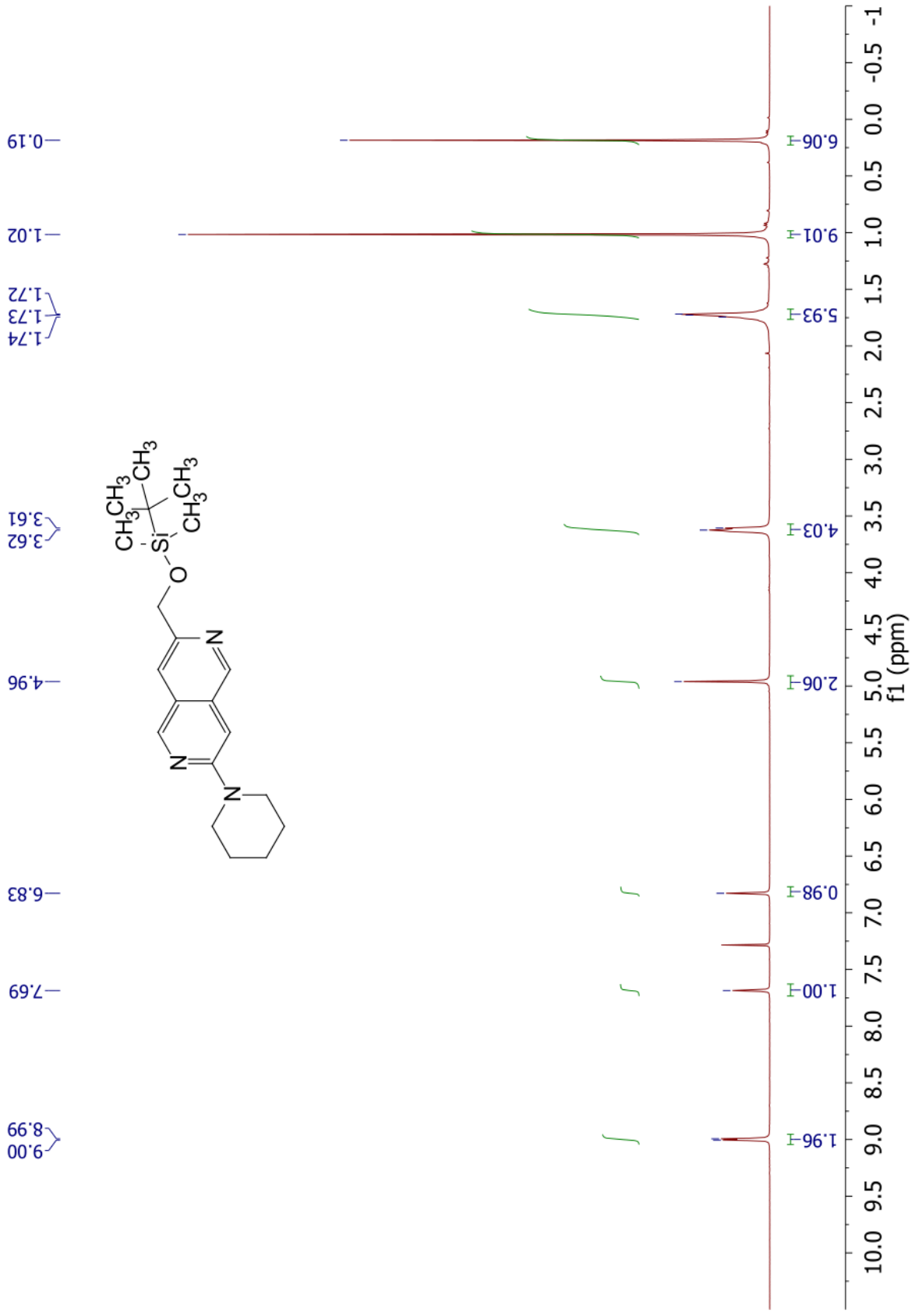
0.19
1.02
1.72
1.73
1.74
3.61
3.62
4.96
6.83
7.69
8.99
9.00
6.06
9.01
5.93
4.03
2.06
0.98
1.00
1.96
10.0 9.5 9.0 8.5 8.0 7.5 7.0 6.5 6.0 5.5 5.0 4.5 4.0 3.5 3.0 2.5 2.0 1.5 1.0 0.5 0.0 -0.5 -1
f1 (ppm)
CH3
CH3
CH3
CH3
Si
O
N
N
N

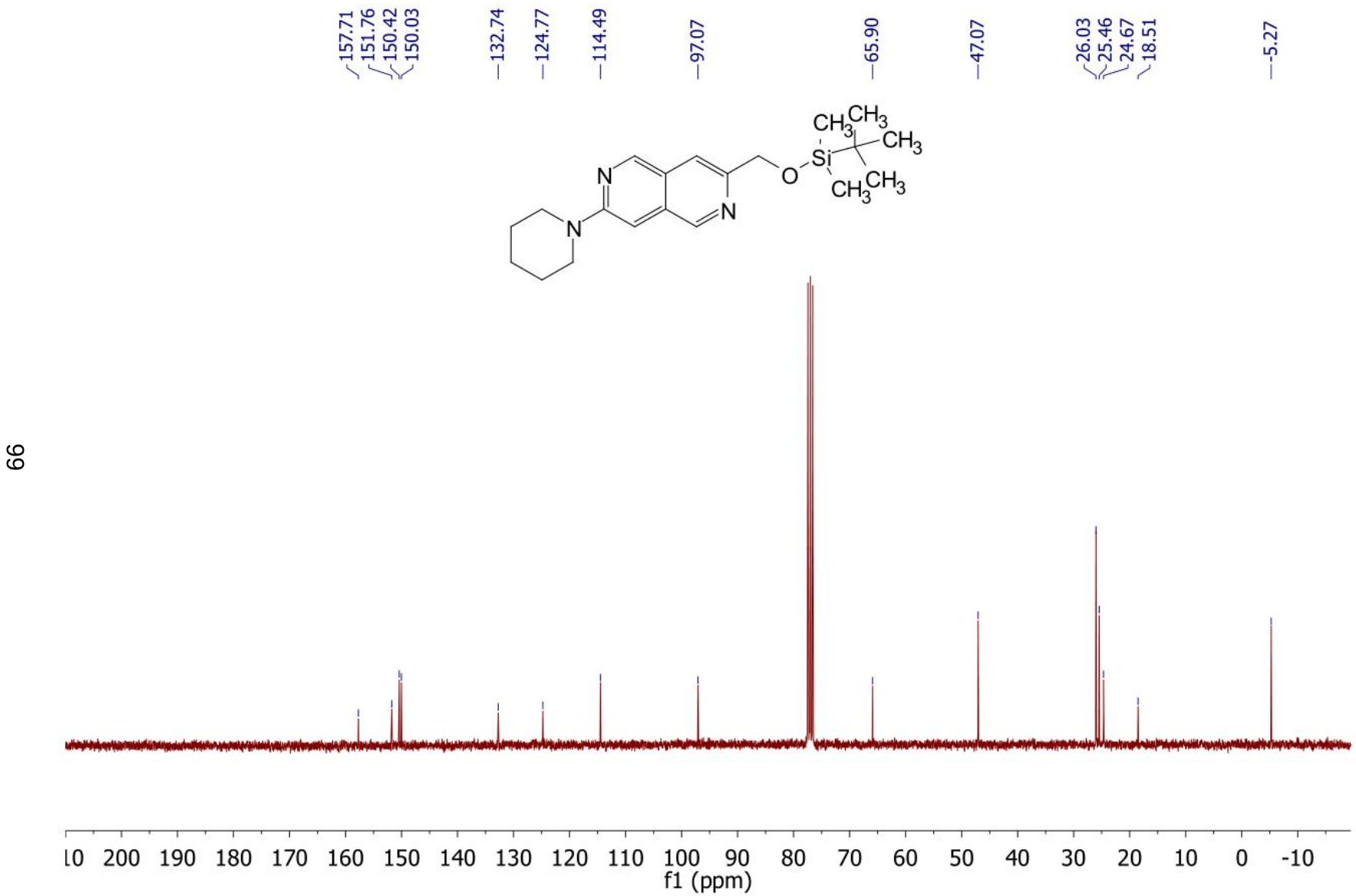
157.71
151.76
150.42
150.03
132.74
124.77
114.49
97.07
65.90
47.07
26.03
25.46
24.67
18.51
-5.27
N
N
N
O
Si
CH3
CH3
CH3
CH3
CH3
f1 (ppm)

9.02
8.96
7.54
7.26
4.85
3.62
1.70
0.86
0.86
0.91
1.00
2.05
4.24
6.17
OH
N
N
N
10.0
9.5
9.0
8.5
8.0
7.5
7.0
6.5
6.0
5.5
5.0
4.5
4.0
3.5
3.0
2.5
2.0
1.5
1.0
0.5
0.
f1 (ppm)

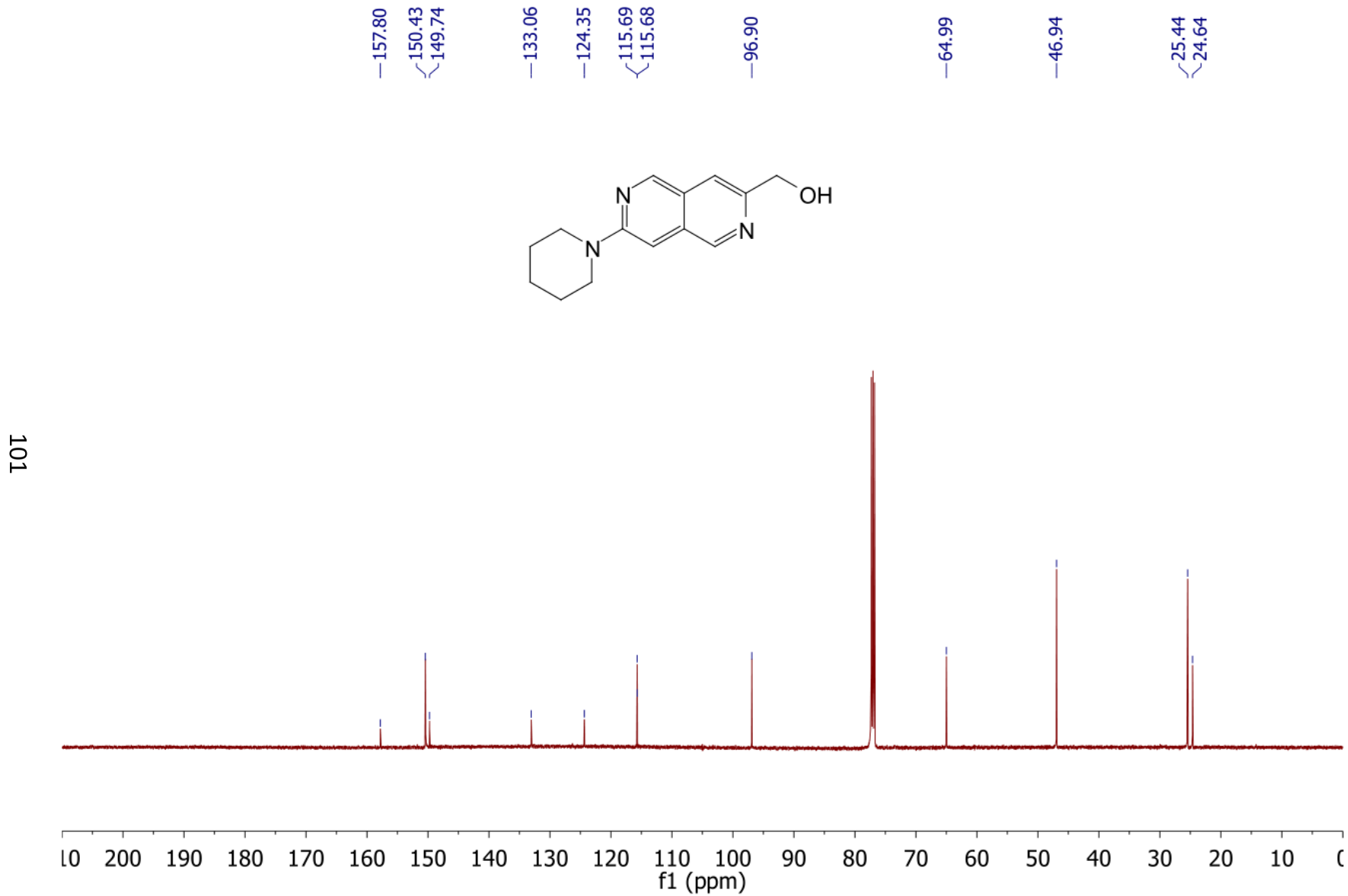
157.80
150.43
149.74
133.06
124.35
115.69
115.68
96.90
64.99
46.94
25.44
24.64
N
N
N
OH
f1 (ppm)

101

10.11
9.07
8.23
6.81
3.75
1.72
0.88
1.98
1.00
1.20
4.12
6.30
f1 (ppm)

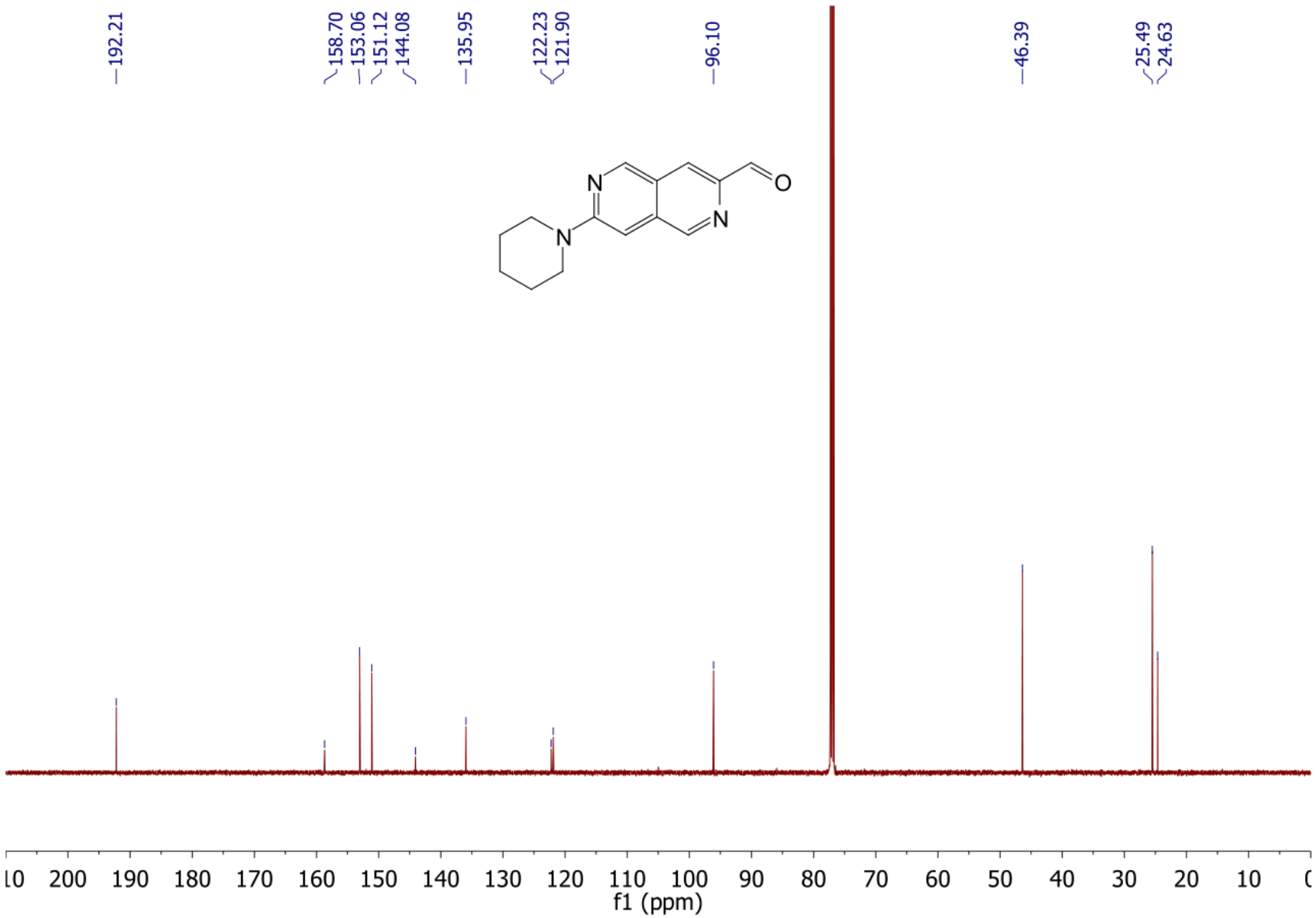
192.21
158.70
153.06
151.12
144.08
135.95
122.23
121.90
96.10
46.39
25.49
24.63
N
N
N
O
f1 (ppm)

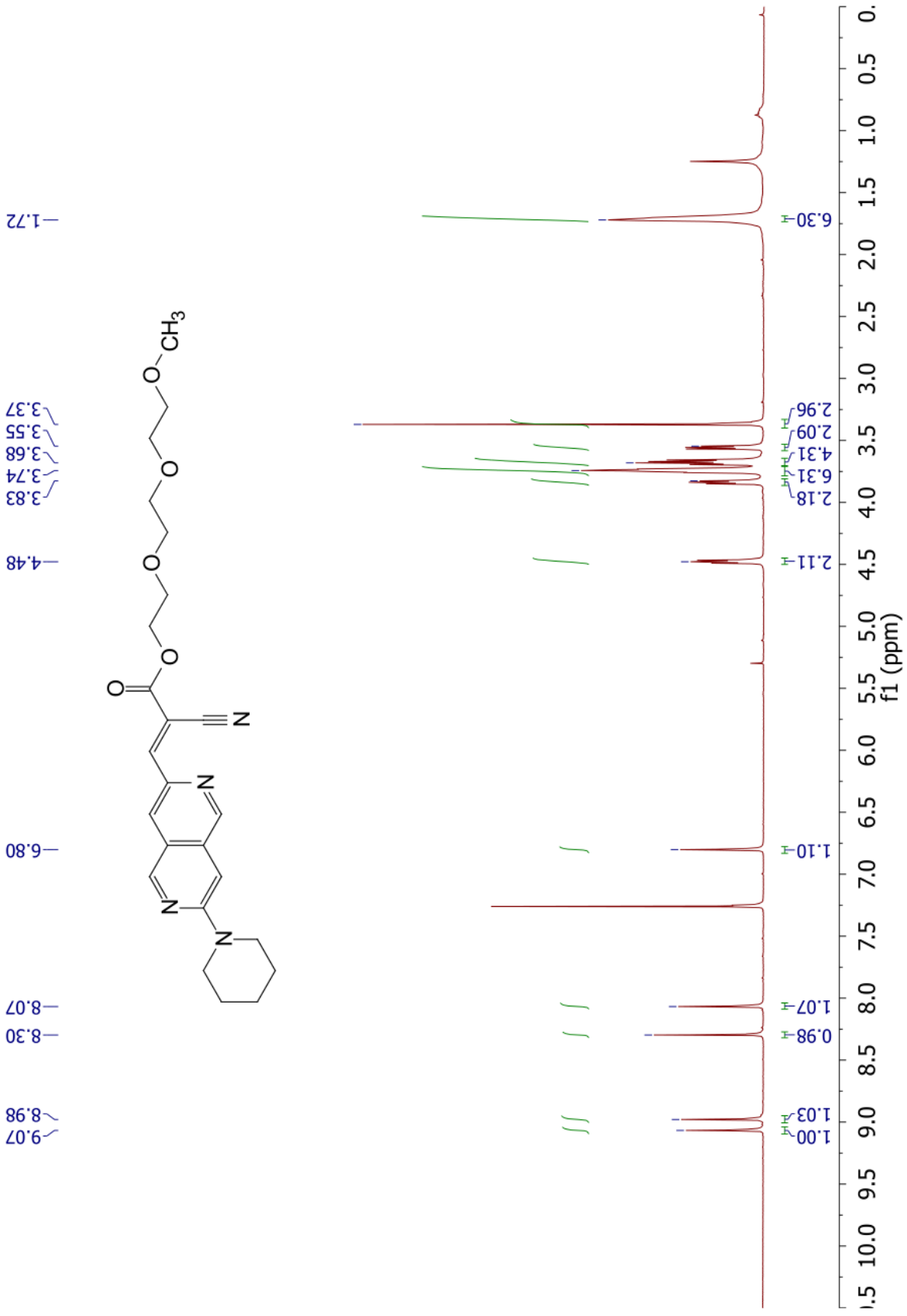
1.72
3.37
3.55
3.68
3.74
3.83
4.48
6.80
8.07
8.30
8.98
9.07
6.30
2.96
2.09
4.31
6.31
2.18
2.11
1.10
1.07
0.98
1.03
1.00
f1 (ppm)

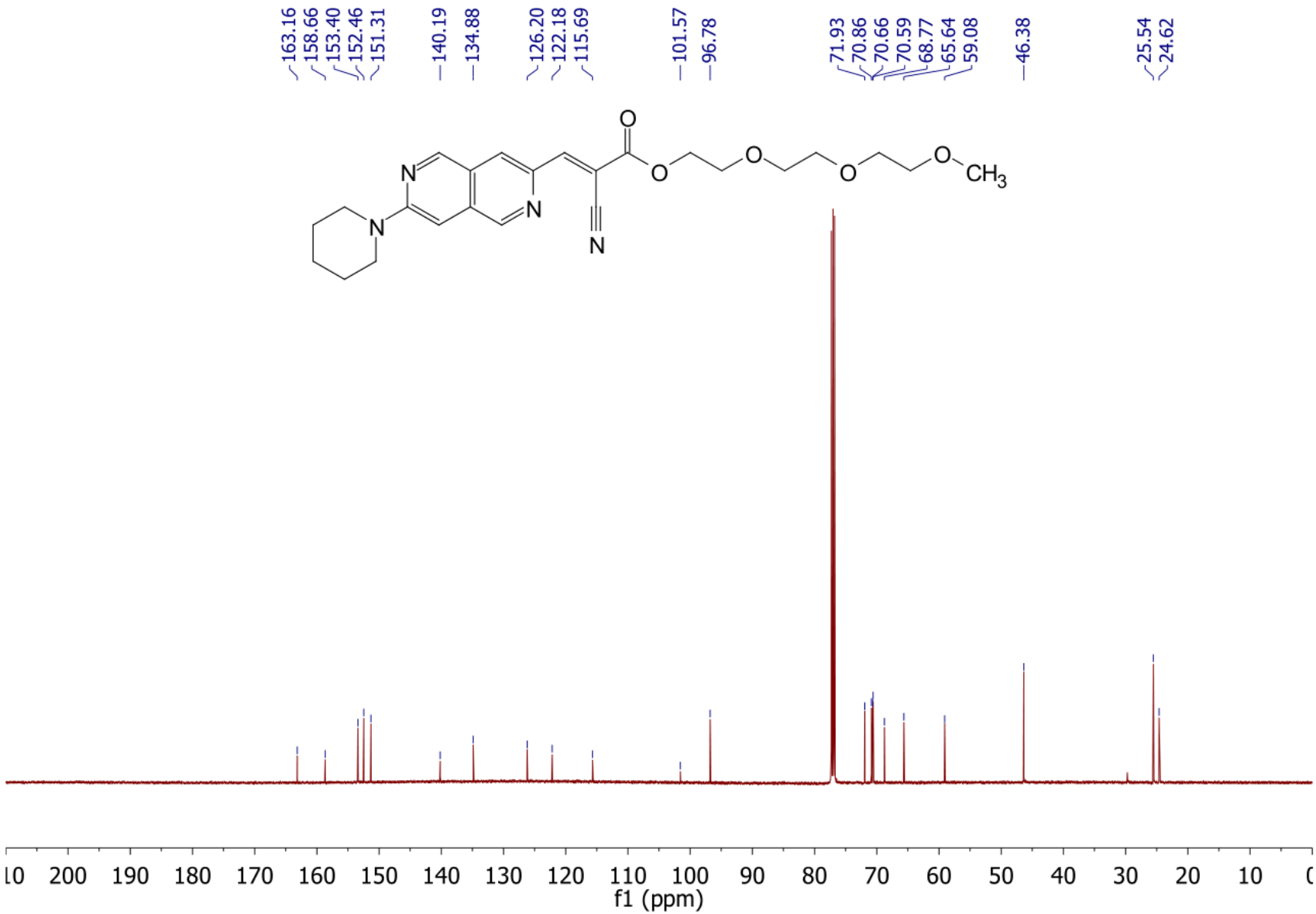
163.16
158.66
153.40
152.46
151.31
140.19
134.88
126.20
122.18
115.69
101.57
96.78
71.93
70.86
70.66
70.59
68.77
65.64
59.08
46.38
25.54
24.62
O
N
N
N
O
O
O
O
CH3
N
200
190
180
170
160
150
140
130
120
110
100
90
80
70
60
50
40
30
20
10
f1 (ppm)

References

1. Gordon, P. F.; Gregory, P., *Organic chemistry in colour*. Springer-Verlag: Berlin ; New York, 1983; p xi, 322 p.

2. Fabian, J.; Hartmann, H., *Light absorption of organic colorants : theoretical treatment and empirical rules*. Springer-Verlag: Berlin ; New York, 1980; p viii, 245 p.

3. Pauling, L., A Theory of the Color of Dyes. *Proceedings of the National Academy of Sciences of the United States of America* **1939,** *25* (11), 577-582.

4. Bahnick, D. A., Use of Huckel Molecular Orbital Theory in Interpreting the Visible Spectra of Polymethine Dyes: An Undergraduate Physical Chemistry Experiment. *Journal of Chemical Education* **1994,** *71* (2), 171.

5. Pariser, R.; Parr, R. G., A Semi-Empirical Theory of the Electronic Spectra and Electronic Structure of Complex Unsaturated Molecules. I. *The Journal of Chemical Physics* **1953,** *21* (3), 466-471.

6. Ruedenberg, K.; Scherr, C. W., Free-Electron Network Model for Conjugated Systems. I. Theory. *The Journal of Chemical Physics* **1953,** *21* (9), 1565-1581.

7. Hoijtink, G. J., The polarographic reduction of conjugated hydrocarbons: VI. Comparison of Hückel's and Wheland's m.o. approximation with experimental half-wave potentials of various alternant and non-alternant hydrocarbons. *Recueil des Travaux Chimiques des Pays-Bas* **1955,** *74* (12), 1525-1539.

8. Milian-Medina, B.; Gierschner, J., pi-Conjugation. *Wires Comput Mol Sci* **2012,** *2* (4), 513-524.

9. Bureš, F., Fundamental aspects of property tuning in push–pull molecules. *RSC Advances* **2014,** *4* (102), 58826-58851.

10. El-Shishtawy, R. M.; Asiri, A. M.; Aziz, S. G.; Elroby, S. A. K., Molecular design of donor-acceptor dyes for efficient dye-sensitized solar cells I: a DFT study. *Journal of Molecular Modeling* **2014,** *20* (6), 2241.

11. Ip, C. M.; Troisi, A., Does the Donor-π-Acceptor Character of Dyes Improve the Efficiency of Dye-Sensitized Solar Cells? *The Journal of Physical Chemistry Letters* **2016,** *7* (15), 2989-2993.

12. Hagfeldt, A.; Boschloo, G.; Sun, L.; Kloo, L.; Pettersson, H., Dye-Sensitized Solar Cells. *Chemical Reviews* **2010,** *110* (11), 6595-6663.

13. Šarlah, D.; Juranovič, A.; Kožar, B.; Rejc, L.; Golobič, A.; Petrič, A., Synthesis of Naphthalene-Based Push-Pull Molecules with a Heteroaromatic Electron Acceptor. *Molecules* **2016,** *21* (3).

14. Chang, W. M.; Dakanali, M.; Capule, C. C.; Sigurdson, C. J.; Yang, J.; Theodorakis, E. A., ANCA: A Family of Fluorescent Probes that Bind and Stain Amyloid Plaques in Human Tissue. *ACS Chemical Neuroscience* **2011,** *2* (5), 249-255.

15. Sustmann, R., Frontier Orbitals and Properties of Organic Molecules. (Reihe: Ellis Horwood Books in Organic Chemistry, Reihenherausgeber: J. Mellor.) Von V. F. Traven. Ellis Horwood, Chichester, 1990), XVI, 401 S., geb. 111.00 $. — ISBN 0-13-327487-X. *Angewandte Chemie* **1994,** *106* (2), 245-246.

16. Burke, K., Perspective on density functional theory. *Journal of Chemical Physics* **2012,** *136*, 150901-150901.

17. Cohen, A. J.; Mori-Sánchez, P.; Yang, W., Insights into Current Limitations of Density Functional Theory. *Science* **2008,** *321* (5890), 792.

18. Solà, M., Forty years of Clar's aromatic π-sextet rule. *Frontiers in Chemistry* **2013,** *1*, 22.

19. Yadav, Jhillu S.; Reddy, Basi V. S.; Basak, Ashok K.; Visali, B.; Narsaiah, Akkirala V.; Nagaiah, K., Phosphane-Catalyzed Knoevenagel Condensation: A Facile Synthesis of α-Cyanoacrylates and α-Cyanoacrylonitriles. *European Journal of Organic Chemistry* **2004,** *2004* (3), 546-551.

20. Smith, J. A.; Jones, R. K.; Booker, G. W.; Pyke, S. M., Sequential and selective Buchwald− Hartwig amination reactions for the controlled functionalization of 6-bromo-2-chloroquinoline: synthesis of ligands for the Tec Src Homology 3 domain. *The Journal of organic chemistry* **2008,** *73* (22), 8880-8892.

21. Mills, W. H.; Smith, J. L. B., CCCXXVIII.—The reactivity of methyl groups in heterocyclic bases. *Journal of the Chemical Society, Transactions* **1922,** *121* (0), 2724-2737.

22. Fieser, L. F.; Lothrop, W. C., The structure of naphthalene. *Journal of the American Chemical Society* **1935,** *57*, 1459-1464.

23. Bryson, A., The effects of substituents in the naphthalene ring. Part I. The basic strengths of the mononitro-napthylamines. *Transactions of the Faraday Society* **1949,** *45* (0), 257-264.

24. Bradamante, S.; Facchetti, A.; Pagani, G. A., Heterocycles as donor and acceptor units in push–pull conjugated molecules. Part 1. *Journal of Physical Organic Chemistry* **1997,** *10* (7), 514-524.

25. Albert, I. D. L.; Marks, T. J.; Ratner, M. A., Large Molecular Hyperpolarizabilities. Quantitative Analysis of Aromaticity and Auxiliary Donor−Acceptor Effects. *Journal of the American Chemical Society* **1997,** *119* (28), 6575-6582.

26. Janietz, S.; Bradley, D. D. C.; Grell, M.; Giebeler, C.; Inbasekaran, M.; Woo, E. P., Electrochemical determination of the ionization potential and electron affinity of poly(9,9-dioctylfluorene). *Applied Physics Letters* **1998,** *73* (17), 2453-2455.

27. D'Andrade, B. W.; Datta, S.; Forrest, S. R.; Djurovich, P.; Polikarpov, E.; Thompson, M. E., Relationship between the ionization and oxidation potentials of molecular organic semiconductors. *Organic Electronics* **2005,** *6* (1), 11-20.

28. Tsuneda, T.; Song, J.-W.; Suzuki, S.; Hirao, K., On Koopmans' theorem in density functional theory. *The Journal of Chemical Physics* **2010,** *133* (17), 174101.

29. Bredas, J.-L., Mind the gap! *Materials Horizons* **2014,** *1* (1), 17-19.

30. Cardona, C. M.; Li, W.; Kaifer, A. E.; Stockdale, D.; Bazan, G. C., Electrochemical Considerations for Determining Absolute Frontier Orbital Energy Levels of Conjugated Polymers for Solar Cell Applications. *Advanced Materials* **2011,** *23* (20), 2367-2371.

31. Cao, K.; Farahi, M.; Dakanali, M.; Chang, W. M.; Sigurdson, C. J.; Theodorakis, E. A.; Yang, J., Aminonaphthalene 2-Cyanoacrylate (ANCA) Probes

Fluorescently Discriminate between Amyloid-β and Prion Plaques in Brain. *Journal of the American Chemical Society* **2012,** *134* (42), 17338-17341.

32. Parasassi, T.; Krasnowska, E. K.; Bagatolli, L.; Gratton, E., Laurdan and Prodan as Polarity-Sensitive Fluorescent Membrane Probes. *Journal of Fluorescence* **1998,** *8* (4), 365-373.

33. Shin, J.; Kepe, V.; R Barrio, J.; W Small, G., *The merits of FDDNP-PET imaging in Alzheimer's disease*. 2011; Vol. 26 Suppl 3, p 135-45.

34. Gellibert, F.; Woolven, J.; Fouchet, M.-H.; Mathews, N.; Goodland, H.; Lovegrove, V.; Laroze, A.; Nguyen, V.-L.; Sautet, S.; Wang, R.; Janson, C.; Smith, W.; Krysa, G.; Boullay, V.; de Gouville, A.-C.; Huet, S.; Hartley, D., Identification of 1,5-Naphthyridine Derivatives as a Novel Series of Potent and Selective TGF-β Type I Receptor Inhibitors. *Journal of Medicinal Chemistry* **2004,** *47* (18), 4494-4506.

35. Narine, A. e. a., Preparation of azolobenzazine compounds, compositions comprising these compounds and their use for controlling invertebrate pests. *2016113272* **2016**.